UNIVERSIDAD COMPLUTENSE DE MADRID
FACULTAD DE MEDICINA

TESIS DOCTORAL

Papel de la fosfatasa de regeneración hepática 1 (PRL-1) durante el ensamblaje de la sinapsis inmunológica y la activación de los linfocitos T

Role of phosphatase of regenerating liver 1 (PRL-1) during immunological synapse assembly and T cell activation

MEMORIA PARA OPTAR AL GRADO DE DOCTOR

PRESENTADA POR

Patricia Castro Sánchez

Director

Pedro Roda Navarro
i

Madrid 2018

Universidad Complutense de Madrid

Facultad de Medicina

Doctorado en Investigación Biomédica

TESIS DOCTORAL

Papel de la fosfatasa de regeneración hepática 1 (PRL-1) durante el ensamblaje de la sinapsis inmunológica y la activación de los linfocitos T

Role of phosphatase of regenerating liver 1 (PRL-1) during immunological synapse assembly and T cell activation

Patricia Castro Sánchez

Director: Pedro Roda Navarro

Madrid, 2017

Universidad Complutense de Madrid

Facultad de Medicina

Doctorado en Investigación Biomédica

TESIS DOCTORAL

Papel de la fosfatasa de regeneración hepática 1 (PRL-1) durante el ensamblaje de la sinapsis inmunológica y la activación de los linfocitos T

Role of phosphatase of regenerating liver 1 (PRL-1) during immunological synapse assembly and T cell activation

Patricia Castro Sánchez

Director: Pedro Roda Navarro

Madrid, 2017

CONTENTS

RESUMEN 9

SUMMARY 15

ABBREVIATIONS 21

INTRODUCTION 27

1. CD4 T cells 27

2. The IS 28

2.1 Formation and structure of the IS 29

2.2 Signaling at the IS 31

2.3 Regulation of actin polymerization at the IS 33

3. Subsets of effector Th cells 34

3.1 Th1 and Th2 35

3.2 Th17 36

3.3 Treg 36

4. Protein tyrosine phosphatases 37

4.1 Classification of the PTP superfamily 37

4.2 PRLs 40

HYPOTHESIS AND OBJECTIVES 47

MATERIALS AND METHODS 51

1. Materials 51

1.1 Reagents 51

1.2 Kits 52

1.3 Primers 52

1.4 Plasmids 54

1.5 Antibodies 54

1.6 Buffers 55

1.7 Equipment 56

2. Methods 56

2.1 Purification of primary cells 56

2.2 In vitro Th1 polarization and restimulation 56

2.3 Cell lines and culture 57

2.4 Generation of knock in GFP-PRL-1 J77 cell line 57

2.5 Cell transfection 59

2.6 Cell stimulation 59

CONTENTS

2.7 Conjugation assays, immunofluorescence and microscopy 59
2.8 Flow cytometry 61
2.9 PCR from genomic DNA 62
2.10 Real- time quantitative PCR (qPCR) 62
2.10 ELISA 63
2.11 Western Blot 63
2.12 Data analysis and statistics 64
RESULTS 67
1. Expression profile of PTPs associated to Th1 polarization 67
1.1 Expression of classical PTPs 69
1.2 Expression of NC PTPs 71
2. Expression of NC PTPs during stimulation of Th1 cells 72
3. PRLs participate in T cell activation 74
4. Recruitment of PRL-1 to the IS 75
5. PRL-1 contributes to T cell activation 85
6. PRL-1 regulates actin dynamics and PLCγ1 at the IS 87
Movie legends 90
DISCUSSION 93
1. Expression profile of NC PTPs during Th1 differentiation and restimulation 93
1.1 Regulators of cytokine signaling and secretion 93
1.2 MAPK regulators 94
1.3 Cell cycle regulators 98
1.4 Phosphoinositide phosphatases 98
1.5 SSHs 99
2. Regulated expression of PRLs during T cell activation 99
3. Recruitment of PRL-1 to the IS 101
4. Contribution of PRL-1 to T cell activation 104
5. PRL-1 regulates actin dynamics at the IS 106
CONCLUSIONS 111
REFERENCES 115
ADDENDA 131
1. Curriculum vitae 131
2. Publications relevant to this thesis 136

RESUMEN

RESUMEN

INTRODUCCIÓN

Los linfocitos CD4 naíf se diferencian a distintos subtipos de células efectoras Th (Th1, Th2, Th17 y Treg) tras ser estimulados por células presentadoras de antígeno (APCs) en el ganglio linfático. Las células Th generadas migran a la periferia, donde un segundo encuentro con el mismo antígeno presentado por APCs conducirá a su activación y función efectora. Tanto la activación inicial de la célula naíf en el ganglio como la reactivación de la célula efectora en la periferia tienen lugar en el contexto de la sinapsis inmunológica (IS), un contacto dinámico y especializado entre una APC y un linfocito. El contacto inicial entre el linfocito T y la APC ocurre en el lamelipodio, donde la estimulación del receptor de la célula T (TCR) y la señalización a través de moléculas de adhesión y de coestimulación induce reordenamientos en el citoesqueleto que estabilizan el contacto, conduciendo a la formación de una IS madura. La estimulación por TCR y moléculas coestimuladoras desencadena redes de señalización que conducen a la activación del linfocito T y su función efectora. La dinámica de actina juega un papel fundamental tanto en el establecimiento de la IS como en la progresión de la señalización necesaria para alcanzar la completa activación del linfocito T. Las redes de señalización inducidas durante la estimulación y diferenciación de la célula T están controladas por fosfo/defosforilación tanto de proteínas como de fosfoinosítidos. Miembros de la familia de las proteínas fosfatasas de tyrosina (PTPs) defosforilan estos sustratos. Más de la mitad de las PTPs pueden también defosforilar residuos de serina y treonina, y pueden definirse como PTPs no clásicas (NC). El papel de un gran número de PTPs NC en la regulación de la diferenciación Th, en el ensamblaje de la IS y en la activación de la célula T son desconocidos.

HIPÓTESIS Y OBJETIVOS

Dado que los linfocitos T expresan un gran número de PTPs, que son importantes reguladores de los niveles de fosforilación en la célula, nuestra hipótesis fue que algunas PTPs NC son reguladores de la activación y diferenciación T. Para verificar esta hipótesis, decidimos (i) estudiar cambios en el perfil de expresión de PTPs NC durante la polarización y reestimulación Th1 y (ii) estudiar el reclutamiento a la IS y el papel regulador en el ensamblaje de la IS y en la señalización por el TCR de la PTP NC PRL-1.

RESULTADOS Y DISCUSIÓN

El estudio del perfil de expresión de PTPs durante la polarización y reestimulación Th1 reveló cambios en los niveles de expresión de varias PTPs, algunas de las cuales tienen una función desconocida en la activación y diferenciación T. Entre las PTPs reguladas durante la reestimulación Th1, la familia de las fosfatasas de regeneración hepática (PRLs) mostró

diferente regulación de cada uno de sus tres miembros: la expresión de PTP4A1 (que codifica para PRL-1) y de PTP4A2 (que codifica para PRL-2) incrementó y disminuyó, respectivamente, mientras que la de PTP4A3 (que codifica para PRL-3) no cambió. Además, el tratamiento con un inhibidor de la actividad catalítica de las PRLs redujo la expresión de CD69 y la secreción de IL-2, sugiriendo que las PRLs participan en la activación T. El aumento de expresión de *PTP4A1* durante la estimulación T y su papel como regulador del citoesqueleto de actina descrito en la literatura nos condujo a estudiar su reclutamiento a la IS. PRL-1 se reclutaba inicialmente a las membranas que escanean la APC, y posteriormente se polarizaba a la IS junto con el compartimento endosomal. Además, PRL-1 colocalizaba con LFA-I y CD3 en la sinapsis madura. Experimentos de microscopía de reflexion interna total confirmaron copresencia de PRL-1 y CD3ζ en la IS y durante el contacto inicial con superficies activadoras. En conjunto, estos datos sugieren que PRL-1 participa en la dinámica y señalización del TCR en la IS. El reclutamiento inicial de PRL-1 a las membranas que escanean la APC nos llevó a estudiar el papel de esta proteína en la dinámica de actina durante el ensamblaje de la IS. La sobreexpresión de PRL-1 provocó un defecto en el aclaramiento de actina y en la extensión de la célula T sobre superficies activadoras, mientras que la inhibición de la actividad catalítica provocó una disminución en la polimerización de actina en la IS. Estos efectos sobre el citoesqueleto de actina podrían deberse a la regulación de las Rho GTPasas Rac1, Cdc42 y RhoA por PRL-1. Por último, la sobreexpresión de PRL-1 condujo a mayores niveles de inducción de CD69, de secreción de IL-2 y de activación de fosfolipasa C γ 1 (PLCγ1), mientras que la inhibición de la actividad catalítica de PRL-1 tuvo el efecto opuesto. La activación de PLCγ1 requiere una adecuada polimerización de actina en la IS. Por tanto, en nuestro sistema, la disminución en la polimerización de actina cuando PRL-1 es inhibido podría causar una deficiente activación de PLCγ1, disminuyendo la secreción de IL-2. Por el contrario, el aumento en la polimerización de actina en el área de contacto inducido por la sobreexpresión de PRL-1 resultaría en una mayor activación de PLCγ1, conduciendo a mayor secreción de IL-2.

CONCLUSIONES

En este trabajo, hemos descrito que el perfil de expresión de PTPs NC se modifica de manera significativa durante la polarización Th1, sugiriendo que las células naíf y las células efectoras requieren distintos niveles de estas enzimas. Además, mostramos que la expresión de diversas NC PTPs se regula durante la estimulación Th1, lo que sugiere que algunas de estas enzimas podrían ser nuevos reguladores de las respuestas T. Respecto a la regulación de las PRLs, encontramos que durante la estimulación T la expresión de PTP4A1 y PTP4A2 se equilibra. Los estudios realizados en PRL-1 mostraron que ésta se recluta a la IS, donde regula los

reordenamientos de actina y donde regula positivamente la activación de PLCγ1 y la secreción de IL-2. En conjunto, nuestros datos alientan futuras investigaciones sobre el papel de PTPs NC en las respuestas T y proporcionan evidencias de que PRL-1 es un regulador positivo de la estimulación T.

SUMMARY

SUMMARY

INTRODUCTION

Stimulation of naïve CD4 T cells in the lymph node by antigen presenting cells (APCs) induces their differentiation into effector T helper (Th) cells. Effector Th cells then migrate to peripheral sites, where a secondary encounter with the same antigen presented by APCs will lead to their activation and effector function, including secretion of appropriate cytokines. Both the initial activation of naïve cells in the lymph node and the reactivation of effector cells in the periphery take place in the context of the immunological synapse (IS). The IS is a specialized dynamic contact between an APC and a lymphocyte. Initial contact between a migrating T cell and an APC takes place at the leading lamellipodium, where T cell receptor (TCR) engagement and signaling through adhesion and costimulatory molecules induces cytoskeletal rearrangements that stabilize the contact, leading to the formation of a mature IS. Recognition of the antigen by the TCR, together with costimulation, triggers the activation of signaling networks that lead to full T cell activation and effector function. Actin dynamics play a central role in both the establishment of the IS and the progression of sustained signaling required for full T cell activation. One of the subsets in which naïve CD4 T cells can differentiate is the Th1. This subset produces interferon γ (IFNγ) and is specific for intracellular pathogens. Polarization to the Th1 phenotype is promoted by IL-12 and IFNγ, and is initiated during stimulation at the IS. The signaling networks induced during T cell stimulation and differentiation are controlled by phospho/dephosphorylation of both proteins and phosphoinositides. Protein tyrosine phosphatases (PTPs) dephosphorylate a wide range of substrates. This family is formed of more than a hundred genes, among which more than a half are also able to dephosphorylate serine or threonine residues, and can be defined as non classical (NC) PTPs. Interestingly, the role of a high number of NC PTPs in the regulation of Th differentiation, IS assembly and T cell activation remains unknown.

HYPOTHESIS AND OBJECTIVES

Given that T cells express a high number of PTPs, which are key regulators of phosphorylation levels in the cell, we hypothesized that some NC PTPs are yet unknown regulators of T cell activation and differentiation. To verify this hypothesis, we decided (i) to study the changes in the expression profile of NC PTPs during Th1 polarization and restimulation and (ii) to study the recruitment to the IS and the regulatory role in IS assembly and signaling downstream the TCR exerted by the NC PTP PRL-1.

RESULTS AND DISCUSSION

Study of the expression profile of PTPs during Th1 polarization and restimulation revealed changes in the expression levels of several PTPs, some of them with unknown function in T cell activation and differentiation. Among the PTPs regulated during Th1 restimulation, the family of phosphatases of regenerating liver (PRLs) showed differential regulation of each of its three genes: the expression of *PTP4A1* (coding for PRL-1) and *PTP4A2* (coding for PRL-2) were up- and downregulated, respectively, while *PTP4A3* (coding for PRL-3) did not change. Besides, treatment of CD4 T cells with an inhibitor of PRL catalytic activity resulted in reduced CD69 expression and IL-2 secretion, suggesting that PRLs participate in T cell activation. The upregulation of *PTP4A1* during T cell stimulation and its role as regulator of the actin cytoskeleton reported in the literature prompted us to study its delivery to the IS. We found an initial delivery of PRL-1 to scanning membranes of T cells, and a later delivery to the stablished IS with the endosomal compartment. Besides, PRL-1 colocalized with LFA-I and CD3 at the mature IS. Total internal reflection microscopy experiments further confirmed copresence of PRL-1 and CD3ζ at the stablished IS and during initial contact with activating surfaces. Altogether, these data suggest that PRL-1 participates in TCR dynamics and signaling downstream the TCR and LFA-I at the IS. Consistent with this idea, we found that PRL-1 overexpression leads to increased CD69 induction and IL-2 secretion, while inhibition of PRL-1 catalytic activity had the opposite effect, indicating that PRL-1 regulates T cell activation. Initial delivery of PRL-1 to scanning membranes prompted us to study the role of this protein in actin dynamics during IS assembly. Overexpression of PRL-1 resulted in defective actin clearance and impaired cell spreading, while inhibition of PRL-1 catalytic activity resulted in decreased actin polymerization at the IS. These effects on actin dynamics could be due to regulation of the Rho family GTPases Rac1, Cdcd42 and RhoA by PRL-1. Proper actin polymerization at the IS is critical for phospholipase C γ 1 activation. Interestingly, we found that PRL-1 overexpression leads to increased PLCγ1 activation, while PRL-1 inhibiton has the opposite effect. Hence, in our system, decreased actin polymerization when PRL-1 is inhibited could cause defective PLCγ1 activation, leading to deficient IL-2 secretion. By contrast, increased actin polymerization at the area of contact induced by PRL-1 overexpression would result in enhanced PLCγ1 activation, leading to increased IL-2 secretion.

CONCLUSIONS

In this work, we found that the expression profile of NC PTPs is significantly modified during Th1 polarization, suggesting a different requirement of these enzimes in naïve versus effector cells. Besides, we showed that the expression of several NC PTPs is regulated during Th1

stimulation, suggesting that some of these enzimes could be novel regulators of T cell responses. Regarding regulation of PRL phosphatases, we found that after activation, PTP4A1 and PTP4A2 have a more balanced expression than before activation. Focusing on PRL-1, we found that it is recruited to the IS, where it regulates actin rearrangements during IS assembly and where it positively regulates PLCγ-1 activation and IL-2 secretion. Altogether, our data encourage further research on the role of NC PTPs in T cell responses and provide evidences that PRL-1 is a positive regulator of T cell stimulation.

ABBREVIATIONS

ABBREVIATIONS

Table A1. List of abbreviations

Abbreviation	Full name
A3	Analog 3
AP-1	Activator protein-1
APC	Antigen presenting cell
ARP 2/3	Actin-related protein 2/3
Asp	Aspartic acid
ATF	Activating transcription factor
bp	Base pairs
CDC14(s)	Cell division cycle-14 protein(s)
CDC25(s)	Cell division cycle-25 protein(s)
CDK(s)	Cyclin-dependent kinase(s)
CMAC	7-amino-4-chloromethyl coumarin
CRISPR	Clustered regularly interspaced short palindromic repeats
cSMAC	Central SMAC
Cys	Cysteine
DAG	Diacylglycerol
DC	Dendritic cell
DCT	Delta CT
DNA	Deoxyribonucleic acid
DSB	Double strand break
dSMAC	Distal SMAC
DSP(s)	Dual specific phosphatase(s)
ELISA	Enzyme-Linked Immunosorbent Assay
ERK1/2	Extracellular signal activated kinase1/2
Eya(s)	Eyes absent phosphatase(s)
F-actin	Filamentous actin
FAK	Focal-adhesion kinase
FCS	Fetal calf serum
Foxp3	Forkhead box P3
GADS	Grb2-Related Adaptor Downstream of Shc
GATA3	GATA-binding protein 3
GEF	Guanine nucleotide exchange factor
GFP	Green fluorescent protein
Grb2	Growth factor receptor-bound protein 2
HA	Homology arm
HS1	Hematopoietic lineage cell-specific protein 1
ICAM-1	Intercellular adhesion molecule 1
IFNγ	Interferon γ
IFNγ-R	IFNγ receptor
IP	Immunoprecipitation
IP_3	Inositol 1,4,5-triphosphate
IS	Immunological synapse
ITAM(s)	Immunotyrosine-based activation motif(s)
Itk	Interleukin-2-inducible tyrosine kinase

Table A1. List of abbreviations (continuation)

Abbreviation	Full name
JNK	c-Jun N-terminal kinase
KDa	Kilodalton
LAT	Linker for activation of T cells
Lck	Leukocyte C-terminal Src kinase
LFA-I	Lymphocyte function-associated antigen 1
LIMK	LIM kinase
LMPTP	Low-molecular-weight PTP
MAPK	Mitogen-activated protein kinase
MHC-II	Major histocompatibility complex
MKP(s)	MAPK phosphatase(s)
mRNA	Messenger ribonucleic acid
MTM(s)	Myotubularin(s)
MTOC	Microtubule organizing center
NC	Non classical
Nck	Non-catalytic region of tyrosine kinase
NF-κB	Nuclear factor κ B
NFAT	Nuclear factor of activated T cells
NRPTPs	Non receptor PTPs
PAM	Protospacer adjacent motif
PBS	Phosphate-buffered saline
PB3	Procyanidin B3
PD	Phosphatase dead
PMA	phorbol 12-myristate 13-acetate
PIP_2	Phosphatidylinositol (4,5)-biphosphate
PIP_3	phosphatidylinositol (3,4,5)-triphosphate
$PI(3,5)P_2$	phosphatidylinositol (3,5)-biphosphate
PI3K	Phosphatidylinositol 3 kinase
PI3P	Phosphatidylinositol 3-phosphate
PKC-θ	Protein kinase C θ
PLCγ1	Phospholipase C γ 1
PRL(s)	Protein(s) of regenerating liver
pSMAC	Peripheral SMAC
PTEN(s)	Phosphatase and tensin homolog(s)
PTP(s)	Protein tyrosine phosphatase(s)
ROCK	Rho-associated protein kinase
RORγt	RAR-related orphan receptor γt
RPTPs	Receptor type PTPs
SEE	Staphylococcal enterotoxin E
Ser	Serine
Sg	Single guide
SLP76	SH2 domain-containing leukocyte protein of 76 kDa
SMAC	Supramolecular activation cluster
STAT	Signal transducer and activator of transcription
SSH(s)	Slingshot(s)
TCR	T cell receptor
TGF-β	Transforming growth factor β

Table A1. List of abbreviations (continuation)	
Abbreviation	**Full name**
Th	T helper
Thr	Threonine
TIRFM	Total internal reflection fluorescence microscopy
TP	Thienopyridone
Treg	T regulatory
Tyr	Tyrosine
VHR	Vaccinia H1-related protein
WASp	Wiskott Aldrich syndrome protein
WB	Western Blot
ZAP70	ζ-chain associated protein kinase 70

INTRODUCTION

INTRODUCTION

1. CD4 T cells

The immune system is formed of two types of immunity: the innate and the adaptive. The innate immunity is important in the initial containment of the infection, and generates an environment where cells of the adaptive immunity activate, proliferate, and differentiate into cells with effector functions appropriate for an efficient response. CD4 or helper T cells (Th) are fundamental players of adaptive immunity, due to the heterogeneity of their effector functions and their capacity to induce memory (1). They are characterized by the expression of the costimulatory molecule CD4 and the capacity to recognize antigens presented in the context of the class II major histocompatibility complex (MHC-II) by antigen presenting cells (APCs). In addition to their pivotal role in the defence against pathogens, Th cells have been shown to be essential players in autoimmune and inflammatory diseases (2). Therefore, understanding the mechanisms that regulate CD4 T cell responses could open new possibilities for therapy of both infectious and autoimmune diseases.

Generation of differentiated effector Th cells involves several processes in different compartments of the body (Figure I1). T cell precursors migrate from the bone marrow to the thymus, where they undergo a maturation process that includes positive and negative selection (3). Mature CD4 T cells leave the thymus as naïve T cells, characterized by the expression of the RA splicing variant of the CD45 phosphatase (CD45RA) (4). Naïve CD4 T cells circulate in the bloodstream until they reach the lymph nodes, where they scan dendritic cells (DCs) for specific peptides presented in the MHC-II (5). After a first phase of serial contacts, naïve T cells establish long-lasting contacts with DCs, in which antigen presentation by the APC results in T cell activation, proliferation and differentiation into effector T cells (6). Antigen-experienced cells loose expression of CD45RA and express CD45RO, a shorter form of CD45 (4). The encounter with the antigen presented by DCs also determines the differentiation of CD4 T cells into one of at least four subsets of effector Th cells: Th1, Th2, Th17 and Treg (7). Generated effector Th cells can either remain within the lymph node to help B cells or leave the organ through the efferent lymphatic vessels to reach sites of infection. Once in the infected tissue, Th cells exert their effector functions upon additional activation by APCs. All the initial activation of naïve T cells in the lymph node by DCs, the cooperation with B cells and

the secondary activation in infected tissues involve the formation of a specialized contact between the T cell and the APC, called the immunological synapse (IS) (8).

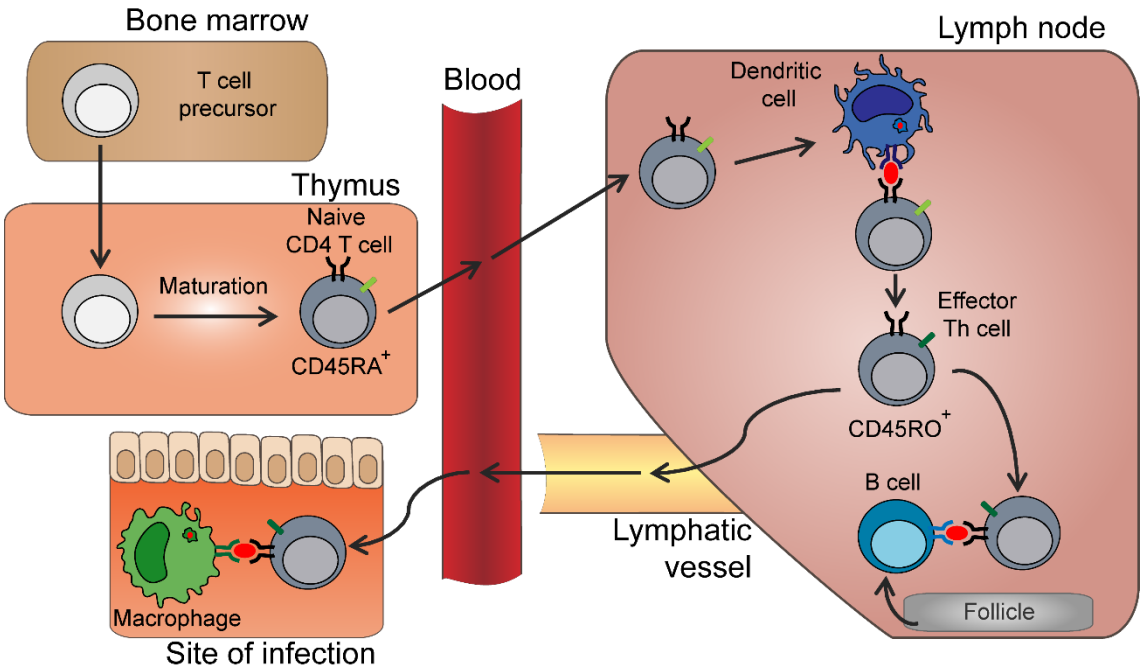

Figure I1. Generation of effector CD4 T cells. The main compartments of the body where take place the initial T cell maturation, antigen encounter, generation of effector Th cells, cooperation with B cells and effector function at the periphery are schematized.

2. The IS

As mentioned before, in vivo T cell activation involves the formation of the IS, an organized, dynamic contact between a lymphocyte and an APC. This structure allows for bidirectional exchange of information between cells, although in this work we will focus on the T cell side of the IS. Signaling downstream the T cell receptor (TCR), costimulatory molecules and integrins takes place in the context of the IS and leads to full T cell activation, differentiation, and effector function.

2.1 Formation and structure of the IS

The formation of the IS starts when a T cell that expresses a TCR for a specific peptide-MCH (p-MCH) complex interacts with an APC presenting the same p-MCH complex. The initial contact takes place at the leading lamellipodium, where p-MHC recognition by the TCR enhances LFA-I (lymphocyte function-associated antigen 1)-mediated adhesion, generating an adhesive surface that, together with the action of the actin cytoskeleton, stops T cell migration and induces the formation of an increasingly stable cell contact with the APC (Figure I2) (9).

LFA-I-mediated adhesion, costimulation by CD28, and TCR signaling trigger actin polymerization at the lamellipodium, which leads to cell spreading over the APC (10). Activated TCRs, CD28, adaptors such as SH2 domain-containing leukocyte protein of 76 KDa (SLP-76) and kinases such as protein kinase C θ (PKC-θ) or ζ-chain associated protein kinase 70 (ZAP70) form microclusters at the periphery of the IS, where signaling starts (11) (Figure I2). At the periphery of the interaction, addition of actin monomers to branched actin filaments and actin severing by depolymerizing factors generates a centripetal retrograde flow of actin that, together with contraction of acto-myosin arcs, drives movement of microclusters to the centre of the interaction (12), where signal extinction takes place (11, 13, 14) (Figure I2). The actin flow is critical for sustaining signaling to achieve T cell activation (15). Besides, the microtubule organizaing center (MTOC) is translocated to the IS within minutes after cell contact, together with the surrounding endosomal compartment (16, 17) (Figure I2). Positioning of the MTOC and microtubule dynamics has been shown to be critical for sustaining TCR signaling, supplying molecules from intracellular pools and maintaining IS architecture (18, 19). In addition, microtubules underlying the IS provide the tracks for movement of signaling microclusters to the center of the interaction in a mechanism that requires dynein (20).

While microclusters migrate, the bull's eye pattern first described by Kupfer and co-workers (21) is formed. This pattern consists of three concentrical structures called SMACs (supramolecular activation clusters) (Figure I2). The central SMAC (cSMAC) is enriched in TCR, costimulatory molecules such as CD28, and intracellular signalling molecules such as protein kinase C θ (PKC-θ) (21). Further analysis of the cSMAC has reveleaded that this area can be further subdivided in a central $CD3^{high}$ region, where TCR and CD3 accumulate prior to internalization and degradation (14, 22), and a surrounding $CD3^{low}$ region enriched in other signaling molecules (Figure I2) (23, 24). A peripheral ring named peripheral SMAC (pSMAC) with high density of LFA-1 and its associated protein talin surrounds the cSMAC (21). Finally,

the more distal zone of the interaction is called distal SMAC (dSMAC), and contains molecules that are excluded from the IS due to its large size, such as CD43 (25). Regarding the actin cytoskeleton, the dSMAC is enriched in a branched filamentous actin (F-actin) network that gives way to a zone of actomyosin arcs at the pSMAC, while the cSMAC is depleted of F-actin (26) (Figure I2).

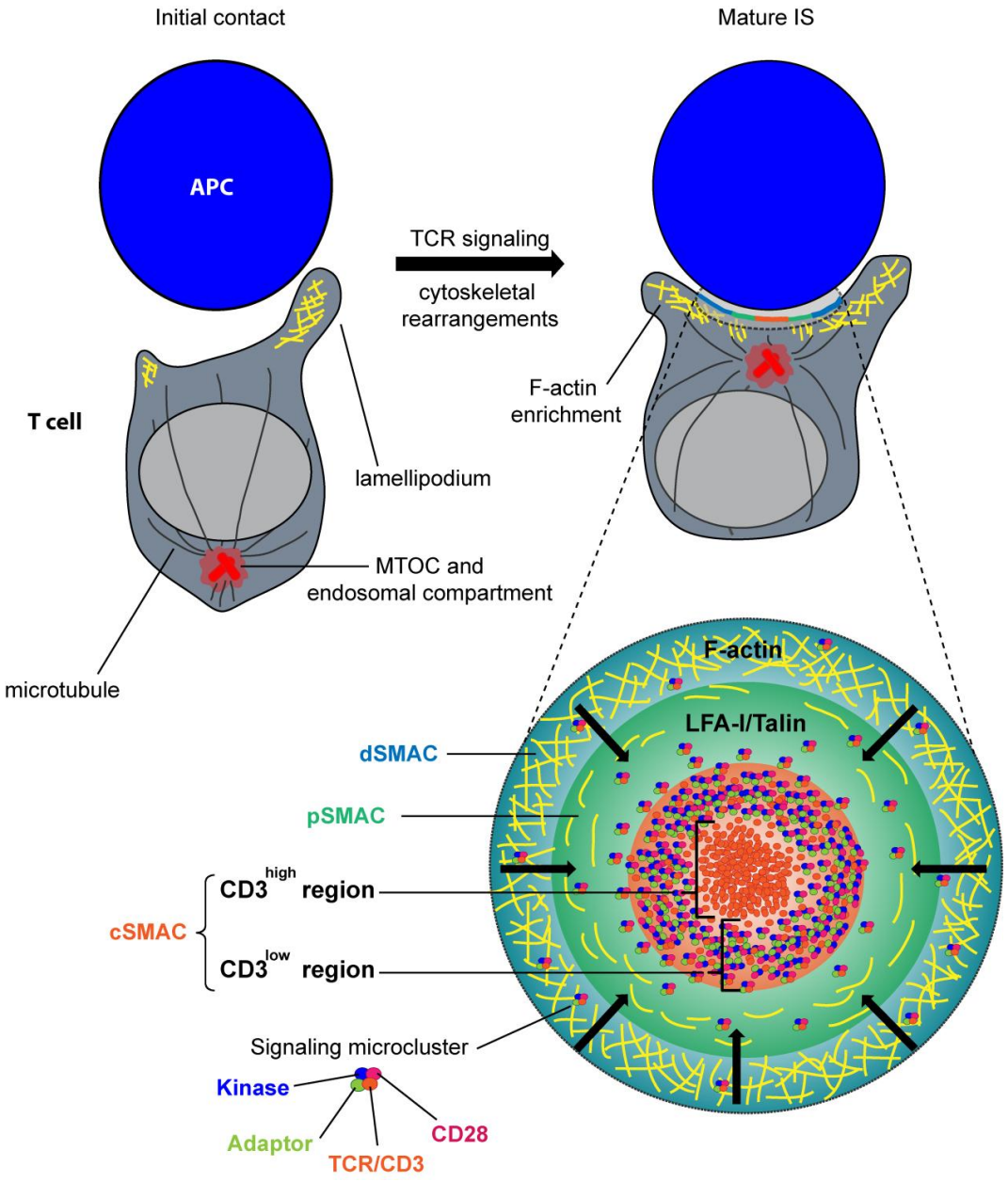

Figure I2. Formation and structure of the IS. In the upper side, a migrating T cell establishing contact with an APC through the leading lamellipodium is shown (left). TCR signaling and actin rearrangements lead to the formation of a mature IS (right). In the lower part, a frontal view of the T cell side of the mature IS as described by Saito and co-workers using planar bilayers (23, 24) is depicted. Filamentous actin is indicated as a yellow network. Actomyosin arcs are represented as yellow curved lines in the pSMAC. Centripetal movement of microclusters is represented by black arrows. Figure inspired by Alarcón *et al* (27).

2.2 Signaling at the IS

Antigen recognition by the TCR and engagement of costimulatory and adhesion molecules triggers signaling through different pathways that lead to T cell activation and regulation of gene expression (Figure I3).

Binding of the MHC/antigen to the TCR induces TCR/CD3 clustering and a conformational change in the CD3 chains, which result in the recruitment of adaptors and protein tyrosine kinases (28, 29). Phosphorylation of the immunotyrosine-based activation motifs (ITAMs) of CD3 chains by the leukocyte C-terminal Src kinase (Lck), which is activated by the phosphatase CD45 (30), results in the recruitment of proteins containing SH2 domains, such as ZAP70 (31). Once activated by Lck, ZAP70 phosphorylates the scaffolds protein linker for activation of T cells (LAT) and SLP76, which leads to the formation of a molecular complex with the adaptors SLP76, Grb2-Related Adaptor Downstream of Shc (GADS) and Nck (non-catalytic region of tyrosine kinase), the guanine nucleotide exchange factor (GEF) Vav1, and the interleukin-2-inducible tyrosine kinase (Itk) (Figure I3A). Costimulation by CD28 also contributes to the formation of this molecular complex. CD28 induces signaling via Vav1/SLP76 complexes through interaction with growth factor receptor-bound protein 2 (Grb2) (32). In addition, CD28 promotes phosphatidylinositol 3 kinase (PI3K) recruitment and activation at the IS (33). PI3K converts membrane-bound phosphatidylinositol 4,5-biphosphate (PIP_2) to phosphatidylinositol (3,4,5) triphosphate (PIP_3). PIP_3 then serves as a docking site for Itk, keeping it close to Lck and hence facilitating Lck-mediated activation of Itk (34) (Figure I3A).

The signaling complex formed around LAT recruits phospholipase C γ 1 (PLCγ1), which is activated by Itk (Figure I3B). Active PLCγ1 catalyzes the hydrolysis of PIP_2 into the secondary messengers diacylglycerol (DAG) and inositol 1,4,5-triphosphate (IP_3). IP_3 generated by active PLCγ1 drives intracellular calcium raise. Increased calcium levels activate calcineurin and induce the nuclear translocation of nuclear factor of activated T cells (NFAT) that, together with activator protein-1 (AP-1) and nuclear factor κ B (NF-κB), induce gene expression changes upon T cell activation (35, 36). On the other hand, local accumulation of DAG triggers the activation of PKCθ, which, together with the microtubule motor dynein, drives MTOC polarization to the IS (18, 37, 38). Besides, DAG promotes the polarization and activation of Ras, triggering the activation of the MAPK (mitogen-activated protein kinase) Erk1/2 (extracellular signal activated kinase 1/2) (39). Other members of the MAPK signaling module are also activated downstream the TCR (Figure I3B). Activation of p38 upon T cell stimulaton

has been proposed to occur through activation of the classical MAPK cascade by Vav1 and the Rho-family GTPase Rac (40), but also through an alternative pathway involving direct phosphorylation of p38 by ZAP70 (41). Both pathways seem to coexist in T cells (42). The mechanism of activation of the c-Jun N-terminal kinase (JNK) during T cell activation requires CD28 costimulation (43), and seems to involve Rac and PKCθ (44, 45).

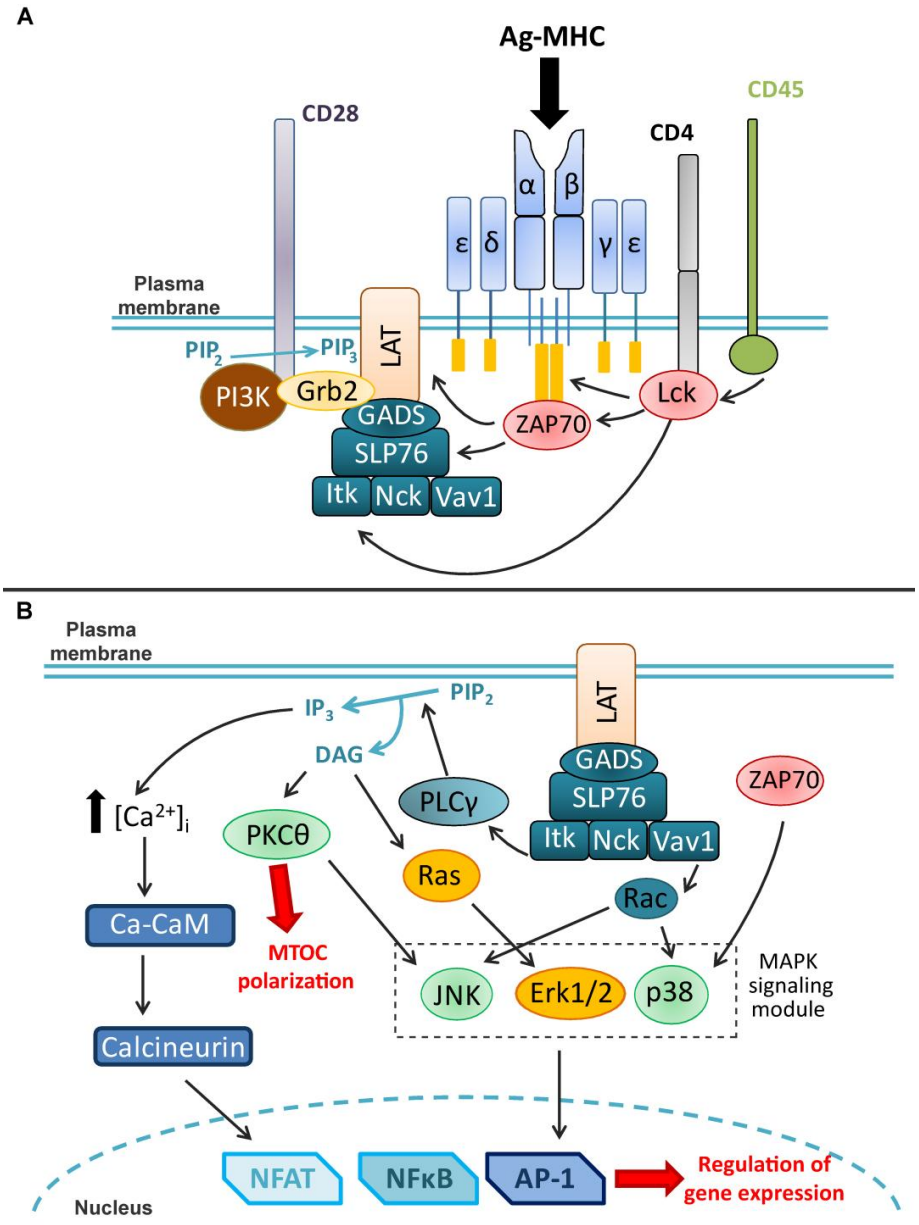

Figure I3. Signaling at the IS. The main signaling pathways induced downstream the TCR and costimulatory molecules are schematised. **A**. Initial steps of TCR and CD28 signaling leading to formation of a molecular complex around LAT and Itk activation. **B.** Signaling events downstream LAT/Itk leading to regulation gene expression and MTOC polarization. **(A** to **B)** Grey arrows indicate activation. Light blue arrows indicate phosphoinositide modifications. Red arrows indicate induction of cellular processes.

As mentioned before, the integrin LFA-1 expressed on the T cell surface binds its ligand intercellular adhesion molecule 1 (ICAM-1) on the APC, providing adhesive forces that stabilize the IS. In addition, LFA-1 acts as a costimulatory molecule by activating SLP76 (46), inducing signaling trough Erk1/2 (47) and PI3K (48), and contributing to AP-1 transcriptional regulation (49).

2.3 Regulation of actin polymerization at the IS

Actin polymerization at the IS is regulated by several signaling pathways that converge from the TCR, the costimulatory molecules, and integrins. The GEF Vav1, present at signalling complexes downstream the TCR, CD28 and LFA-I, activates the Rho family GTPases CDC42 and Rac1, that, in turn, activate the actin nucleation factors WASp (Wiskott Aldrich syndrome protein) and Wave2, respectively (48, 50) (Figure I4). Indeed, both proteins have been shown to be recruited to the IS (51), where Wave2 is important for lamellipodium formation (52). Together with the hematopoietic lineage cell-specific protein 1 (HS1), which is phosphorylated downstream TCR signaling (53), WASp and Wave2 promote actin polymerization through actin-related protein 2/3 (ARP2/3) complex (54, 55) (Figure I4). However, proper actin depolymerization is also required to maintain actin dynamics at the IS. The protein cofilin severs actin filaments and depolymerizes F-actin, providing new barbed ends that serve as substrates for elongation factors (56). It has been shown that cofilin activity is required for proper IS formation and T cell activation (57). Cofilin is activated upon T cell stimulation downstream Ras and PI3K (58), in a mechanism that could also involve the phosphatase Slingshot 1 (SSH1), which specifically dephosphorylates cofilin (59, 60) (Figure I4). Cofilin activation is counteracted by LIM kinase (LIMK), which inhibits cofilin by phosphorylation (61) downstream the small GTPase RhoA and the Rho-associated protein kinase (ROCK) (62) (Figure I4). Hence, a highly regulated balance between actin polymerization and depolymerization has to be maintained for proper T cell signalling progression and T cell stimulation.

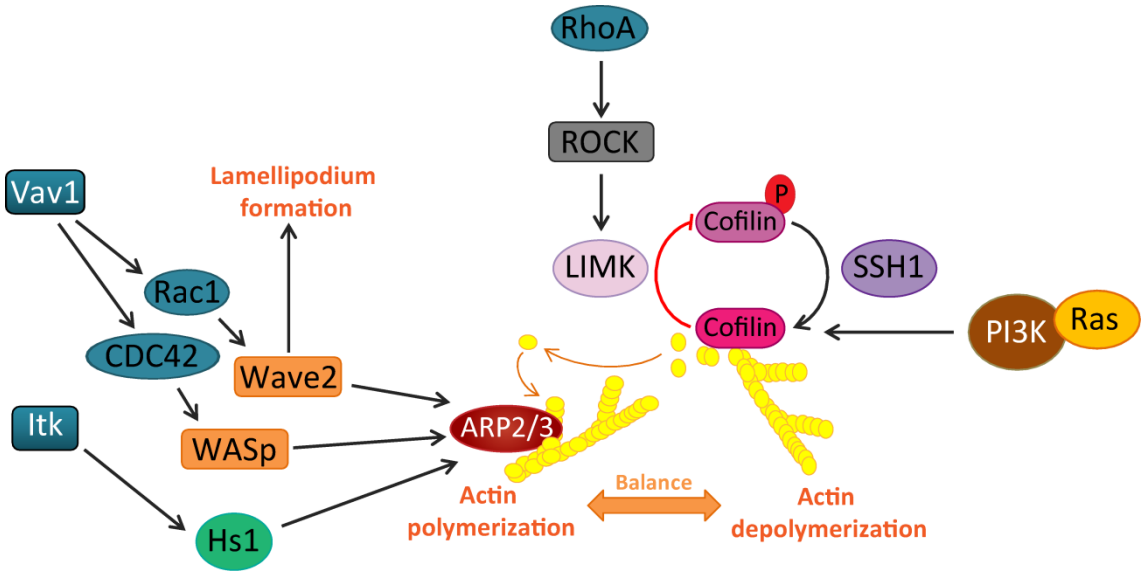

Figure I4. Regulation of actin dynamics at the IS. The main signaling pathways regulating actin dynamics at the IS are schematised. Grey arrows indicate activation. Red line indicates inhibition. Orange arrows indicate dynamics of actin.

3. Subsets of effector Th cells

Upon antigen recognition, naïve CD4 T cells differentiate into effector Th cells, which will be able to respond faster and with higher magnitude in subsequent stimulations by APCs. At least four effector Th subsets or lineages have been described: Th1, Th2, Th17 and Treg (Figure I5) (7). Differentiation into (or polarization to) one of these subsets is initiated by signaling of cytokines present in the environment at the moment of antigen presentation and stabilized by a lineage-specifying transcription factor through epigenetic mechanisms (1). Once differentiated, each Th subset will produce distinct signature cytokines and exert different effector functions (Figure I5). Although the factors driving polarization to each Th subset are well known (7), the structure and dynamics of the underlying molecular networks remain to be fully elucidated. The four main Th subsets are briefly described below.

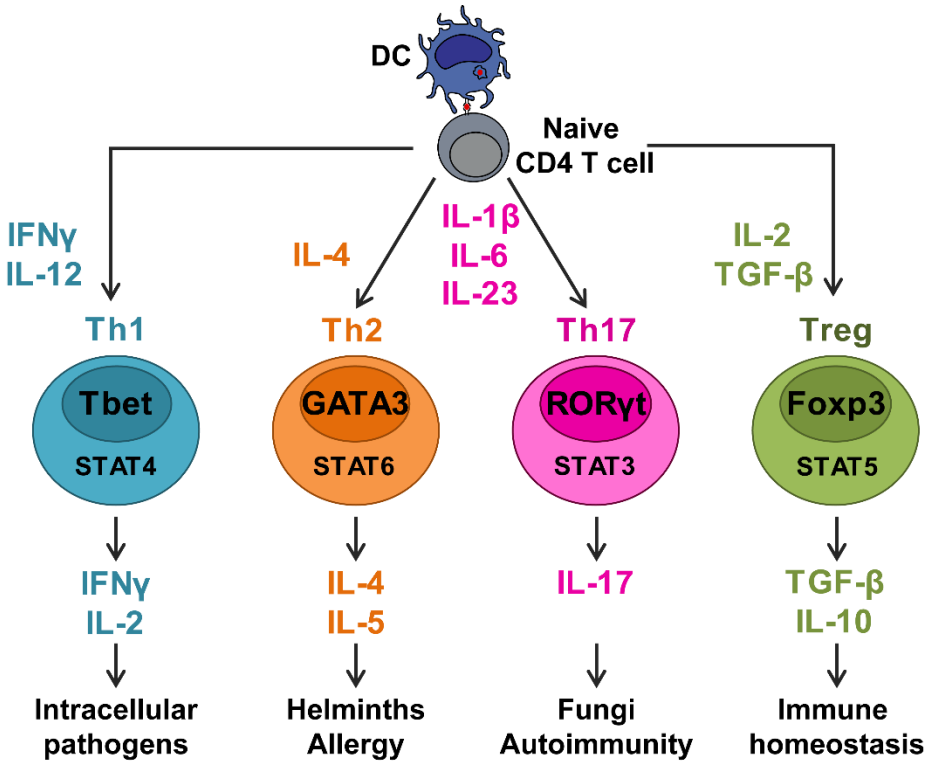

Figure I5. Th subsets. The four main subsets of Th cells and the cytokines driving their differentiation are shown in the upper part. The main transcription factor and STAT protein involved in each subset commitment are depicted inside each Th cell. The cytokines produced and the physiological function of each subtype are shown in the lower part of the scheme.

3.1 Th1 and Th2

Th1 cells produce interferon γ (IFNγ) and IL-2, and mediate immune responses against intracellular pathogens (7). Th1 polarization is initiated by the cytokine IL-12 through activation of the transcription factor signal transducer and activator of transcription (STAT) 4, and amplified by IFNγ-mediated activation of STAT1. These pathways converge in the induction of the master regulator of Th1 polarization, the transcription factor Tbet (63, 64).

Th2 cells produce IL-4, which induces B cell switching to IgE production, and IL-5, which recruits eosinophils (7). Hence, Th2 responses are predominant in allergy and helminthic infections (65). Th2 polarization is promoted by IL-4 through activation of STAT6 (66), which induces the master regulator of Th2 differentiation, GATA-binding protein 3 (GATA3) (67). Th2 polarization has also been shown to be promoted by antigens with weak affinity, which seem to induce GATA3 activation and IL-4 production (68, 69).

The distribution of cytokine receptors during the IS has been proposed to be a mechanism for controlling Th1 and Th2 differentiation. It has been reported that in absence of exogenous cytokines the IFNγ receptor (IFNγ-R) is recruited to the IS in naïve cells upon TCR activation, while IL-4 receptor is not. By contrast, when IL-4 was added during TCR stimulation, IFNγ-R recruitment was blocked in a STAT6-dependent manner (70). In addition, phosphorylated (active) STAT1 was corecruited with the TCR and the IFNγ-R at the IS in absence of IL-4 (71). Hence, the differential recruitment of cytokine receptor to the IS would determine the predominant cytokine signals received by the T cell during antigenic stimulation and, consequently, Th1/Th2 commitment. These findings highlight the importance of spatial regulation at the IS in determining T cell responses. In addition, these evidences also suggest that naïve CD4 T cells are prone to differentiate to Th1 cells instead of the other Th phenotypes, a notion supported by other groups (72).

3.2 Th17

Th17 cells produce IL-17, which triggers neutrophil recruitment, being important in the defense against fungi (7). IL-17 also triggers inflammation, and has a pathogenic role in autoimmunity (73). Th17 cells differentiate in presence of IL-1β, IL-6 and IL-23 (74), which signal through STAT3 to induce IL-17 production (75). Some groups have reported that transforming growth factor β (TGF-β) is also required for Th17 cell polarization (76), although other studies sustain that it is not (74). The master regulator of Th17 cells is the RAR-related orphan receptor γt (RORγt) (77).

3.3 Treg

T regulatory (Treg) cells produce IL-10 and TGF-β, and exert anti-inflammatory functions (78). Treg cells differentiate in presence of IL-2 and TGF-β (7), which induces the expression of the master regulator of Treg differentiation, the transcription factor Forkhead box P3 (Foxp3) (79, 80). The action of STAT5 is also required for Foxp3 expression (81). In addition, strong TCR signals have been shown to inhibit Foxp3 and as a consequence Treg differentiation (82).

4. Protein tyrosine phosphatases

As explained in the preceding sections, signaling downstream the TCR and costimulatory molecules occurs through a cascade of phosphorylation events that is tightly regulated by kinases and phosphatases. In fact, treatment of Jurkat cells with pervanadate, a potent inhibitor of protein tyrosine phosphatases (PTPs) (83), results in induction of proximal TCR signaling and production of IL-2, mimicking TCR crosslinking (84). Hence, the experiments with pervanadate show that, in general, tyrosine phosphatases are important for maintaining T cells in the resting state in absence of antigenic stimulation. This does not mean, however, that all the tyrosine phosphatases are negative regulators of signaling downstream the TCR. In fact, some PTPs such as CD45 are required for T cell activation (85), while others such as the low-molecular-weight PTP (LMPTP) positively regulate signaling downstream the TCR (86). T cells express a high number of the more than a hundred PTPs present in the human genome (87, 88), but the role of the majority of them during T cell stimulation and IS assembly has not been addressed.

4.1 Classification of the PTP superfamily

In humans there are 107 genes that encode members of the PTP superfamily, based on their conserved catalytic motifs and PTP domains (87). It is important to note that a large number of the so-called PTPs are able to dephosphorylate serine (Ser) and threonine (Thr) in addition to tyrosine (Tyr) residues, while others can dephosphorylate messenger ribonucleic acid (mRNA) or phospholipids. Besides, there are catalytically inactive PTPs that exert functions non-dependent on dephosphorylation (89-91). Hence, the PTP superfamily includes members with different substrate specificities that can regulate a broad range of cellular processes. In addition, the members of the PTP superfamily are heterogeneous in their subcellular localization, ranging from transmembrane receptor-like proteins, to enzymes localized in cytosolic, endosomal, and nuclear compartments. PTPs can be classified in four classes based on the sequences of their catalytic domains (Figure I6). Class I, II and III PTPs base their catalytic mechanism in a residue of cysteine (Cys), while the catalytic residue in Class IV is an aspartic acid (Asp). The four classes have evolved independently, and Class II and III seem to be more ancient than class I, having evolved from bacterial enzymes. Class I is the largest, with 99 members, and can be further divided in two groups: classical PTPs, which are specific for Tyr residues, and dual specific phosphatases (DSPs), able to dephosphorylate a wide range of

substrates. Classes II, III and IV, in contrast, consist of 1, 3 and 4 members, respectively (Figure I6). Here we will refer DSPs and PTPs from classes II, III and IV as non classical (NC) PTPs.

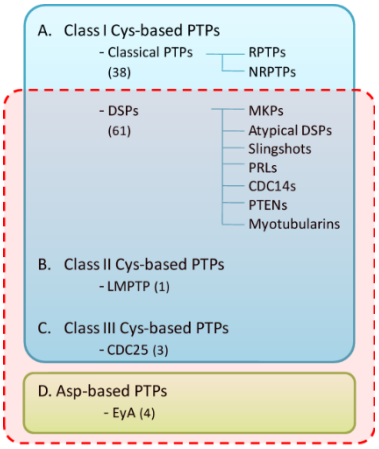

Figure I6. Classification of the PTP superfamily into four classes. The numbers in brackets indicate the number of PTPs in each subgroup. Figure based on Alonso *et al* (87).

4.1.1 Classical PTPs

The group of classical PTPs, formed by 38 members, is a well-known group of enzymes specific for Tyr residues. It can be divided in two subgroups, the receptor type PTPs (RPTPs), such as CD45, which have a transmembrane domain, and the nonreceptor PTPs (NRPTPs), which are intracellular.

4.1.2 DSPs

The group of DSPs is the more diverse in terms of substrate specificity and its 61 members can be further divided in seven subgroups:

- MAP kinase phosphatases (MKPs): these enzymes have specific MAPK targeting motifs, and can dephosphorylate both Tyr and Thr residues. There are ten catalytically active MKPs in humans: the ERK-selective cytoplasmic DUSP6, DUSP7 and DUSP9, the JNK/p38-selective DUSP8, DUSP10 and DUSP16, and the nuclear DUSP1, DUSP2, DUSP4 and DUSP5, which also dephosphorylate ERK. In addition, the phosphatase dead (PD) MK-STYX is also classified in this group (92).
- Atypical DSPs: the nineteen enzymes that form this group lack specific MAPK targeting motifs and can dephosphorylate either Tyr or Thr residues, with the exception of PIR1, which dephosphorylates mRNA (93), Laforin, which dephosphorylates glycogen (94), the mRNA capping enzyme RNGTT, and the PD STYX.

- Slingshots (SSHs): this group includes three enzymes (SSH1, SSH2 and SSH3), that dephosphorylate and consequently activate cofilin in Ser, and that have actin-bundling activity (60).
- Phosphatases of regenerating liver (PRLs): this group includes three enzimes (PRL-1, PRL-2 and PRL-3, enconded by the genes PTP4A1, PTP4A2 and PTP4A3, respectively) with unknown substrates that have been implicated in cancer progression (95).
- Cell division cycle-14 proteins (CDC14s): the members of this group (CDC14A, CDC14B and CDKN3) inactivate cyclin-dependent kinases (CDKs) to induce mitotic exit and are also involved in mitotic spindle formation (96, 97).
- Phosphatase and tensin homologs (PTENs): this group is formed by five members, four of which are active phosphatases that dephosphorylate the position 3 of phosphoinositides (98).
- Myotubularins (MTMs): the members of this group dephosphorylate the position 3 of PI3P and PI(3,5)P_2 (98). Among the sixteen members of this group, nine are catalytically active, while the other seven are thought to be PD enzimes that bind to the active members of the group, regulating their activity (91).

4.1.3 Class II Cys-based PTPs

This class is composed by only one member, LMPTP, encoded by the gene ACP1. LMPTP is able to dephosphorylate Tyr residues, but not Ser o Thr (99), and in T cells has been described to dephosphorylate ZAP70 (86) and focal-adhesion kinase (FAK) (100).

4.1.4 Class III Cys-based PTPs

This group is formed by the three cell division cycle-25 proteins (CDC25s): CDC25A, CDC25B and CDC25C, that dephosphorylate cyclin-dependent kinases (CDKs) in Tyr and Thr residues, promoting entry into mitosis (101).

4.1.5 Asp-based PTPs

The eyes absent (Eya) phosphatases that form this class have the peculiarity of using an Asp as catalytic residue to dephosphorylate their substrates in Tyr (102, 103). Eya phosphatases are encoded by four genes in humans (Eya1, Eya2, Eya3 and Eya4) and act as transcriptional regulators during organogenesis (103, 104).

4.2 PRLs

The first PRL identified was PRL-1, and was given its name because it was found as a gene induced in rats upon hepatectomy (105, 106). Mouse PRL-2 and PRL-3 were identified later as proteins with high homology to PRL-1 (107). The most relevant features of PRLs will be outlined below.

4.2.1 Structure, regulation and substrate specificity

The PRLs are relatively small proteins of around 19 KDa, although according to the *Gene* database (NCBI), smaller isoforms of PRL-2 and PRL-3 exist in humans. Considering the full-length isoform, the aminoacid identity between the three human PRLs is very high (Figure I7): 87% between PRL-1 and PRL-2, 79% between PRL-1 and PRL-3, and 76% between PRL-2 and PRL-3 (95). The motifs of the PRLs and their localization are highlighted in the sequences shown in Figure I7.

The PTP domain contains the active site, which shares the common PTP signature motif (I/V)HCXXGXXR(S/T) (108). This sequence contains the catalytic Cys (Cys 104 in PRL-1 and PRL-3, Cys 101 in PRL-2), which exerts a nucleophilic attack to the phosphate group on the substrate creating a cysteinyl-phosphate intermediate (109). Release of the dephosphorylated substrate requires the participation of an Asp (Asp 72 in PRL-1 and PRL-3, Asp 69 in PRL-2), situated in the adjacent WPD loop (110). Unlike other PTPs, however, PRLs have an Alanine instead of the Ser/Thr at the end of the active site, and this difference might be the cause of the low activity of PRLs *in vitro* (110, 111). Next to the PTP domain is found a polybasic region (Figure I7) that has been reported to contribute to localization of PRL-1 at the inner face of the plasma membrane (112). Finally, the CAAX motif situated in the C-terminal region of the PRLs provides a signal for farnesylation on the first Cys (113) that is required for subcellular distribution of PRLs at the plasma membrane and endosomes (112, 114-116). It has been reported that the second Cys of the CAAX motif of PRL-3 can be palmitoylated, a modification that could reversibly regulate the subcellular distribution of the molecule (117). Whether palmitoylation also takes place in PRL-1 and PRL-2 remains to be determined.

Redox regulation of these proteins has been proposed (118), and for PRL-1, reversible oxidation of the catalytic Cys has been shown to inactivate the protein in mammalian retina (119). Another mechanism for regulation of PRL localization and activity might be the

formation of trimers, as shown for PRL-1 (Figure I7B) (112, 120). The structure of the trimer positions the CAAX motif of each monomer in the upper side of the trimer, allowing for binding to membranes, while the regions involved in catalysis (the WPD loop and the catalytic motif) remain at the outer face of the trimer, leaving space for substrate binding in each monomer.

A

```
                                                                  WPD loop                                                                  Catalytic motif
PRL-1           MARMNRPAPVEVTYKNMRFLITHNPTNATLNKFIEELKKYGVTTIVRVCEATYDTTLVEK   60
PRL-2           ---MNRPAPVEISYENMRFLITHNPTNATLNKFTEELKKYGVTTLVRVCDATYDKAPVEK   57
PRL-3           MARMNRPAPVEVSYKHMRFLITHNPTNATLSTFIEDLKKYGATTVVRVCEVTYDKTPLEK   60
                   ********  *  **************  * * ***** ** ****  ***    **

                                                                  WPD loop                                                                  Catalytic motif
PRL-1           EGIHVLDWPFDDGAPPSNQIVDDWLSLVKIKFREEPGCCIAVHCVAGLGRAPVLVALALI   120
PRL-2           EGIHVLDWPFDDGAPPPNQIVDDWLNLLKTKFREEPGCCVAVHCVAGLGRAPVLVALALI   117
PRL-3           DGITVVDWPFDDGAPPPGKVVEDWLSLVKAKFCEAPGSCVAVHCVAGLGRAPVLVALALI   120
                 ** * **********    * *** * * ** * ** * ********************

                                                Polybasic region                                                                  CAAX motif
PRL-1           EGGMKYEDAVQFIRQKRRGAFNSKQLLYLEKYRPKMRLRFKDSNGHRNNCCIQ          173
PRL-2           ECGMKYEDAVQFIRQKRRGAFNSKQLLYLEKYRPKMRLRFRDTNGH---CCVQ          167
PRL-3           ESGMKYEDAIQFIRQKRRGAINSKQLTYLEKYRPKQRLRFKDPHTHKTRCCVM          173
                * ******* ********** ***** ******** **** *   *    **
```

B

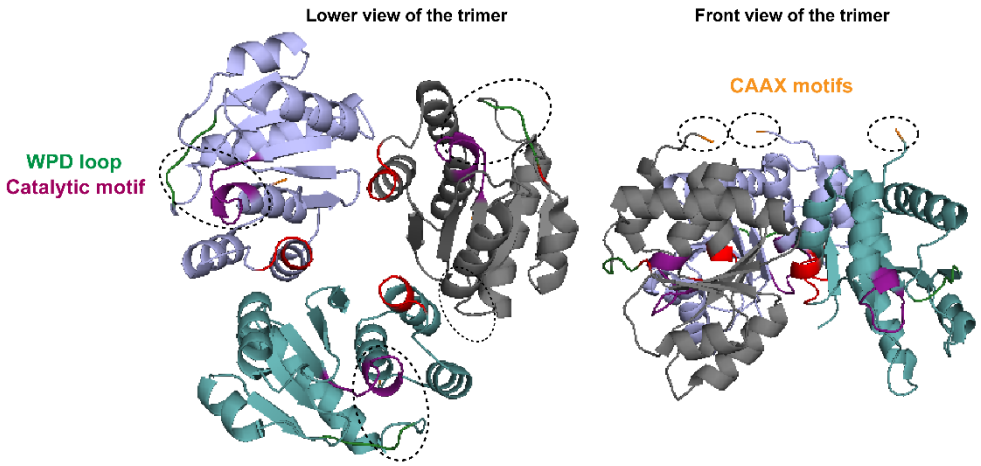

Figure I7. Structure of the PRLs. A. The alignment of the amino acid sequences of the three PRLs is shown. Motifs are highleted by squares. The number of the last aminoacid of each row is indicated on the righ. Asterisks indicate identic residues. The alignment was performed with the MAFFT version 7 software. **B.** Ribbon diagram of the tridimensional structure of the trimer formed by PRL-1 as described by Jeong and coworkers (120). In each monomer, the WPD loop (green), the catalytic motif (purple), the polybasic region (red) and the CAAX motif (yellow) are highlighted. Tridimensional structures were obtained from the Protein Data Bank and represented using Pymol software.

The substrates of the PRLs are currently unknown (95), and the study of their structure has not provided clues of their substrate specificity. In fact, the phosphatases structurally most closely related to PRLs are PTEN, vaccinia H1-related phosphatase (VHR or DUSP3), and CDC14s, but, compared with them, PRLs lack regions important for substrate recognition (95, 120). In addition, these related phosphatases show different substrate specificities, ranging from

phosphoinositides (PTEN) (98), to Tyr (VHR) (121) and Ser/Thr (CDC14s) (122, 123). The only substrate proposed for PRL-1 is the activating transcription factor 7 (ATF-7), although interaction between the two proteins and dephosphorylation of ATF-7 by PRL-1 has been reported only *in vitro* (124). Regarding PRL-3, it has been proposed to dephosphorylate ezrin (125) and PI(4,5)P_2 (126), although further confirmation will be needed to identify these molecules as canonic substrates of PRL-3.

4.2.2 Expression

In normal adult tissues, PRL-1 and PRL-2 are ubiquitously expressed, showing detectable expression in a wide range of tissues and cell types, including lymph nodes, thymus, and peripheral blood lymphocytes (127, 128). However, their role in lymphocyte activation has not been addressed. PRL-3 mRNA is expressed mainly in normal skeletal muscle, heart, and pancreas (129), as well as in developing blood vessels and pre-erythrocytes (130). In the hematopoietic system, PRL-2 has the highest expression among PRLs, followed by PRL-1, while the expression of PRL-3 is very low (131). In addition, the three PRLs are upregulated in several cancer types. Both PRL-1 and PRL-2 have been shown to be overexpressed in cancer cell lines when compared with untransformed cells (114, 132). PRL-3, the most studied PRL in this regard, is upregulated in several cancer types, including breast, gastric, and ovarian carcinomas, where PRL-3 overexpression correlates with poor prognosis (133-135). Overexpression of PRLs has also been described in hematological malignancies (131). Hence, it was soon recognized that the three PRLs promote tumor progression, invasion, and metastasis.

4.2.3 PRLs in intracellular signaling and function

PRLs promote cell proliferation, migration and invasion, having oncogenic properties (136). Several signaling pathways and cellular processes have been shown to be affected by these proteins, some of which seem to explain their oncogenicity. Firstly, PRLs induce cell migration and invasion. In fact, knock down or inhibition of the catalytic activity of PRLs decreased p130Cas phosphorylation and protein levels in cancer cells, resulting in less anchorage-independent tumor cell growth (137). p130Cas is a scaffold protein that participates in migration and invasion downstream the oncogenic protein Src (138). Consistently, overexpression of PRL-1 increased Src and p130Cas phosphorylation in HEK-293 cells (139).

Secondly, PRLs promote cell survival and proliferation through several signaling pathways. The three PRLs have been shown to induce ERK1/2 activation in cancer cells (132, 139, 140), although the mechanism remains to be determined. Interestingly, it has been proposed that PRL-1-mediated activation of ERK1/2 takes place through binding of PRL-1 to the MEKK1 inhibitor p115 RhoGAP (141). Whether PRL-2 and PRL-3 act through the same mechanism remains to be determined. In addition, PRL-3 induces PI3K/Akt signaling in cancer cell lines (142), an effect that might be mediated by downregulation of PTEN levels (143).

In physiological conditions, PRLs also seem to regulate cell proliferation. In fact, PRL-1 localizes to the centrosome and the mitotic spindle, where it regulates normal mitosis (114), while PRL-2 promotes cell proliferation in mouse placenta by activating the Akt kinase through downregulation of the tumor suppressor PTEN (144). Interestingly, PRL-2 seems to be important in the development of the hematopoietic system. Analysis of knockout mice for PRL-2 has shown that this PRL is required for hematopoietic stem cell self-renewal, since it promotes proliferation of hematopoietic stem cells (145). In addition, loss of PRL-2 decreases lymphocyte count in peripheral blood and blocks development of T lymphocytes at the double negative stage (131, 145). Recently, it has also been shown that PRL-2 is an effector of the Notch signaling pathway in T cell progenitors, being required for generation and maturation of T cells (146). These findings point to important roles of PRLs not only during cancer progression, but also in normal tissues.

Several findings suggest the PRLs might be involved in the organization of the actin cytoskeleton through regulation of Rho GTPases. In fact, it has been shown that overexpression of PRL-1 or PRL-3 leads to inhibition of Rac and activation of RhoA and RhoC (116, 147), while silencing of PRL-1 decreases Rac and Cdc42 activation in cancer cells (148).

The reported role of PRLs as regulators of the actin cytoskeleton, together with the reported expression of PRL-1 and PRL-2 in lymphocytes, suggest that PRLs could be regulators of IS assembly and T cell signaling.

HYPOTHESIS AND OBJECTIVES

HYPOTHESIS AND OBJECTIVES

PTPs are key regulators of phosphorylation levels, which control T cell activation and differentiation. Although T cells express a high number of NC PTPs, the role of the majority of these enzymes in T cell activation and differentiation is unknown. Our hypothesis was that some NC PTPs are yet unknown regulators of T cell activation and differentiation. We payed particular attention to PRLs due to their regulatory role on actin dynamics reported in the literature.

The general aim of this work was to study the changes in the expression of NC PTPs during T cell responses and the role of the PRLs during IS assembly and T cell activation. To address this general aim, we posed the following specific objectives:

1. To study the changes in the expression profile of NC PTPs during Th1 differentiation and restimulation

2. To study the expression of PRLs during T cell activation

3. To study the contribution of the catalytic activity of PRLs to T cell activation

4. To study the delivery of PRL-1 to the IS

5. To study the contribution of PRL-1 to T cell activation and its regulatory role in IS assembly and signaling downstream the TCR

MATERIALS AND METHODS

MATERIALS AND METHODS

1. Materials

1.1 Reagents

Table MM1. Reagents

Product	Source
Agarose	Sigma-Aldrich
Analog 3	Enamine
AseI	New England Biolabs
Blocking reagent	Roche
Brefeldin A	Sigma-Aldrich
BsrGI	New England Biolabs
CellTracker™ Blue CMAC Dye	Molecular probes
Distilled water	Gibco
DMEM w/o phenol red	Lonza
Dynabeads Human T-Activator CD3/CD28	Gibco
E Superantigen (SEE)	Toxin Technology
EDTA	Panreac
Fetal Calf Serum (FCS)	Gibco
Hepes	Gibco
Homology arms (HA DNA)	IDT
Human IgG	Sigma-Aldrich
ICAM-Fc	Carlos Cabañas, PhD
ImmunoCult™ Human CD3/CD28 T Cell Activator	StemCell technologies
Ionomycin	Sigma-Aldrich
L-Glutamine	Lonza
Latex beads	Sigma-Aldrich
Lymphoprep™	Rafer
MluI	New England Biolabs
Mouse serum	Sigma-Aldrich
NheI	New England Biolabs
Non-essential aminoacids	Gibco
Paraformaldehyde	Sigma-Aldrich
PCR Nucleotide Mix	Roche
PCR Reaction Buffer, 10X	Roche
Penicillin 10000 U/mL-Streptomycin 10000 µg/mL	Lonza
Phalloidin-488	Molecular Probes
Phosphate buffered saline (PBS)	Gibco
Phorbol 12-myristate 13-acetate	Sigma-Aldrich
Pierce™ ECL Plus Substrate	Thermo Scientific
Poly-L-Lysine	Sigma-Aldrich
Procyanidin B3 (PB3)	ChemFaces
Recombinant human IL-12	Preprotech
RPMI 1640	Lonza

Table MM1. Reagents (continuation)	
Product	**Source**
Saponin	Sigma-Aldrich
Sodium pyruvate	Gibco
SpeI	New England Biolabs
Taq DNA polymerase	Roche
Taqman® gene expression master mix	Applied Biosystems
Thienopyridone (TP)	Enamine
TMB	Calbiochem
Triton X-100	Sigma-Aldrich
Trizma® base	Sigma-Aldrich
T4 DNA Ligase	New England Biolabs
U0126	Cell Signaling
XhoI	New England Biolabs

1.2 Kits

Table MM2. Kits	
Product	**Source**
Amersham Cy3 mAb Labelling Kit	GE Healthcare
Amaxa™ Human T Cell Nucleofector™ Kit	Lonza
Amaxa™ Cell Line Nucleofector™ Kit V	Lonza
Dynabeas™ untouched™ Human CD4 T cells kit	Invitrogen
Human IL-2 ELISA Set	BD OptiEA
Naïve CD4+ T cell Isolation Kit II	Miltenyi
Absolutely RNA Microprep Kit	Agilent Technologies
Illustra™ DNA Extraction Kit BACC2	GE Healthcare
QIAquick Gel Extraction Kit	QIAGen

1.3 Primers

1.3.1 Primers for PCR (Sigma-Aldrich)

Table MM3. Primers for PCR			
Target	**Application**	**Sequence Forward (5'-3')**	**Sequence Reverse (5'-3')**
5'HA-GFP	Amplification	AAAGAAAACAACTATCGAAAGGG	GGTGCAGATGAACTTCAGGGTC
GFP-3'HA	Amplification	TCAAGGTGAACTTCAAGATCCG	TGAGATCATGCCACTGCACTC
5'HA-GFP	Sequencing	CAAAAATGTAACAATGGGTTTGG	GCTGAACTTGTGGCCGTTTACG
GFP-3'HA	Sequencing	GACAACCACTACCTGAGCACCC	GACAGAACGAGACTCCATCTC

1.3.2 TaqMan assays for qPCR and Low-Density Arrays (Applied Biosystems)

Table MM4. TaqMan assays

Target		Assay number	Target		Assay number
Gene	Protein		*Gene*	Protein	
CDC14A	CDC14A	Hs00186432_m1	*MTMR4*	MTMR4	Hs00608314_m1
CDC14B	CDC14B	Hs00372920_m1	*MTMR5*	SBF1	Hs00959744_g1
CDC25A	CDC25A	Hs00947994_m1	*MTMR6*	MTMR6	Hs00395064_m1
CDC25B	CDC25B	Hs00244740_m1	*MTMR7*	MTMR7	Hs00952738_m1
CDC25C	CDC25C	Hs00156411_m1	*MTMR8*	MTMR8	Hs00250307_m1
CDKN3	KAP	Hs00193192_m1	*MTMR9*	MTMR9	Hs00209995_m1
CD69	CD69	Hs00934033_m1	*MTMR10*	MTMR10	Hs01107504_m1
DUSP1	MKP1	Hs00610256_g1	*MTMR11*	MTMR11	Hs00916722_m1
DUSP2	PAC-1	Hs01091226_g1	*MTMR12*	MTMR12	Hs00539666_m1
DUSP3	VHR	Hs01115776_m1	*MTMR13*	SBF2	Hs00293588_m1
DUSP4	MKP-2	Hs01027785_m1	*MTMR14*	MTMR14	Hs00560430_m1
DUSP5	DUSP5	Hs00244839_m1	*MTMR15*	MTMR15	Hs00429686_m1
DUSP6	MKP-3	Hs04329643_s1	*PTEN*	PTEN	Hs02621230_s1
DUSP7	MKP-X	Hs00997002_m1	*PTPDC1*	PTPDC1	Hs01115183_m1
DUSP8	DUSP8	Hs00792712_g1	*PTPN1*	PTP1B	Hs00942477_m1
DUSP9	MKP-4	Hs01046584_g1	*PTPN2*	TCPTP	Hs00959886_g1
DUSP10	MKP-5	Hs00200527_m1	*PTPN4*	PTP-MEG1	Hs00267762_m1
DUSP11	PIR1	Hs01061375_m1	*PTPN6*	SHP1	Hs00169359_m1
DUSP12	DUSP12	Hs00170898_m1	*PTPN7*	HePTP	Hs00978680_m1
DUSP13	DUSP13	Hs00969203_m1	*PTPN9*	PTP-MEG2	Hs00361739_m1
DUSP14	MKP-6	Hs01877076_s1	*PTPN12*	PTP-PEST	Hs00184747_m1
DUSP15	VHY	Hs01566654_m1	*PTPN13*	PTP-BAS	Hs01106214_m1
DUSP16	MKP-7	Hs00411837_m1	*PTPN18*	PTP20	Hs01079757_g1
DUSP18	DUSP20	Hs01036622_g1	*PTPN22*	LYP	Hs01587518_m1
DUSP19	DUSP17	Hs00369901_m1	*PTPRA*	RPTPα	Hs00160751_m1
DUSP21	DUSP21	Hs00254403_s1	*PTPRC*	CD45	Hs04189704_m1
DUSP22	VHX	Hs00414885_m1	*PTPRJ*	CD148	Hs01119326_m1
DUSP23	DUSP23	Hs00367783_m1	*PTPRK*	RPTPκ	Hs00267788_m1
DUSP26	VHP	Hs00225167_m1	*PTP4A1*	PRL-1	Hs00743856_s1
DUSP27	DUSP27	Hs01367756_m1	*PTP4A2*	PRL-2	Hs00754750_s1
EPM2A	Laforin	Hs00194655_m1	*PTP4A3*	PRL-3	Hs02341135_m1
EYA1	Eya1	Hs00166804_m1	*RNGTT*	RNGTT	Hs01016926_m1
EYA2	Eya2	Hs00193347_m1	*SSH1*	SSH1	Hs00368014_m1
EYA3	Eya3	Hs00544914_m1	*SSH2*	SSH2	Hs00810681_m1
EYA4	Eya4	Hs00187965_m1	*SSH3*	SSH3	Hs00215309_m1
GATA3	GATA3	Hs00231122_m1	*STYX*	STYX	Hs00377042_m1
GNB2L1	GNB2L1	Hs00272002_m1	*Tbet*	TBX21	Hs00203436_m1
IL-2	IL-2	Hs00174114_m1	*TENC1*	TENC1	Hs00539247_m1
MK-STYX	MK-STYX	Hs01555207_m1	*TNS1*	Tensin	Hs00917032_m1
MTM1	MTM1	Hs00896978_m1	*TPTE*	PTEN2	Hs04186747_m1
MTMR1	MTMR1	Hs00395009_m1	*TPIP*	TPIPα	Hs01685756_m1
MTMR2	MTMR2	Hs01547438_m1	*18S*		Hs99999901_s1
MTMR3	MTMR3	Hs00221562_m1			

1.4 Plasmids

Table MM5. Plasmids	
Plasmid	**Source**
β-Actin speckle	Miguel Vicente-Manzanares, PhD (HUP)
CD3ζ-mCherry	Balbino Alarcón, PhD. (CBMSO)
GFP C1 (GFP)	Clontek
GFP-PRL-1	Rocío Ramírez, MSc (UCM)
GFP-PRL-1-ΔCAAX	Rocío Ramírez, MSc (UCM)
GFP-PRL-3	Patricia Castro, MSc (UCM)
mCitrine-PRL-1 (mCit-PRL-1)	Max Planck Institute
mCitrine-PRL-2 (mCit-PRL-2)	Max Planck Institute
LifeAct RFP	Ibidi
LV C9	Raúl Torres, PhD (CNIO)
YFP	Clontek

CBMSO, Centro de Biología Molecular Severo Ocha. CNIO, Centro Nacional de Investigaciones Oncológicas. HUP, Hospital Universitario de la Princesa. UCM, Universidad Complutense de Madrid.

1.5 Antibodies

1.5.1 Primary antibodies

Table MM6. Primary antibodies					
Antigen	**Fluorophore**	**Clone**	**Host**	**Application**	**Source**
α Tubulin	---	DM1A	Mouse	WB	Sigma-Aldrich
α Tubulin	FITC		Mouse	IF	Molecular Probes
CD3ε	APC	HIT3a	Mouse	FC	BD Pharmingen
CD3ε	---	T3b	Mouse	IF	Francisco Sánchez-Madrid, PhD
CD3ε	---	UCHT1	Mouse	Stimulation	Purified from hybridome
CD3ζ	---	448	Rabbit	IF	Balbino Alarcón, PhD
CD4	PE	13B8.2	Mouse	FC	Beckman Coulter
CD19	PerCP	A3-B1	Mouse	FC	Immunostep
CD28	---	CD28.2	Mouse	Stimulation	BD Pharmingen
CD45RA	FITC	ALB11	Mouse	FC	Beckman-Coulter
CD69	APC	CH/4	Mouse	FC	Molecular Probes
ERK1/2	---	L34F12	Mouse	WB	Cell Signaling
ERK1/2-pT202/Y204	---		Rabbit	WB	Cell Signaling
GFP	---	Polyclonal	Rabbit	FC/WB	Life Technologies
IFNγ	FITC	B27	Mouse	FC	BD Pharmingen
PLCγ	---	Polyclonal	Rabbit	WB	Cell Signaling
PLCγ-pY783	---	Polyclonal	Rabbit	WB	Cell Signaling
PRL-1	---/Cy3	---	Mouse	FC/WB	Qi Zeng, PhD
PRL-1/2	---	42	Mouse	WB	Merck

APC, allophycocyanin. FC, flow cytometry. FITC, fluorescein. IF, immunofluorescence. PE, phycoerythrin. PerCP, peridinin chlorophyll protein. WB, western blot.

1.5.1 Isotype controls

Table MM7. Isotype controls

Fluorophore	Clone	Host	Application	Source
---	MOPC	Mouse	IF/FC	Sigma-Aldrich
APC	B11/6	Mouse	FC	Immunostep
PerCP	MOPC-21	Mouse	FC	Immunostep

FC, flow cytometry. IF, immunofluorescence

1.5.2 Secondary antibodies

Table MM8. Secondary antibodies

Antibody	Conjugation	Application	Source
Donkey Anti-Mouse	Alexa Fluor 594	IF	Life Technologies
Donkey Anti-Rabbit	Alexa Fluor 488	IF	Life Technologies
Goat Anti-Mouse	APC	FC	Life Technologies
Goat Anti-Mouse	IRDye 680RD	WB	LICOR
Goat Anti-Rabbit	Alexa Fluor 594	IF	Life Technologies
Goat Anti-Rabbit	IRDye 800RD	WB	LICOR
Goat anti-Rabbit	HRP	WB	Merck

FC, flow cytometry. IF, immunofluorescence. WB, western blot

1.6 Buffers

Table MM9. Buffers

Buffer	Composition
Carbonate buffer	0,1 M $NaHCO_3$; 32 mM Na_2CO_3
IP Lysis buffer	10 mM Tris-HCl pH 7,5; 0,5% NP-40; 150 mM NaCl; 0,5 mM EDTA; 1X protease inhibitor cocktail; 10 mM NaF; 1 mM PMSF; 1 mM Na_3VO_4
RIPA buffer	20 mM Tris-HCl pH 7,5; 1% NP-40; 0,5% sodium deoxycholate; 0,1% SDS; 150 mM NaCl; 10 mM β-glicerophosphate; 1X protease inhibitor cocktail; 10 mM NaF; 1 mM PMSF; 1 mM Na_3VO_4
TBS	20 mM Tris-HCl pH 7,5; 150 m M NaCl
TNB	TBS + 0,5 % blocking reagent
WB Lysis buffer	20 mM Tris-HCl pH 7,5; 0.2% Triton X-100; 1% NP-40; 150 mM NaCl; 2mM EDTA; 1,5 mM $MgCl_2$; 10mM Glycerophosphate; 1X protease inhibitor cocktail; 1 mM Pyrophosphate; 1 mM NaF; 2 mM Na_3VO_4; 1 mM PMSF

1.7 Equipment

Table MM10. Equipment

Device	Manufacturer
AM TIRF MC M system	Leica
Amaxa™ Nucleofector™ II system	Lonza
Digital sonifier	Branson
DMI 6000B microscope	Leica
ELx800™ Absorbance Microplate Reader	BioTek
FACSAria III cell sorter	BD Biosciences
FacsCalibur flow cytometer	BD Biosciences
FV-1200 CLS microscope	Olympus
Neon™ transfection system	Invitrogen
7900HT Fast Real-Time PCR System	Applied Biosystems

2. Methods

2.1 Purification of primary cells

Peripheral blood from healthy adult donors (< 65 years old) was obtained from buffy coats processed at the transfusion centre of the "Comunidad de Madrid", Spain. Blood was diluted five times in phosphate-buffered saline (PBS) and peripheral blood mononuclear cells were obtained by centrifugation on Lymphoprep™ density gradient for 35 minutes at 600 g. After three washes with PBS, cells were counted and used for cell purification. Total CD4 T cells were isolated by negative selection using the Dynabeas™ untouched™ Human CD4 T cells kit. Naïve CD4 T cells were isolated by negative selection using the Naïve CD4+ T cell Isolation Kit II. Purities over 95% were typically obtained as assessed by flow cytometry.

2.2 In vitro Th1 polarization and restimulation

Naïve CD4 T cells were cultured for 12 days in RPMI 1640 supplemented with 10% fetal calf serum (FCS), 100 U/mL penicillin, 100 µg/mL streptomycin and 2mM L-Glutamine in presence of Dynabeads Human T-Activator CD3/CD28 and 10 ng/ml of IL-12. Th1 cells were then restimulated for 4 hours with 10 ng/mL phorbol 12-myristate 13-acetate (PMA) plus 1 µM Ionomycin (Th1-PI). Th1 polarization was assessed by analysing the induction of the master regulators *Tbet* and *GATA3* and the production of IFNγ in response to restimulation with PMA

and Ionomycin. For analysis of IFNγ production Th1 cells were restimulated in presence of 5 µg/mL Brefeldin A, and intracellular content of the cytokine was measured by flow cytometry.

2.3 Cell lines and culture

The B cell line Raji and the T cell line Jurkat clone J77 (149) were cultured in RPMI 1640 supplemented with 10% FCS, 2 mM L-Glutamine, 100 U/mL penicillin, 100 µg/ml streptomycin, 1 mM sodium pyruvate and 1x non-essential aminoacids.

2.4 Generation of knock in GFP-PRL-1 J77 cell line

The genome of Jurkat J77 cells was edited to generate a knock in cell line (KI) expressing a chimeric endogenous GFP-PRL-1 protein (where GFP is the green fluorescent protein), using the clustered regularly interspaced short palindromic repeats (CRISPR)/Cas9 technology (150-152). Two single guides (Sg) specific for PRL-1 gene targeting (Figure MM1A) were designed by Raúl Torres at Centro Nacional de Investigaciones Oncológicas (CNIO, Madrid, Spain) and cloned into the pLV C9 plasmid using restriction sites BsrGI and SpeI. This expression vector allows for the ectopic expression of the Cas9 endonuclease under the cytomegalovirus promoter and of the Sg RNA under the U6 promoter. The Sg RNA is complementary to a region of around 20 base pairs (bp) on the target gene, called protospacer. To allow Cas9 recognition, the protospacer has to be followed by a protospacer adjacent motif (PAM) with the NGG sequence (where N is any nucleotide and G is guanine). Hence, the Cas9 is recruited to the gene of interest, where it performs a double strand break (DSB) three nucleotides upstream the PAM. In the absence of a donor DNA (deoxyribonucleic acid), this DSB will be repaired by non homologous end joining, but if a donor DNA is provided, homologous recombination will take place. To promote homologous recombination we generated a donor DNA (Figure MM1B). The expression vector GFP C1 was digested with AseI and NheI restriction enzimes to eliminate the promoter region of the GFP gene. A 5' homology arm (5'HA) containing the 685 bp upstream the start codon of genomic PRL-1 was digested with AseI and NheI and inserted replacing the promoter region of GFP gene in the GFP C1 plasmid. Both the generated 5'HA-GFP plasmid and a 3' homology arm (3'HA), containing the 677 bp downstream the start codon of genomic PRL-1 were then digested with XhoI and MluI and ligated. The generated vector 5'HA-GFP-3'HA (Figure MM1B, right) allows for the insertion of the open reading frame of the GFP upstream of, and in phase with, PRL-1 gene. The resulting edited gene encodes an endogenous chimeric GFP-PRL-1 protein (Figure MM1B, left).

Jurkat J77 cells were electropored using Neon™ transfection system with the parameters: 1,325 v, 10 ms, 3 pulses. Transfected cells were maintained in culture until GFP-PRL-1 expression was detected by flow cytometry. Then, edited cells (GFP+) were sorted using a FACSAria III cell sorter.

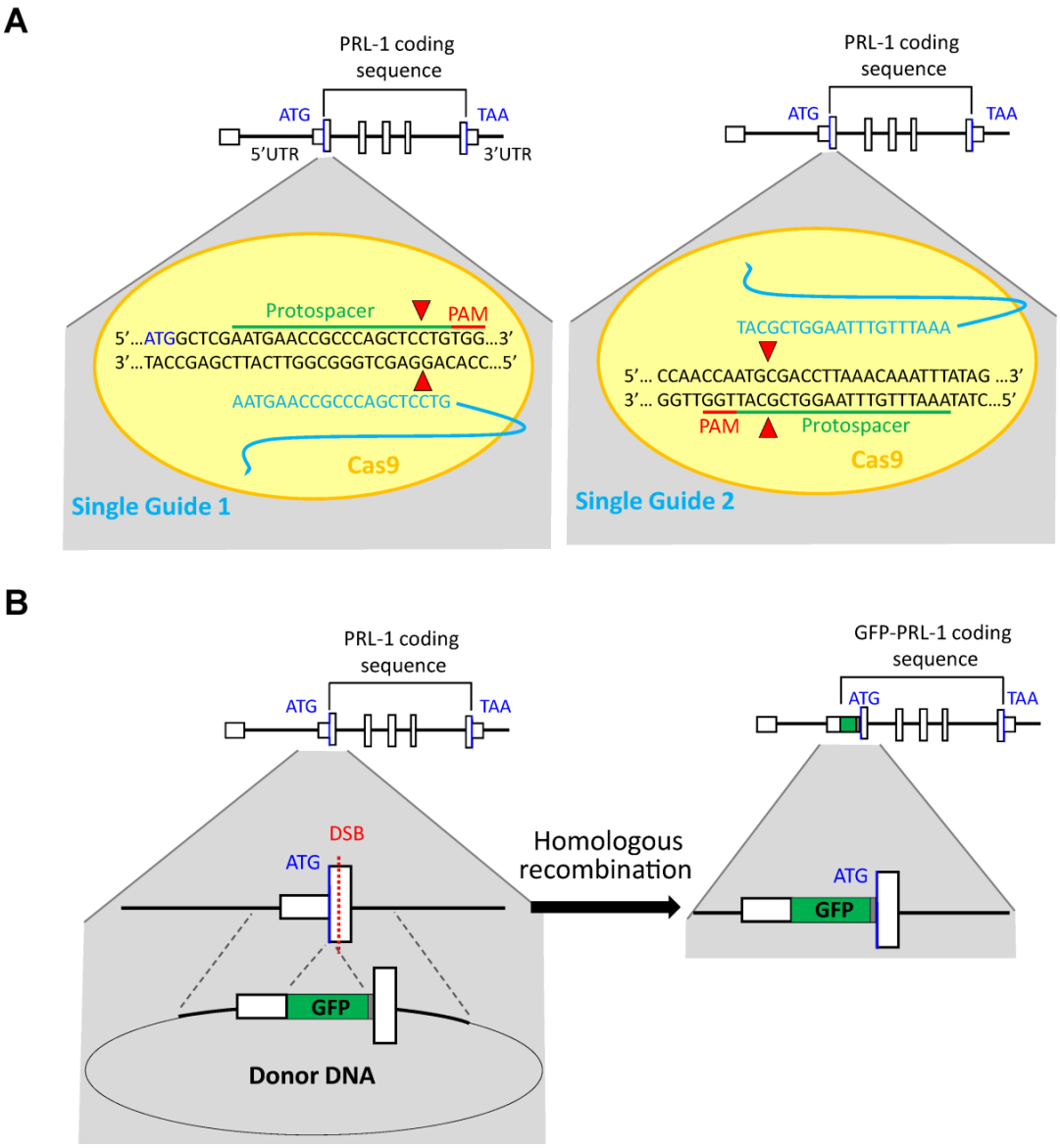

Figure MM1. Strategy for generation of a KI GFP-PRL-1 cell line. A. Two vectors carrying the gene coding for the Cas9 nuclease and one single guide each (Single Guide 1 or 2) were generated. Each Single guide was complementary to a sequence in the second exon of genomic PRL-1 (region called protospacer), followed by a PAM. Cas9 performs a DSB three nucleotides upstream the PAM (red arrowheads). **B**. After DSB, homologous recombination using the donor DNA takes place. As a result, the GFP cassette is inserted upstream the starting codon for PRL-1 (ATG), generating a GFP-PRL-1 coding sequence.

2.5 Cell transfection

Cells were nucleofected using the Amaxa™ Nucleofector™ II system. The Jurkat clone J77 was nucleofected using Amaxa™ Cell Line Nucleofector™ Kit V. Two million cells were nucleofected with 4 µg of plasmid using program X-001. Primary CD4 T cells were nucleofected using Amaxa™ Human T Cell Nucleofector™ Kit. 5-10 million cells were nucleofected with 5 µg of plasmid using program U-014. 24 hours after transfection, living cells were isolated by centrifugation on Lymphoprep™ before further experimental procedures.

2.6 Cell stimulation

For PRL-1 and PRL-2 expression studies, CD4 or Th1 cells were stimulated for 10, 30, 60, 120 and 240 minutes with 10 ng/mL PMA plus 1 µM Ionomycin.

For CD69 and IL-2 induction, J77 cells, transfected with either pOPIN N mCitrine-PRL-1 (mCit-PRL-1) or YFP, were mixed with Raji cells loaded or not with the indicated concentration of staphylococcal enterotoxin E superantigen (SEE), at a cell ratio 1:1. Mixtures were cultured O/N and stained for flow cytometry analysis. CD4 T cells were stimulated for 6h with Dynabeads™ Human T-Activator CD3/CD28 at a ratio 1:1. When specified, cells were preincubated for 1 hour with the indicated inhibitor before stimulation. The inhibitors used were Thienopyridone (TP, 20 µM), Analog 3 (A3, 75 µM), Procyanidin B3 (PB3, 12,5 to 75 µM) and U0126 (20 µM). The inhibitors were maintained during the whole stimulation time. Cells were then washed and stained for flow cytometry data acquisition. Supernatants of cell cultures were collected for analysis of IL-2 production by Enzyme-Linked Immunosorbent Assay (ELISA).

For Western Blot analysis, Raji cells were loaded with SEE (1 µg/mL), washed and mixed with J77 cells at 1:10 (RAJI:J77) ratio. Cell mixtures were incubated for 0, 5, 15 or 30 minutes at 37ºC. Primary CD4 T cells were stimulated with ImmunoCult™ Human CD3/CD28 T Cell Activator for the same time as J77 cells. When needed, cells were preincubated for 1 h with 50 µM PB3 which was maintained during the whole stimulation time.

2.7 Conjugation assays, immunofluorescence and microscopy

Raji cells were loaded or not with SEE at 1 µg/mL and labelled with 10 µM 7-amino-4-chloromethyl coumarin (CMAC) for one hour at 37ºC. After two washes Raji cells were mixed

with J77 cells at a 1:1 cell ratio, briefly centrifuged, and gently resuspended. 50 µL of such mixture was plated on each poly-L-Lysine-coated coverslip and cells were allowed to interact for 20 minutes at 37ºC.

For conjugates with primary cells, 100 µL of latex beads were coated with 900 µL of carbonate buffer containing 10 µg of anti-CD3ε (UCHT1) and 3 µg of anti-CD28 antibodies. As a negative control, beads were coated with 13 µg of isotype control (MOPC) in the same conditions. CD4 T cells were mixed with coated beads at 1:1 ratio and allowed to interact for 20 minutes at 37ºC. When specified, cells were preincubated for 1 hour with PB3 (25 µM), which was maintained during the whole conjugation time.

Both J77/Raji and CD4/bead conjugates were then fixed with 4% paraformaldehyde in PBS during 5 minutes at room temperature. When required, cells were then permeabilized with 0,1% Triton X-100. Conjugates were blocked with 1:100 human IgG before staining with the indicated antibodies. When staining CD4/bead conjugates, additional blocking with mouse serum was performed. Blocking reagents and antibodies were diluted in TNB buffer.

For live cell time-lapse confocal microscopy, J77 cells were attached to the bottom of LabTek chambered cover glasses coated with 20 µg/ml poly-L-Lysine. Then, Raji cells labelled with CMAC were added. Cells were imaged in DMEM without phenol red supplemented with 5% FCS and 25mM hepes buffer at 37ºC and 5% of CO_2.

Confocal microscopy was performed with a FV-1200 microscope (Olympus Deutschland GmbH, Germany). 405 nm (CMAC), 488 nm (GFP, Alexa488 and mCitrine), 559 nm (Cy3 and RFP) and 594 nm (Alexa594 and mCherry) lines were used. The elapsed time used in time-lapse assays is indicated for each experiment.

For total internal reflection fluorescence microscopy (TIRFM), cells were diluted in imaging medium (HBSS supplemented with 1% fetal bovine serum and 25 mM HEPES) and allowed to settle onto glass bottom dishes coated with ICAM-FC (10 µg/ml), anti-CD3ε (UCHT-1, 10 µg/mL) and anti-CD28 (3 µg/ml). Cells were immediately visualized with an AM TIRF MC M system mounted on a DMI 6000B microscope coupled to an Andor-DU8285_VP-4094 camera and fitted with a HCX PL APO 100.0x1.46 OIL objective. Images were processed with the accompanying confocal software. The laser penetrance used was 150 or 200 nm for both laser

channels (488 and 561 nm), using the same objective angle. Synchronization was performed with the accompanying Leica software.

Processing, analysis and quantification of fluorescence images were developed with FIJI free ware (NIH, USA). Polarization of molecules to the synapse was quantified using SynapseMeasures Plugin (153).

2.8 Flow cytometry

2.8.1 Intracellular staining

For each staining, 0,3x10^6 cells were washed with PBS, fixed with PBS + 4% paraformaldehyde for 20 minutes at 4ºC, permeabilized with PBS + 1% FCS + 0,1% saponin for 15 minutes at RT and stained with primary antibodies for 30 minutes at 4ºC. When required, cells were washed and incubated with a secondary antibody for 30 minutes. After two washes, cells were resuspended in PBS + 1 mM EDTA and flow cytometry data were collected using a FacsCalibur flow cytometer.

2.8.1 Extracellular staining

For each staining, 0,1-0,2x10^6 cells were washed with PBS and stained with the indicated antibodies for 30 minutes at 4ºC. Cells were then washed twice with PBS, resuspended in PBS + 1 mM EDTA and flow cytometry data were collected using a FacsCalibur flow cytometer. For analysing CD69 surface expression in J77/RAJI mixtures, CD19/CD69 double staining was performed and J77 cells were identified inside forward scatter/side scatter (FSC/SSC) cell gate by the negative staining for CD19 marker (Figure MM2). Flow cytometry data were analysed using the Flowjo software (Treestar, Inc.).

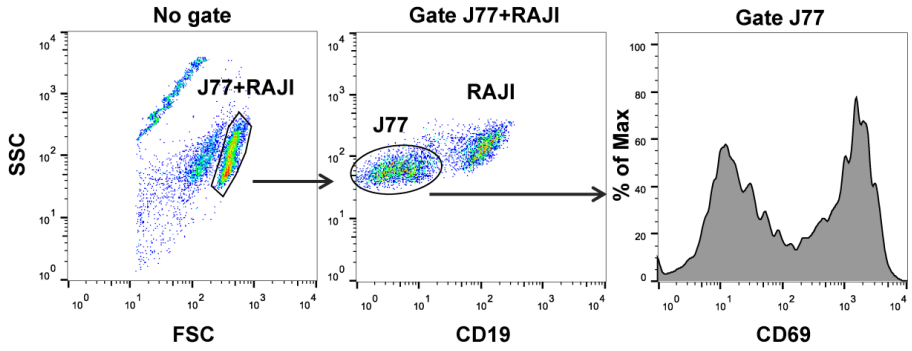

Figure MM2. Gating strategy. The gates performed to analyze CD69 expression in J77 cells stimulated with RAJI cells are shown. A representative histogram of CD69 staining in the J77 gate is shown on the right side.

2.9 PCR from genomic DNA

Genomic DNA from J77 cells was extracted with the Illustra^{TM} DNA Extraction Kit BACC2. PCR reactions were performed with 200 µM of each deoxynucleotide triphosphate (dNTP), 400 nM of each primer, 0,5 units of Taq polymerase and 250 ng of genomic DNA. PCR products were run in a 1% agarose gel and purified using the QIAquick Gel Extraction Kit. Sequencing of purified products was performed in an ABI Prism 3730 DNA analyser using nested primers.

2.10 Real- time quantitative PCR (qPCR)

Total RNA was extracted using the Absolutely RNA Microprep Kit and the RNA integrity was assessed using the Agilent 2100 Bioanalyzer. 2 µg of RNA were used to synthesize cDNA with the High Capacity cDNA Reverse Transcription Kit (Applied Biosystems, USA).

Expression profiles were obtained by qPCR implemented with TaqMan Low Density Arrays (TLDAs) in a 7900HT Fast Real-Time PCR System. Genes with CT values under 33 were considered to be non-expressed. Delta CT (DCT) was calculated by using as housekeeping gene the average of CT values obtained for the genes 18S and GNB2L1.

When analyzing the expression profiles of naïve *vs* Th1 cells, consistent changes in the expression levels were considered significant when the difference in expression was equal to or higher than 1,5 CTs in the majority of donors analyzed and the *p* value of a paired T test was under 0.1. When analyzing expression changes during Th1 restimulation, consistent changes in the expression levels were considered significant when the difference in expression was equal to or higher than 1 CT in the majority of donors analyzed and the *p* value of a paired T test was under 0.1.

Conventional qPCRs were performed using Taqman reagents. Reactions were run in 7900HT Fast Real-Time PCR system. Comparative analysis of the results obtained was done comparing the RQ values. RQ was calculated using the $2^{-\Delta\Delta CT}$ method (154), using GNB2L1 as housekeeping gene.

2.10 ELISA

Supernatants of J77/Raji or CD4/beads co-cultures were collected and stored at -80ºC until analysis. IL-2 production was determined by ELISA assays using the BD OptEIA™ ELISA set. Quantification was done in an ELx800 absorbance microplate reader. Absorbance values were interpolated in a standard curve using Excel software.

2.11 Western Blot

In order to analyze the integrity of plasmids used (Figure R6), transfected cells were lysed for 30 min in ice-cold RIPA buffer and sonicated in a digital sonifier.

In order to analyze phosphorylation of PLCγ and ERK1/2, stimulated cells were lysed for 30 min in ice-cold Western Blot (WB) lysis buffer. Cell lysates were centrifuged at 1000 g for 10 min at 4ºC, and supernatants were collected for further procedure.

For immunoprecipitation (IP), cells were lysed for 30 min in ice-cold IP lysis buffer. Cell lysates were then sonicated in a sonifier. Equilibrated GFP-Trap®_A beads were added to cell lysates and incubated for 2 hours at 4ºC with rotation. After two washes, Laemmli buffer was added and beads were boiled for 10 min at 95ºC to dissociate complexes. WB was performed with the supernatants.

Cell lysates were mixed with 4x Laemmli buffer containing 20% β-mercaptoethanol. Samples were then boiled at 95°C for 5 minutes and proteins were separated by SDS-PAGE in acrylamide gels. Proteins were then transferred to an Immobilon-FL transfer membrane. After transference, membranes were blocked with either LICOR or BSA blocking buffer before O/N incubation with primary mouse or rabbit antibodies. Fluorescently-labelled secondary antibodies IRDye 680 goat anti-Mouse and IRDye 800 goat anti-rabbit were used. In some experiments, HRP-conjugated goat anti-rabbit antibody and Pierce™ ECL Plus Substrate were used. Blots were scanned and fluorescence or quimioluminiscence were quantified with an Odyssey Infrared Imager. When needed, membranes were stripped using PVDF Stripping buffer from LICOR.

2.12 Data analysis and statistics

Hitmap and dendrogram of expression data were generated using MATLAB software. Statistical analysis was implemented with PRISM 6 and Statgraphics Centurion XVII. When comparing three or more samples, one-way ANOVA followed by Bonferroni's multiple comparing test correction was used. When comparing two samples, Student T test was performed. Welch correction was applied when variances between samples were statistically different. Normalized values were analyzed by a one-sample T test. All tests were implemented with two tails unless otherwise stated in figure legends.

RESULTS

RESULTS

1. Expression profile of PTPs associated to Th1 polarization

The expression profile of NC PTPs had not been studied in human CD4 T cells upon differentiation to an effector phenotype and subsequent activation. In addition, the role of the majority of NC PTPs in T cell immune responses is unknown. Therefore, as a first attempt to understand their role in this process, we decided to study the changes in PTP expression during differentiation of naïve CD4 T cells into Th1 effector cells. We studied the expression of 65 NC PTPs present in the human genome according to Alonso *et al* (87), and 14 classical PTPs. The latter were included due to their regulatory role in signaling downstream the TCR and cytokine receptors, or due to their association with autoimmune diseases (Table R1). The complete list of genes included in the study is shown in Table MM4.

Table R1. Classical PTPs included in this study

Phosphatase	Substrate	Function in T cells	Autoimmunity	Reference(s)
PTPRA (RPTPα)	SFK	Regulation of TCR signalling	Not reported	(155)
PTPRC (CD45)	SFK and JAK family kinases	Regulation of TCR and cytokine signalling	MS, AH	(156)
PTPRJ (CD148)	SFK	Regulation of TCR signalling	Not reported	(157, 158)
PTPRK (RPTPκ)	STAT3	Regulation of CD4+ T cell development	NK/T cell lymphoma	(159, 160)
PTPN1 (PTP1B)	STAT6	Not reported	Not reported	(161)
PTPN2 (TC-PTP)	SFK, JAK1, JAK3	Regulation of TCR and cytokine signalling	T1D, CD	(162, 163)
PTPN4 (PTP-MEG1)	CD3ζ	Regulation of TCR signalling	Not reported	(164)
PTPN6 (SHP1)	SFK, ITAMs, ZAP70, SLP-76	Regulation of TCR signalling	PS	(165)
PTPN7 (HePTP)	ERK1/2, p38	Regulation of TCR signalling	Not reported	(166, 167)
PTPN9 (PTP-MEG2)	NSF, STAT3	Regulation of cytokine secretion	Not reported	(168, 169)
PTPN12 (PTP-PEST)	Pyk2	Regulation of secondary T cell responses	Not reported	(170)
PTPN13 (PTP-BAS or PTP-BL)	STAT4, STAT6	Regulation of cytokine signalling	Not reported	(171)
PTPN18 (PTP20)	HER2	Not reported	Not reported	(172)
PTPN22 (LYP)	ZAP70, LCK, FYN	Regulation of TCR signalling	T1D, RA, SLE	(173, 174)

Table R1. Classical PTPs included in this study. Classical PTPs, their known substrates, function in T cells, and role in autoimmune diseases are reported. SFK: Src family kinases, MS: Multiple sclerosis, AH: Autoimmune Hepatitis, T1D: Type I diabetes, CD: Crohn's disease, PS:psoriasis, RA: Rheumatoid Arthritis, SLE: Systemic Lupus Erythematosus.

Human naïve CD4 T cells were isolated and polarized to Th1 conditions as detailed in materials and methods. Th1 polarization was assessed by induction of the Th1 master regulator transcription factor Tbet (Figure R1A). Production of IFNγ by Th1 cells in response to phorbol esters and Ionomycin treatment was also analyzed (Figure R1B).

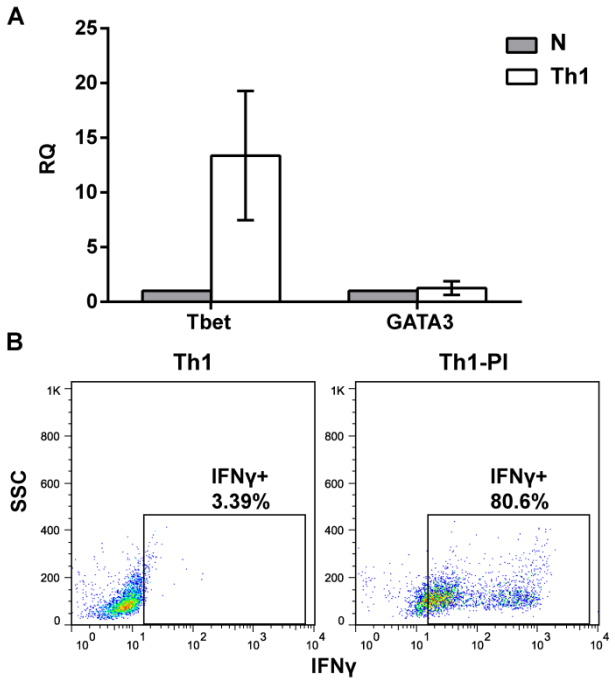

Figure R1. Assessment of Th1 polarization. A. Determination of the RQ of the transcription factors Tbet and GATA3 in naïve and Th1 cells. The average and the standard deviations of 3 donors are shown. **B.** Analysis of IFN*γ* production by *in vitro*-polarized Th1 cells before (Th1) and after (Th1-PI) restimulation with PMA and Iomoycin was analyzed by intracellular flow cytometry. The percentage of IFN*γ* producing cells (IFNγ+) is indicated. A representative experiment is shown. SSC, side scatter.

Expression of PTPs was analyzed in naïve and Th1 cells by using as housekeeping gene the average of the DCT values obtained from the genes 18s and GNB2L1. We found that the mRNA of all 14 classical PTPs and 52 out of 65 NCs was detectable in both the analyzed human naïve and Th1 cells. An agglomerative hierarchical tree (Figure R2) revealed clusters of PTPs, which shared not only the expression levels and profiles during Th1 polarization but also, in some cases, related functions (see section 1 of the Discussion). The PTPs significantly regulated during Th1 polarization are detailed in Table R2.

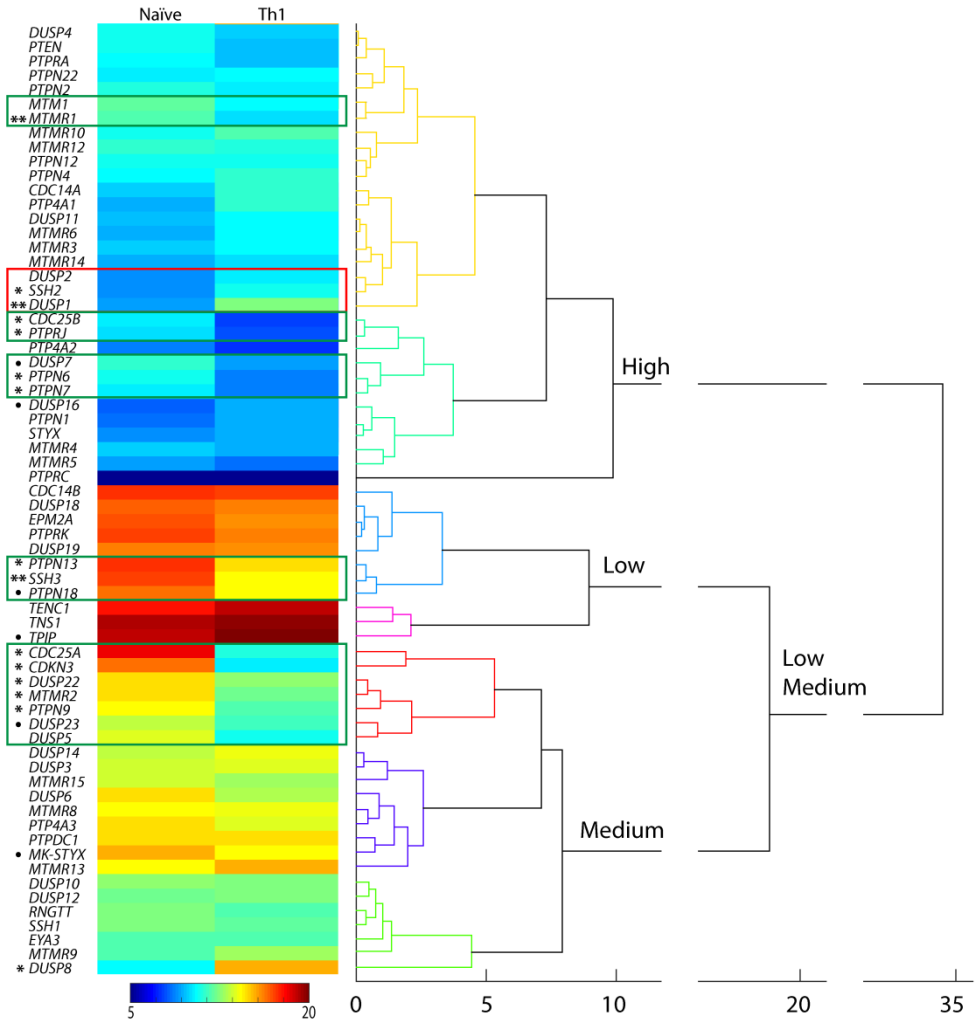

Figure R2. Expression profile of PTPs in naïve and Th1 cells. Agglomerative hierarchical tree of the gene expression patterns in naïve and Th1 cells. Numbers below the tree indicate the Euclidean distance among gene patterns. Hitmap represents the average DCT obtained for each gene in both conditions and 3 donors. The calibration bar is shown between 5 and 20 DCTs. Green and red squares point to clusters of upregulated and downregulated genes, respectively. Clusters of high, medium, and low expressed PTPs are indicated. Asterisks indicate those genes whose expression levels were considered to significantly change following the criterium stated in the main text. •, p≤0.1; *, p≤0.05; **, p≤0.01.

1.1 Expression of classical PTPs

The majority of classical PTPs analyzed (10 out of 14) were found inside the group of high expression, including *PTPRA*, *PTPN22*, *PTPN2*, *PTPN12*, *PTPN4*, *PTPRJ*, *PTPN6*, *PTPN7*, *PTPN1 and PTPRC*. *PTPRC*, an important regulator of Lck activation (175), showed the highest expression levels of all PTPs included in this study. The remaining classical PTPs were found in the group of medium (*PTPN9*) or low (*PTPRK, PTPN13* and *PTPN18)* expression.

Table R2. PTPs regulated during Th1 polarization

Group	Gene	Regulation during Th1 polarization	Average DCT change/p value	Substrate
Classical	*PTPRJ*	Upregulation	2.02/*	SFK
	PTPN6	Upregulation	2.08/*	SFK, ITAMs, ZAP70, SLP-76, Vav1
	PTPN7	Upregulation	1.54/*	ERK1/2, p38
	PTPN9	Upregulation	2.45/*	NSF
	PTPN13	Upregulation	2.40/*	STAT4, STAT6
	PTPN18	Upregulation	1.9/•	HER2
MKPs and Atypical DSPs	*DUSP1*	Downregulation	3.07/**	p38, JNK, ERK
	DUSP7	Upregulation	2.10/•	ERK
	DUSP8	Downregulation	4.55/*	JNK,p38
	DUSP13	Repression	---	JNK,p38
	DUSP16	Downregulation	1.20/•	JNK,p38
	MK-STYX	Upregulation	1.19/•	Catalytically inactive
	DUSP21	Repression	---	Unknown
	DUSP22	Upregulation	2.10/*	JNK,ERK2, Lck
	DUSP23	Upregulation	1.57/**	p38, JNK
Myotubularins and PTEN DSPs	*MTMR1*	Upregulation	1.43/**	PI(3)P, PI(3,5)P2
	MTMR2	Upregulation	2.61/*	PI(3)P, PI(3,5)P2
	MTMR11	Induction	---	Catalytically inactive
	TPIP	Downregulation	1.96/•	PIP
Cell cycle regulators	*CDKN3*	Upregulation	5.81/*	CDK2
	CDC25A	Upregulation	6.80/*	CDKs
	CDC25B	Upregulation	2.45/*	CDKs
	CDC25C	Induction	---	CDKs
Class III Cys-based PTPs	*SSH2*	Downregulation	1.68/*	Cofilin
	SSH3	Upregulation	2.63/**	Cofilin

Table R2. PTPs regulated during Th1 polarization. PTPs whose expression levels were regulated during Th1 polarization are shown. Changes in expression were determined as explained in materials and methods. Dots and asterisks represent the result of the paired T test of DCt values obtained for the comparison of naïve and Th1 cells in 3 donors. • $p<0.1$; * $p\leq0.05$; ** $p\leq0.01$. The absolute value of the average DCT change in the 3 donors is shown. DUSP13 and DUSP21 were considered as repressed genes since their expression was detectable only in naïve but not in Th1 cells. MTMR11 and CDC25C were considered as induced genes since their expression was detectable in Th1 but not in naïve cells.

1.2 Expression of NC PTPs

We did not detect mRNA of the MKP *DUSP9*, the atypical DSPs *DUSP15*, *DUSP26*, and *DUSP27*, the tensin homolog *TPTE*, the myotubularin *MTMR7* and the Asp-based PTPs *EYA1*, *EYA2*, and *EYA4* in either naïve or Th1 cells. Non expressed MKPs in our study matched previous data in mice (176). In contrast, the reported expression of the *Eya1*, *Eya2*, and *Eya3* mouse orthologs (176) suggests a different requirement of this group of PTPs in mice and humans. The same might apply for the myotubularin *MTMR7*, which seems to have a regulatory role in Th polarization in mice (177).

22 NC were found in the group of highly expressed PTPs (Figure R2). Substantial changes in expression levels associated with Th1 polarization were found in genes coding for regulators of the phosphorylation state of phosphoinositides (*TPIP* and MTMs), the MAPK signalling module (MKPs), the actin cytoskeleton (SSHs), and the cell cycle (CDC25s and *CDKN3*) (Table R2). The changes in the expression of these genes will be further discussed in the section 1 of the discussion. Here we will only briefly outline the level of expression (high, medium or low, see Figure R2) of the groups of PTPs.

Among the ten out of eleven classical MKPs whose expression was detected, five (*DUSP1*, *DUSP2*, *DUSP4*, *DUSP7*, and *DUSP16*) were found in the group of highly expressed PTPs, and five (*DUSP5*, *DUSP6*, *DUSP8*, *DUSP10* and *STYXL1)* were found inside the group of medium expressed PTPs.

Among the DSPs, only *STYX* and *DUSP11* were found in the group of higly expressed PTPs, while *DUSP3*, *DUSP12*, *DUSP14*, *DUSP22*, *DUSP23 and RNGTT* where in the group of medium expression. The DSPs with low expression were *DUSP18*, *DUSP19* and *EPM2A.*

Among the tensin homologs only PTEN was highly expressed particularly in Th1 cells. The other components of the PTEN family, *TPIP*, *TNS1* and *TENC1* shared a cluster of very low expression.

Regarding MTMs, 9 out of 16 (*MTM1*, *MTMR1*, *MTMR3*, *MTMR4*, *MTMR6*, *MTMR10*, *MTMR12*, *MTMR14* and *SBF1,* which encodes for MTMR5) were found in the group of highly expressed PTPs, suggesting that these enzymes are important regulators of phosphoinositide levels in T cells. The other MTMs whose expression was detected were in the group of medium

expression (*MTMR2*, *MTMR8*, *MTMR9*, *FAN1*, which encodes for MTMR15, and *SBF2,* which encodes for MTMR13).

Among cell cycle regulators, *CDC14A* and *CDC25B* were found in the group of highly expressed PTPs. *CDC25A*, *CDKN3* and *PTPDC1* were in the group of medium expressed genes.

The cytoskeleton regulators *SSH1*, *SSH2* and *SSH3* were found in the medium, high, and low expression groups, respectively.

Among the PRL phosphatases, PTP4A1 and PTP4A2 were highly expressed, while PTP4A3 was in the group of medium expression.

2. Expression of NC PTPs during stimulation of Th1 cells

The finding that the expression levels of several NC PTPs were regulated during Th1 polarization prompted us to further investigate their expression during the effector functions of Th1 cells at inflammatory sites. We used PMA and Ionomycin (PI) stimulation for 4 hours to mimic strong stimuli that effector cells receive upon extravasation to sites of inflammation. PMA is a DAG analog that induces PKC and RasGRP activation (178, 179), while Ionomycin is an ionophore that trigguers elevation of intracellular Calcium levels (180).

While the cell cycle regulators (CDC14s and CDC25s) were in general downregulated during Th1 stimulation (Figure R3B), all the MAPK regulators (MKPs and atypical DSPs) that showed significant changes in their expression levels upon Th1 stimulation were upregulated (Figure R3A). Consistent with our data, the ERK-specific DUSP5 has been shown to be upregulated in human T cells in response to IL-2 stimulation (181), and it has been reported that both DUSP5 and DUSP6 are upregulated in MCF7 cells upon PMA treatment (182). DUSP8 expression has also been shown to be induced in K562 cells by PMA (183).

Among phosphoinositide phosphatases (PTENs and MTMRs) only *MTMR3* was significantly downregulated, while *MTMR2* and *MTMR11* were upregulated by PI treatment (Figure R3C).

The tensin homolog *TPIP* was repressed with Th1 stimulation and could not be included in Figure R3C.

Two out of three members of the PRL family were significantly regulated during Th1 stimulation (Figure R3E). Interestingly, while *PTP4A1* was upregulated, *PTP4A2* was downregulated, suggesting that despite their high homology, these proteins might play distinct roles in Th1 cell responses. This finding, together with the reported high expression of *PTP4A1* and *PTP4A2* in T cell areas of the lymph node (127) and the proposed role of PRLs as regulators of the actin cytoskeleton (116, 147, 148) prompted us to further analyze the expression of PRLs in CD4 T cells, and their role in IS assembly and T cell activation.

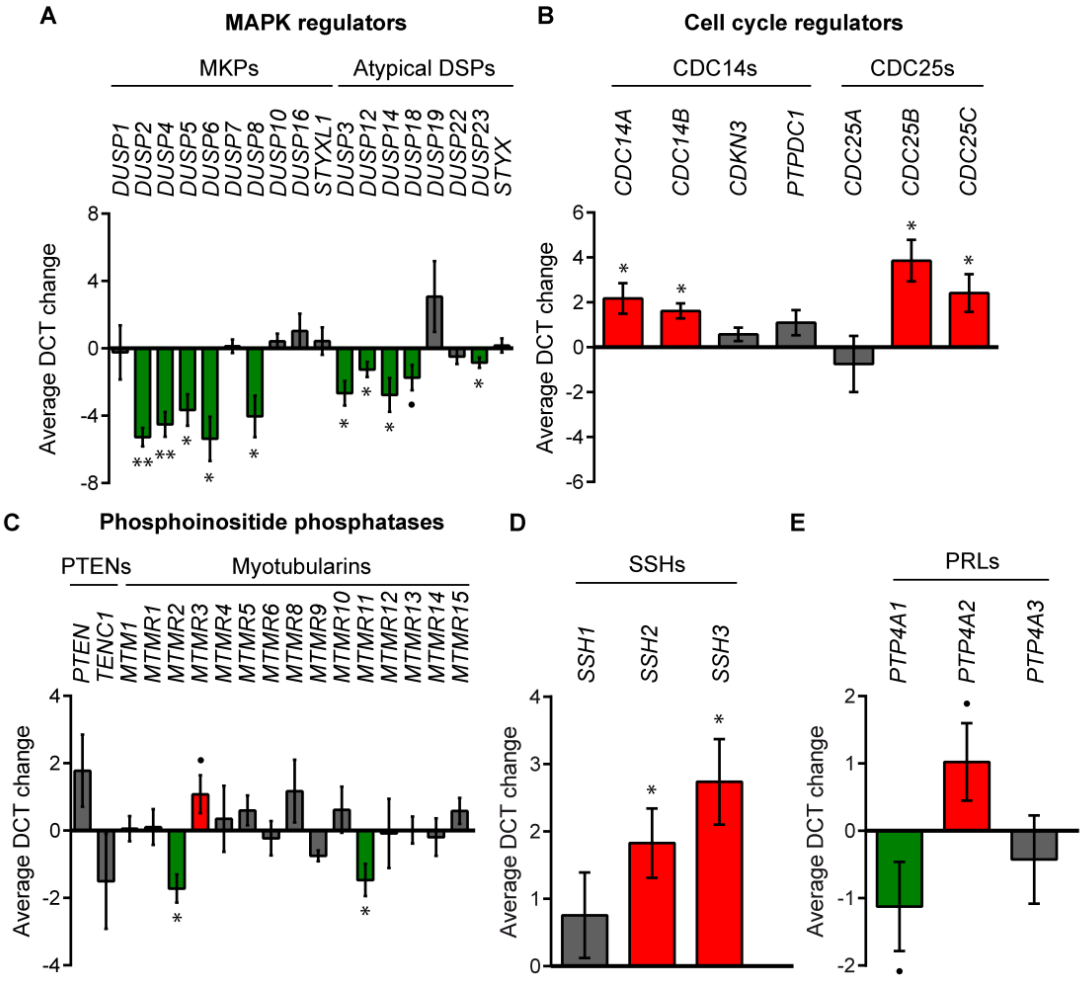

Figure R3. Expression changes of NC PTPs upon Th1 stimulation. In vitro polarized Th1 cells were stimulated with PMA an Iomomycin for four hours and gene expression was measured. The graphs represent the average of the change in DCT between Th1 and restimulated Th1 cells for the main functional groups of PTPs (**A to E**). Genes upregulated and downregulated are labelled in green and red, respectively. Asterisks indicate those genes whose expression levels were considered to significantly change following the criterium stated in materials and methods. The mean ± SD of three donors is shown. • p≤0.1; * p≤0.05; ** p≤0.01.

3. PRLs participate in T cell activation

To further analyze the regulation of PRLs expression during T cell stimulation, we used both *in vitro* generated Th1 and peripheral blood CD4 T cells. As shown in Figure R4A, *PTP4A2* was the most abundant PRL in both cells, followed by *PTP4A1* and *PTP4A3*, successively. In addition, the expression of *PTP4A1* and *PTP4A2* was similar to other PTPs known to regulate T cell responses (88). Next, we performed a time-course experiment stimulating with PMA and Iomomycin both Th1 and peripheral blood CD4 T cells (Figure R4B and C). PKC/RasGRP stimulation and intracellular rise of Ca^{2+} obtained by this treatment caused an up-regulation of *PTP4A1* concomitant to a quick down-modulation of *PTP4A2*. While Th1 effector cells showed a higher and more sustained rise of *PTP4A1* (Figure R4C), a lower transient peak at 30 minutes was observed in *ex vivo* analyzed peripheral blood CD4 T cells (Figure R4B). Interestingly, Th1 cells induced higher levels of both *PTP4A1* and *CD69* (Figure R4D). No consistent changes were observed for *PTP4A3* (data not shown).

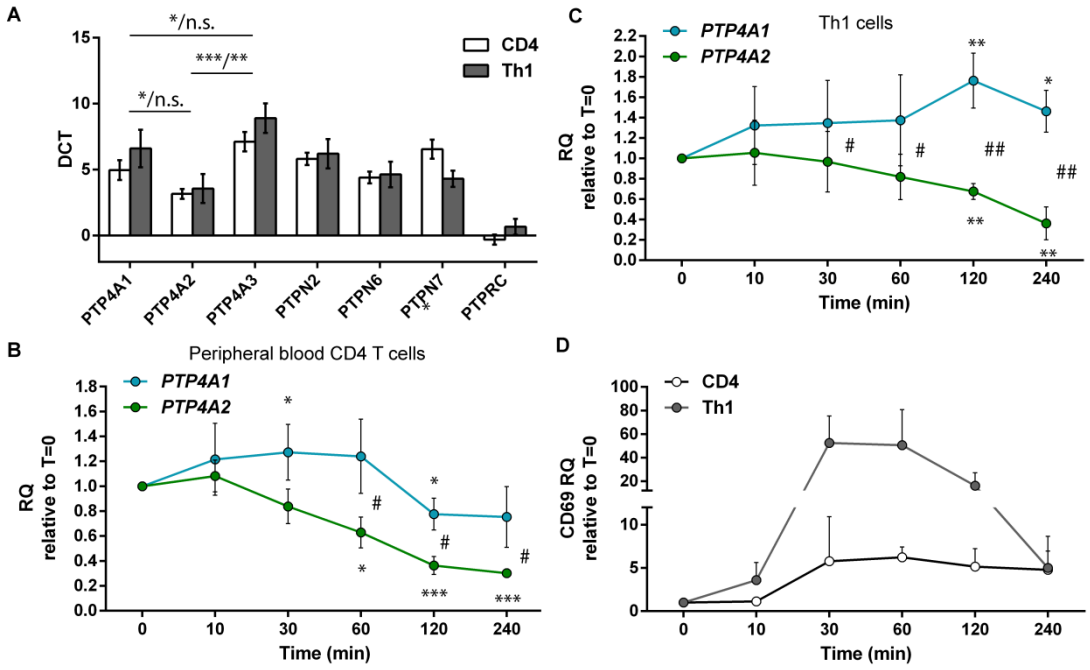

Figure R4. Expression of PRLs in CD4 T cells. A. Gene expression of PRLs and other PTPs in peripheral blood CD4 T cells and *in vitro* polarized Th1 cells from 3 healthy donors was analyzed by qPCR. The mean value of DCT ± SD for each gene is shown. The significance of a one-way ANOVA test in CD4/Th1 cells is indicated with asterisks. n.s. not significant. **B** and **C.** Expression of PTP4A1 and PTP4A2 mRNA in peripheral blood CD4 T cells (B) and Th1 cells (C) during stimulation with PMA and Ionomycin for the indicated times. Asterisks indicate comparison to t=0 using a one sample T test. Hashes indicate comparisons between PTP4A1 and PTP4A2 using a paired T test. **D.** Induction of CD69 mRNA during stimulation. (**B** to **D**) The mean value of RQ ± SD from four different donors is shown. (**A** to **C**) * and # p≤0.05; ## and ** p≤0.01; *** p≤0.001.

Expression data indicated that T cell stimulation leading to PKC/RasGRP activation and Ca^{2+} elevation increased the relative amount of PRL-1 compared with PRL-2. Hence, we hypothesized that these molecules could have a role during T cell activation. To test this hypothesis, we treated peripheral blood CD4 T cell with Thienopyridone (TP), a selective inhibitor of the enzymatic activity of this group of DSPs (137), before and during T cell stimulation with anti-CD3ε and anti-CD28. TP treatment decreased the induction of the activation marker CD69 (184) and the secretion of IL-2 (Figure R5). No clear effects were found when cells were treated with Analog 3 (A3), a less specific drug that also inhibits classical PTPs (185), such as the negative regulator of TCR signaling TC-PTP (162). Although the effect of TP was not as patent as the effect of the MEK inhibitor U0126, these data suggested that the enzymatic activity of PRLs was required for the optimal activation of human CD4 T cells.

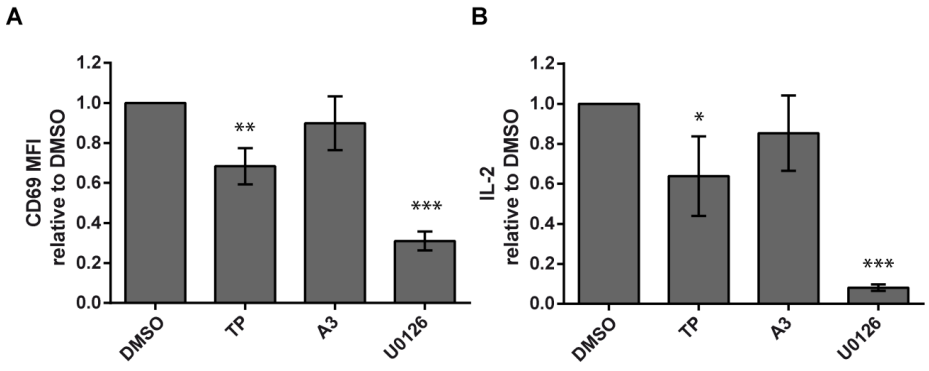

Figure R5. Contribution of catalytic activity of PRLs to T cell activation. Effect of the MEK1 inhibitor U0126, Analog 3 and thienopyridone on CD69 induction (**A**) and IL-2 secretion (**B**) in CD4 T cells in response to T cell stimulation with anti-CD3/anti-CD28 coated beads. Results were normalized to control (DMSO) and the mean ± SD of four experiments is shown. Samples were compared with the control (DMSO) by a one-sample T test. * p≤0.05; ** p≤0.01; *** p≤0.001.

4. Recruitment of PRL-1 to the IS

The obtained expression data, together with the effect of TP on T cell stimulation, suggested that PRLs might play a role in T cell activation. Given that PTP4A1 was the only member of the PRL family that was transiently upregulated during PI treatment, we decided to study its distribution during IS formation. Distribution of endogenous PRL-1 at the T cell side of the IS was imaged in IS-like structures formed by peripheral blood CD4 T cells of healthy donors and latex beads coated with anti-CD3ε and anti-CD28 antibodies as described in materials and methods. PRL-1 staining was performed with a mouse monoclonal antibody kindly provided by Dr. Qi Zeng (Institute of Molecular and Cell Biology, Singapore) that showed specificity to PRL-1 with respect to PRL-2 and PRL-3, as assessed by intracellular staining of chimeric proteins

(Figure R6A, α-PRL-1 panels). By contrast, a commercial antibody recognized both PRL-1 and PRL-2 (Figure R6A and R6C, α-PRL-1/2 panels).

Co-staining with α-tubulin revealed that PRL-1 accumulated at the IS-like structures in cells showing or not polarization of the MTOC, while it was not recruited to interfaces established with non-stimulating control beads (Figure R7A). Interestingly, two pools of PRL-1 were observed; one around the MTOC and another accumulated at the IS (Figure R7B). PRL-1 accumulation at T cell membranes contacting latex beads correlated with the recruitment of CD3ζ (Fig. R7C), indicating that PRL-1 polarization is associated to the activation process.

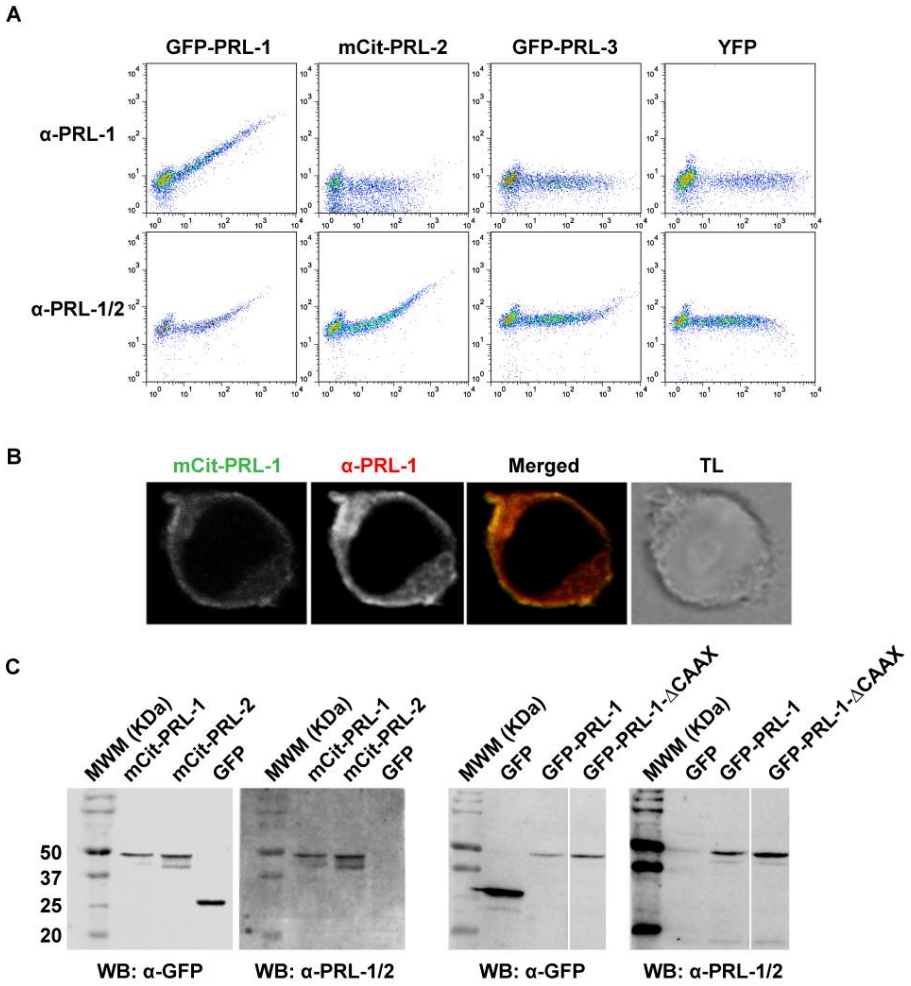

Figure R6. Assessment of α-PRL-1 antibody specificity and plasmid integrity. A. Intracellular staining of overexpressed chimeric proteins in Jurkat cells with a monoclonal antibody α-PRL-1 provided by Dr. Qi Zeng, and a commercial α-PRL-1/2 antibody. Fluorescence of the overexpressed protein is displayed in the X axis; fluorescence of the intracellular staining is displayed in the Y axis. **B**. Immunofluorescence of a Jurkat cell transfected with the mCit-PRL-1 chimeric protein stained with α-PRL-1 antibody. **C**. WB of Jurkat cells transfected with mCit-PRL-1, mCit-PRL-2, GFP-PRL-1, GFP-PRL-1-ΔCAAX or GFP alone, probed with α-GFP or α-PRL1/2 antibodies. TL, Transmitted light; MWM, Molecular weight marker.

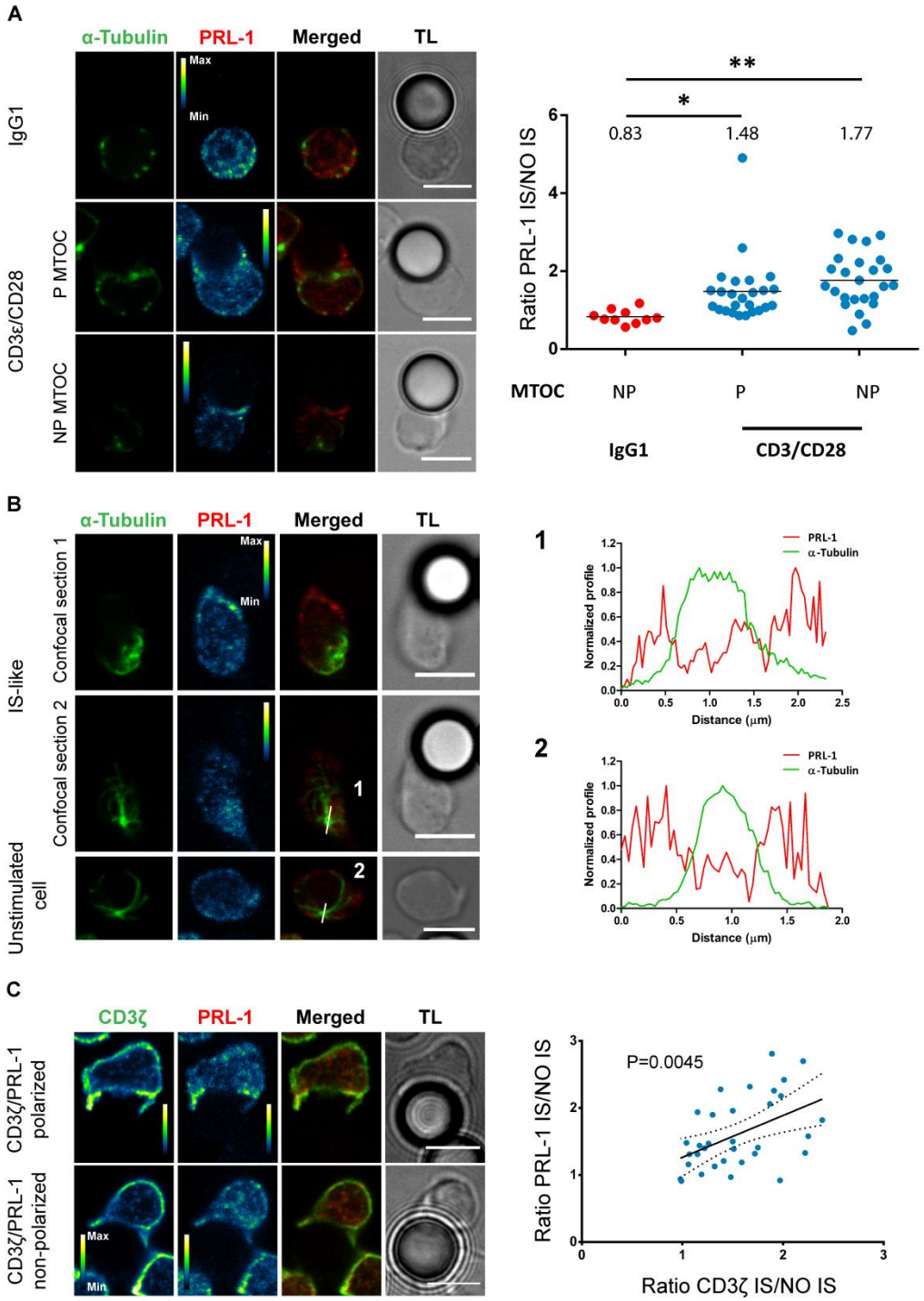

Figure R7. Distribution of endogenous PRL-1 at the IS. A. Representative immunofluorescences of CD4 T cells interacting with microspheres coated with anti-CD3ε and anti-CD28 antibodies (IS-like) or IgG1 as negative control for stimulation. The right panel represents the quantification of PRL-1 redistribution to the IS in relation to MTOC polarization. The numbers represent the mean for each group. Groups were compared by a one-way ANOVA. * p≤0.05, ** p≤0.01. **B.** Representative immunofluorescence of CD4 T cells interacting (IS-like) or not (Unstimulated cell) with microspheres coated with anti-CD3ε and anti-CD28 antibodies. Right panels represent profiles of the fluorescence intensity in the green and the red channel along the line drawn on images. Numbers indicate the correspondence between the cell and the profile. **C.** Representative images of CD4 T cells interacting with microspheres coated with anti-CD3ε and anti-CD28 antibodies. Examples of IS-like interactions showing or not polarization of PRL-1 and CD3ζ are shown. The right panel represents the correlation of PRL-1 and CD3ζ polarization to the IS. The p-value of the Pearson coefficient is shown. (**A to C**) Calibration bar is shown in pseudocolored images. Scale bars 5 µm. Dots represent individual conjugates from two independent experiments.

To study the distribution of PRL-1 in a system with antigenic stimulation, we used the J77 T cell line, which can be stimulated by RAJI cells presenting SEE. To directly visualize endogenous PRL-1 in J77 cells with no antibody staining, we edited the genome of J77 cells. By using Crispr/Cas9 technology, we inserted a GFP cassette in the genome of J77 cells right before the coding sequence of the PRL-1 gene (see materials and methods section 2.4). As a result, we obtained a cell line expressing endogenous PRL-1 coupled to the GFP. As shown in Figure R8A, edited J77 cells (GFP+) were enriched by cell sorting. Proper insertion of the GFP coding sequence in genomic DNA of edited cells was assessed by PCR (Figure R8B) and integrity of the endogenous chimeric protein, as well as the absence of free GFP was confirmed by WB (Figure R8C).

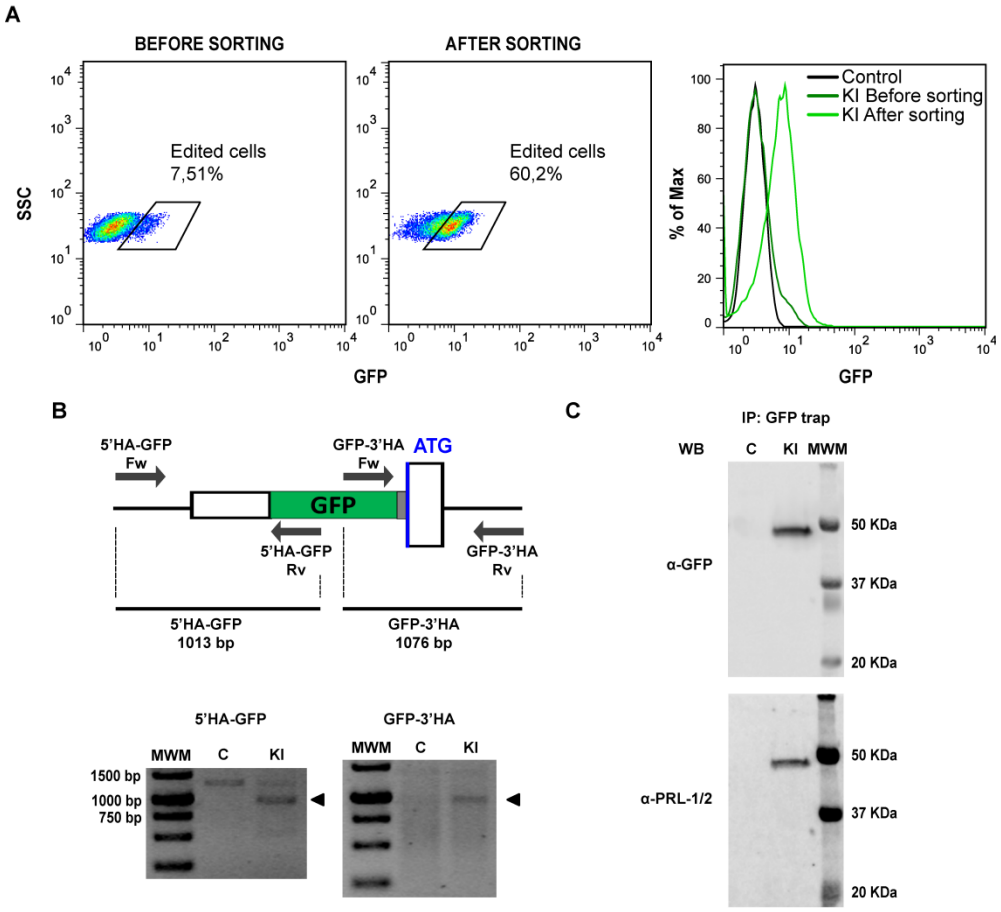

Figure R8. Caracterization of the GFP-PRL-1 J77 KI cell line. A. Dot plots showing the percentage of cells with the GFP cassette inserted in the genome (edited cells) before and after enrichment by cell sorting. Histogram on the right represents fluorescence of control J77 and KI cells before and after sorting. **B.** Insertion of GFP in the PTP4A1 gene was assessed by PCR. PCRs were designed as shown in the scheme to amplify a fragment corresponding to the end of 5'HA and the beginning of the GFP coding sequence (5'HA-GFP) and a fragment corresponding to the end of GFP and the beginning of the 3'HA (GFP-3'HA). Arrows represent the primers used. The start codon of the PRL-1 coding sequence is shown. PCRs were run in agarose gels and visualized with ethidium bromide staining. Arrowheads indicate the specific band. **C.** Immunoprecipitation was performed with GFP traps to pull down the GFP-PRL-1 protein, followed by WB with the indicated antibodies. C, Control; KDa, KiloDalton.

We also transfected J77 cells with plasmids coding for chimeric GFP-PRL-1 or GFP alone to compare the result of overexpression and genomic edition. The overexpressed chimeric protein conserved the epitope recognized by the α-PRL-1 antibody and had the expected molecular weight (Figure R6). In unstimulated cells, overexpressed (o/e) GFP-PRL-1 cells showed a distribution consistent with the previous endogenous PRL-1 staining, with an intracellular pool of GFP-PRL-1 distributed around the MTOC (Figure R9A). Next, we examined GFP-PRL-1 recruitment to the mature IS formed between J77 and RAJI cells presenting SEE. The low expression levels of endogenous PRL-1 in J77 cells difficulted the visualization of endogenous GFP-PRL-1 when fixed cells were permeabilized prior to tubulin staining. Hence, KI cells were stained for surface CD3ε. Both KI and o/e GFP-PRL-1, but not GFP alone, polarized to the zone of contact (Figure R9B). Interestingly, KI GFP-PRL-1 showed polarization rates more similar to the endogenous PRL-1 (mean 1,23 and 1,48, respectively, Figures R7A and R9B) than the o/e GFP-PRL-1 (mean 2,27, Figure R9B). These results indicated that although both systems enabled us to evaluate the polarization to the IS, genomic edition reproduced more accurately the behaviour of the endogenous molecule.

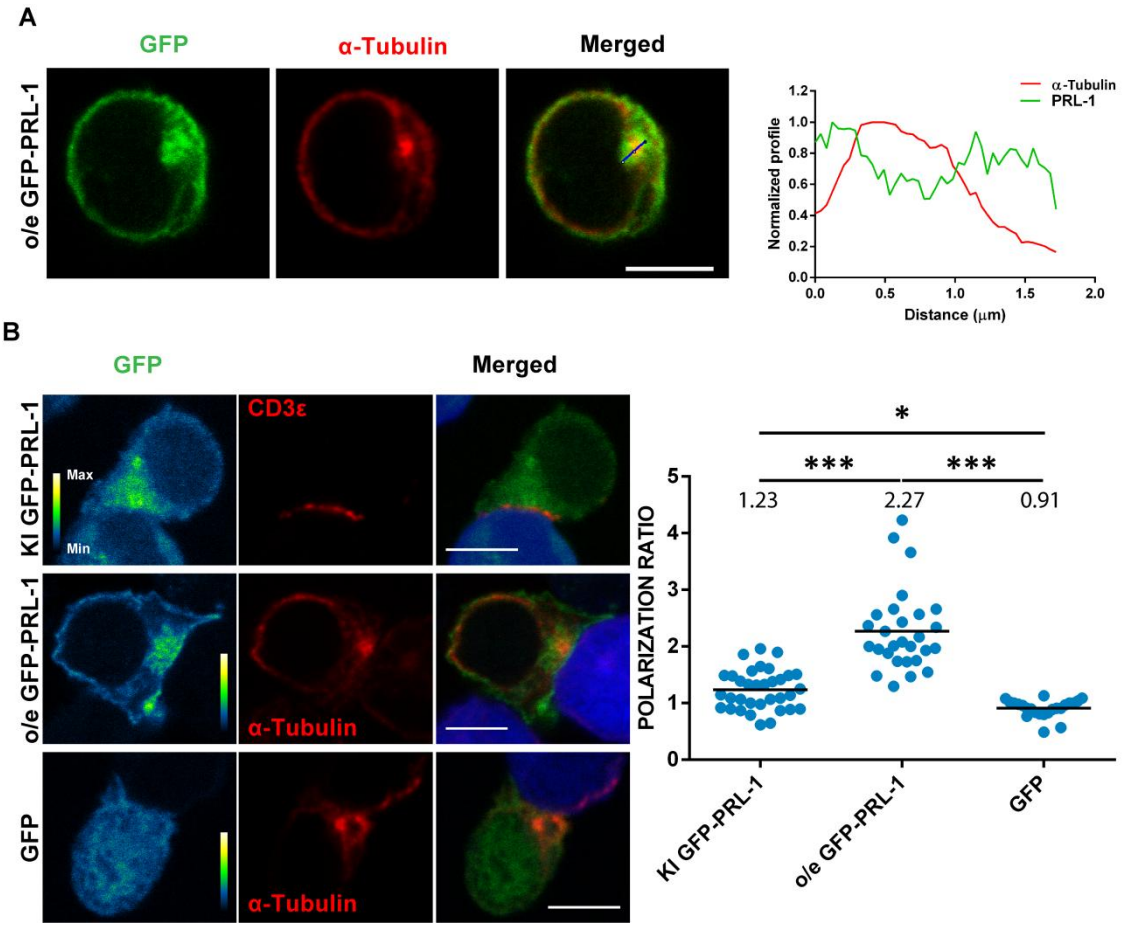

Figure R9. Distribution of GFP-PRL-1 in J77 T cells. A. Representative immunofluorescence of a J77 cell overexpressing GFP-PRL-1 and stained for α-tubulin. The right panel represents the profile of the fluorescence

intensitiy in the green and the red channels along the line drawn in the merged image. **B.** Representative immunofluorescences of cell conjugates formed by J77 KI cells (KI GFP-PRL-1) or J77 cells overexpressing GFP-PRL-1 (o/e GFP-PRL-1) or GFP alone (GFP) and conjugated with SEE-pulsed RAJI cells labeled with CMAC (blue). The right panel represents the quantification of the distribution of GFP-PRL-1 to the IS. The mean of each group is indicated on the graph. Dots represent individual conjugates. Asterisks indicate the p-value of a one-way ANOVA test. * p≤0.05, *** p≤0.001. Scale bars 5 μm.

The accumulation of endogenous PRL-1 at the IS in which the MTOC was not completely polarized (Figure R7A) suggested that PRL-1 was delivered to the contact site before the IS maturation. To further prove this idea the polarization of the GFP-PRL-1 fusion protein was tracked in live cells from the initial scanning of the APC until the complete assembly and maturation of the IS. The low expression levels of endogenous PRL-1 in J77 cells made necessary to increase the laser voltage to visualize GRP-PRL-1 in KI cells, leading to fast bleaching of the chromophore. Hence, time-lapse experiments had to be performed with o/e GFP-PRL-1. Time-lapse confocal microscopy revealed a fast and transient accumulation of PRL-1 at membrane protrusions during initial stages of the APC scanning and a later delivery at the mature IS in the pericentriolar endosomal compartment (Figure R10A and B, white arrows and yellow arrowheads for initial contacts and intracellular compartment, respectively, and Movies 1 and 2). PRL-1 colocalized with CD3ζ at dynamic membrane protrusions scanning the APC surface during the interaction (Figure R10B, white arrows). Plasma membrane targeting and delivery of PRL-1 to the IS was dependent on the CAAX motif, as shown by overexpression of the mutant GFP-PRL-1-ΔCAAX, which lacks this sequence (Figure R11).

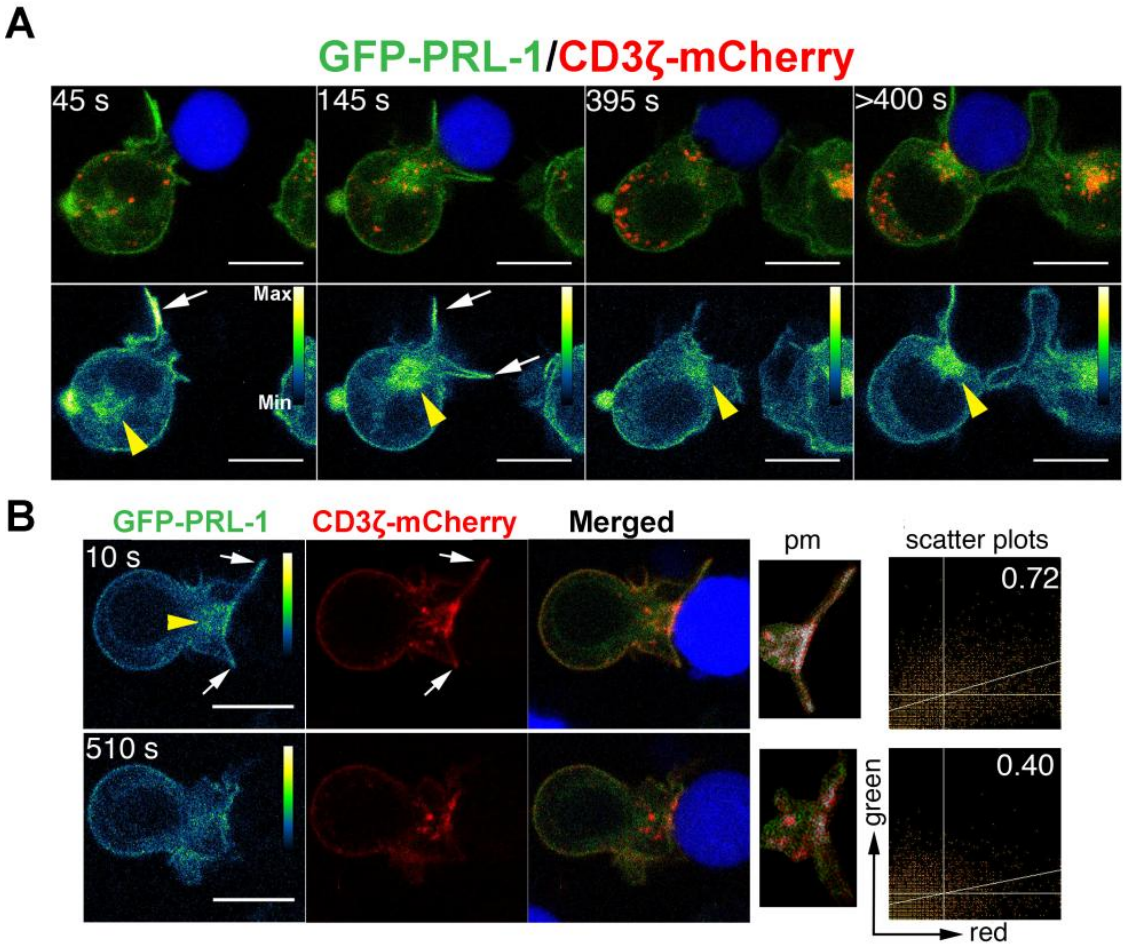

Figure R10. Dynamic distribution of GFP-PRL-1 to the IS. Formation of conjugates between J77 cells overexpressing GFP-PRL-1 (green) and CD3ζ-mCherry (red) and SEE-pulsed RAJI cells (labelled in blue) was imaged by time-lapse confocal microscopy. **A.** Frames of the experiment in Movie 1 are shown. The distribution of GFP-PRL-1 is shown in the pseudocolor (lower panels) and in the merged (upper panels) images. White arrows indicate transient accumulation of GFP-PRL1 at scanning membranes. Yellow arrowheads indicate the pericentriolar location of GFP-PRL-1. **B.** An early and a late frame of the experiment in Movie 2 are shown. The distribution of GFP-PRL-1 is shown in the pseudocolor and merged images. White arrows indicate the colocalization of GFP-PRL1 and CD3ζ-mCherry at scanning membranes. Yellow arrowhead indicates the intracellular compartment containing GFP-PRL-1. Colocalization is shown in a pixel map (pm) obtained at the interaction zone. White pixels indicate colocalization sites. Scatter plots of green and red channels are shown. Numbers indicate the Manders coefficient (MC). Scale bars 5 µm. Time in seconds (s) is indicated for each image.

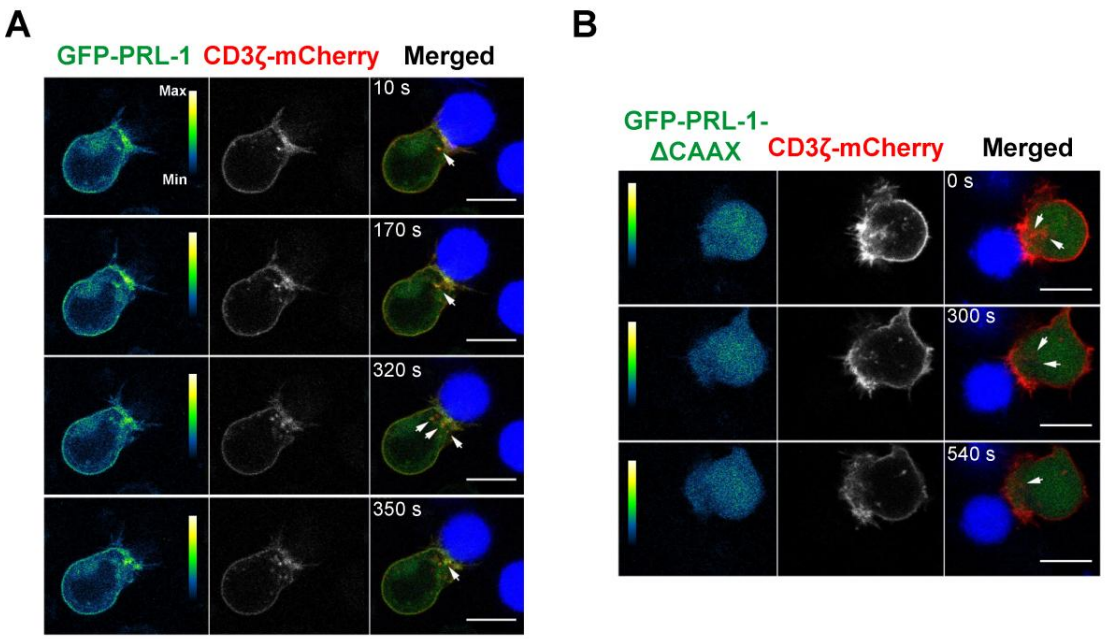

Figure R11. Distribution of GFP-PRL-1-ΔCAAX in J77 cells. Images from time-lapse experiments performed with J77 cells expressing CD3ζ-mCherry and either GFP-PRL-1 (**A**) or GFP-PRL-1-ΔCAAX (**B**) interacting with SEE-pulsed RAJI cells labeled with CMAC (blue). White arrows indicate CD3ζ-mCherry vesicles containing GFP-PRL-1 but not GFP-PRL-1-ΔCAAX. Scale bars 10 µm. Time in seconds (s) is indicated for each image.

Distribution of PRL-1 at the established IS was further studied by confocal microscopy in fixed samples (Figure R12). Overexpressed mCit-PRL-1 clearly colocalized with LFA-1 at the IS. Partial colocalization with surface CD3ε was also observed in more restricted areas. As a negative control, we analyzed colocalization of YFP alone with CD3ε.

To further analyze the colocalization of PRL-1 with CD3ζ we used TIRFM, which allows for higher spatial and temporal resolution. We imaged IS-like structures formed by J77 cells upon stimulation on glasses covered with anti-CD3ε, anti-CD28 and ICAM-1. During early adhesion of T cells to these activating surfaces, GFP-PRL-1 clearly localized in clusters enriched in CD3ζ-mCherry (Figure R13A and Movie 3). These results suggested that PRL-1 could be included in signaling aggregates organized during initial T cell activation, as described for other molecules such as ZAP-70 (186). In already established IS, we observed transient copresence of GFP-PRL-1 and CD3ζ-mCherry at dynamic peripheral sites and central CD3ζ-containing vesicles (Figure R13B, see profile and arrows in magnified areas, and Movie 4) as well as comigration of both molecules towards a more internal area of the interaction (Figure R13C, see kymograph, and Movie 5).

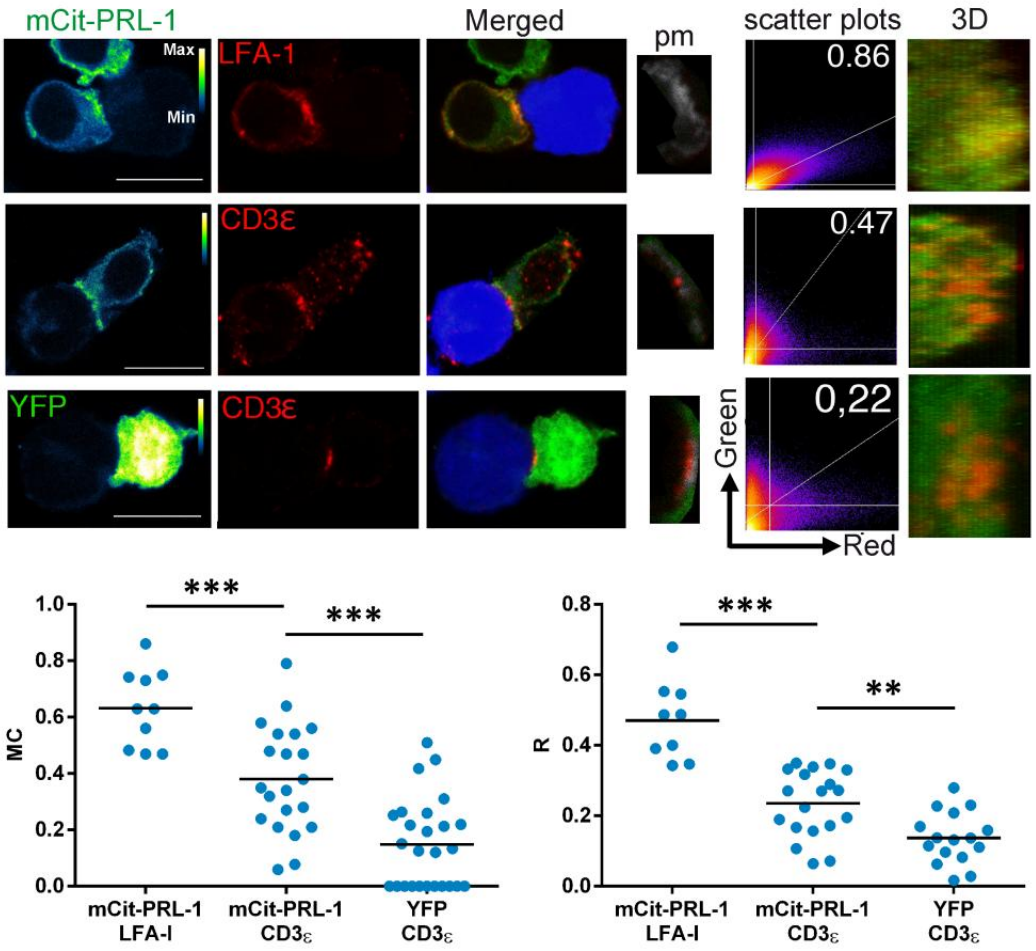

Figure R12. Colocalization of GFP-PRL-1 with LFA-1 and CD3ε at the IS. Upper images: immunofluorescence of cell conjugates formed by J77 cells overexpressing mCit-PRL-1 and SEE-pulsed RAJI cells labeled with CMAC (blue). Co-localization is shown in a pixel map (pm) obtained at the interaction zone. White pixels indicate colocalization sites. Scatter plots of green and red channels are shown. Numbers indicate the Manders coefficient (MC). A 3D reconstruction of the IS where co-localization was analyzed is shown. Scale bars 10 µm. Lower graphs: quantification of the colocalization by Manders and Pearson coefficients (MC and R, respectively). Dots represent individual cell conjugates from at least two experiments. Asterisks represent the p-values of unpaired T tests. ** p≤0.01, ***P≤0.001.

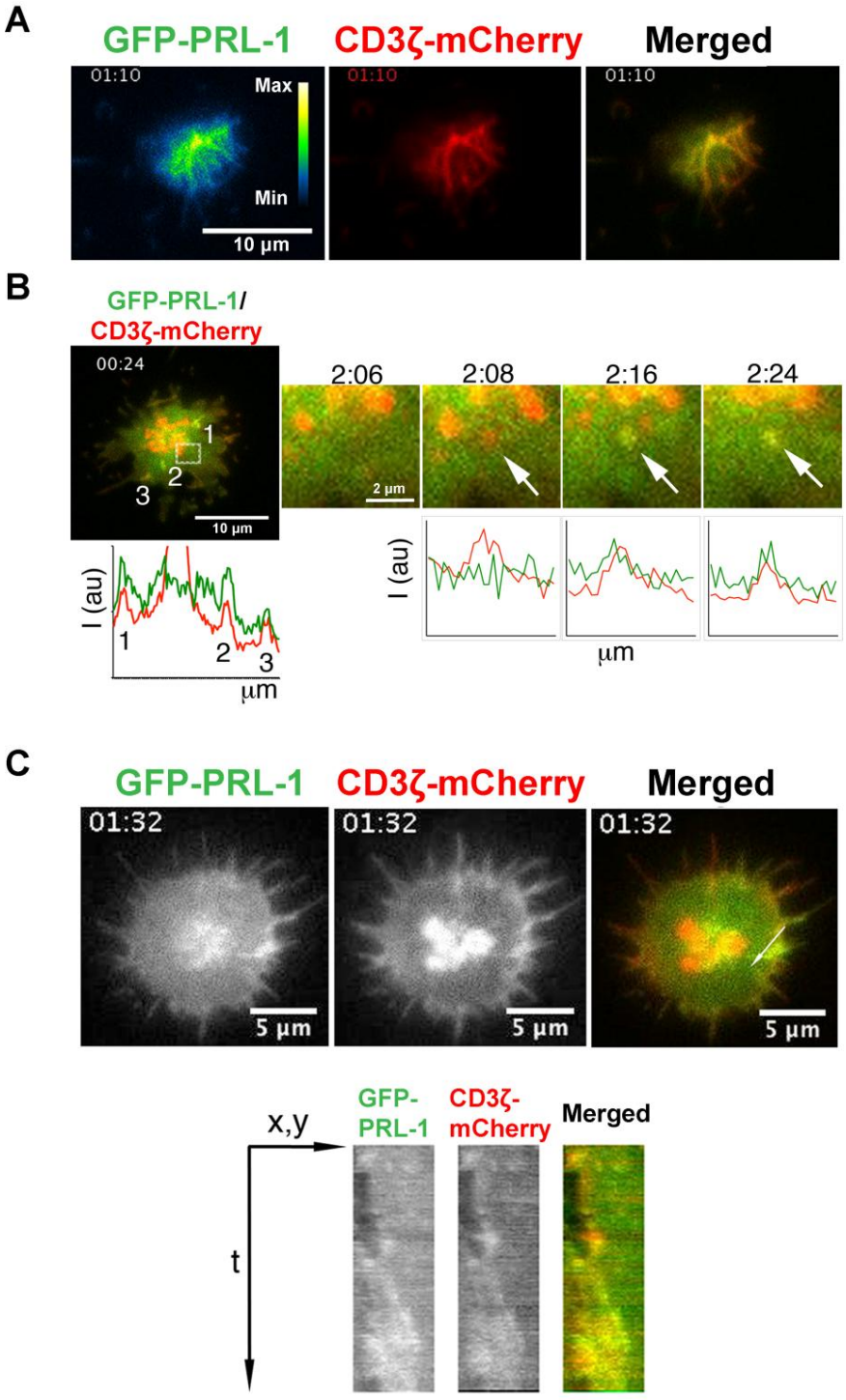

Figure R13. TIRFM imaging of GRP-PRL-1 and CD3ζ-mCherry at the IS. Images from TIRFM experiments performed with J77 cells expressing GFP-PRL-1 and CD3ζ-mCherry plated on glass bottom dishes coated with ICAM-Fc, anti-CD3ε and anti-CD28 antibodies. **A.** Time frame of the experiment in Movie 3. **B.** Merged image of a time frame of the experiment in Movie 4. Lower graph represents the profile of the fluorescence intensity of the green and red channels on the line that would cross the numbered sites in the upper image. A magnified area of the region defined by a square is shown at different time points. White arrows indicate a CD3ζ-mCherry-containing vesicle to which GFP-PRL-1 arrives. Lower graphs represent the profile of the fluorescence intensity of the green and red channels on the line that would cross the vesicle. **C.** Time frame of the experiment in Movie 5. The lower panel shows the kymograph obtained with the arrow drawn in the image. (**A to C**) Time in minutes:seconds is indicated on each image. Penetration depth: A and B, 150 nm. C, 200 nm.

5. PRL-1 contributes to T cell activation

The upregulated expression of PRL-1 upon T cell activation, the delivery to the IS and the colocalization with CD3 suggested that PRL-1 might regulate T cell activation. To address this possibility, we decided to investigate the effect of PRL-1 overexpression and PRL-1 inhibition on the induction of the activation marker CD69 and the production of IL-2. Initially, we performed PRL-1 overexpression (gain-of-function approach, GOF) in J77 cells and inhibition of PRL-1 catalytic activity (loss-of-function approach, LOF) in peripheral blood CD4 T cells (Figure R14A and B). J77 cells transfected with the plasmid coding for mCit-PRL-1 or YFP alone were cultured for 16h with Raji B cells loaded or not with SEE. Then, CD69 surface expression was analyzed by flow cytometry and IL-2 secretion by ELISA. Both CD69 induction and IL-2 secretion were increased in cells overexpressing the mCit-PRL-1 chimera compared with cells expressing YFP alone (Figure R14A). Consistently, pharmacological inhibition of the catalytic activity of PRL-1 by the specific inhibitor Procyanidin B3 (PB3) (187) decreased the amount of IL-2 secreted by peripheral blood CD4 T cells stimulated for 6 hours with beads coated with anti-CD3ε and anti-CD28 monoclonal antibodies (Figure R14B, right panel), although no significant effect was detected on CD69 induction (Figure R14B, left panel). This discrepancy between J77 and CD4 T cells prompted us to test whether PRL-1 overexpression had any effect on CD69 induction in peripheral CD4 T cells. As shown in the graph of Figure R14C, cells expressing increasing amounts of mCit-PRL-1 expressed increasing amounts of CD69 (see gates on the left dot plot and grey series on the graph). By contrast, cells expressing increasing amounts of YFP (see gates on the right dot plot and white series on the graph) showed no difference in CD69 induction. This result suggested that PRL-1 enhanced CD69 expression in a dose-dependent manner. Importantly, negative cells of both transfections (see the *Negative cells* gate in each dot plot, and the first point of the graph for each series) induced equal amounts of CD69, indicating that the same activating stimulus was applied to both conditions.

Altogether, the results of GOF and LOF experiments suggested that PRL-1 contributes to T cell activation by a mechanism involving its catalytic activity. To further investigate this mechanism, we decided to address whether PRL-1 was regulating T cell activation through the regulation of the actin cytoskeleton reported in other cell types (116, 147, 148).

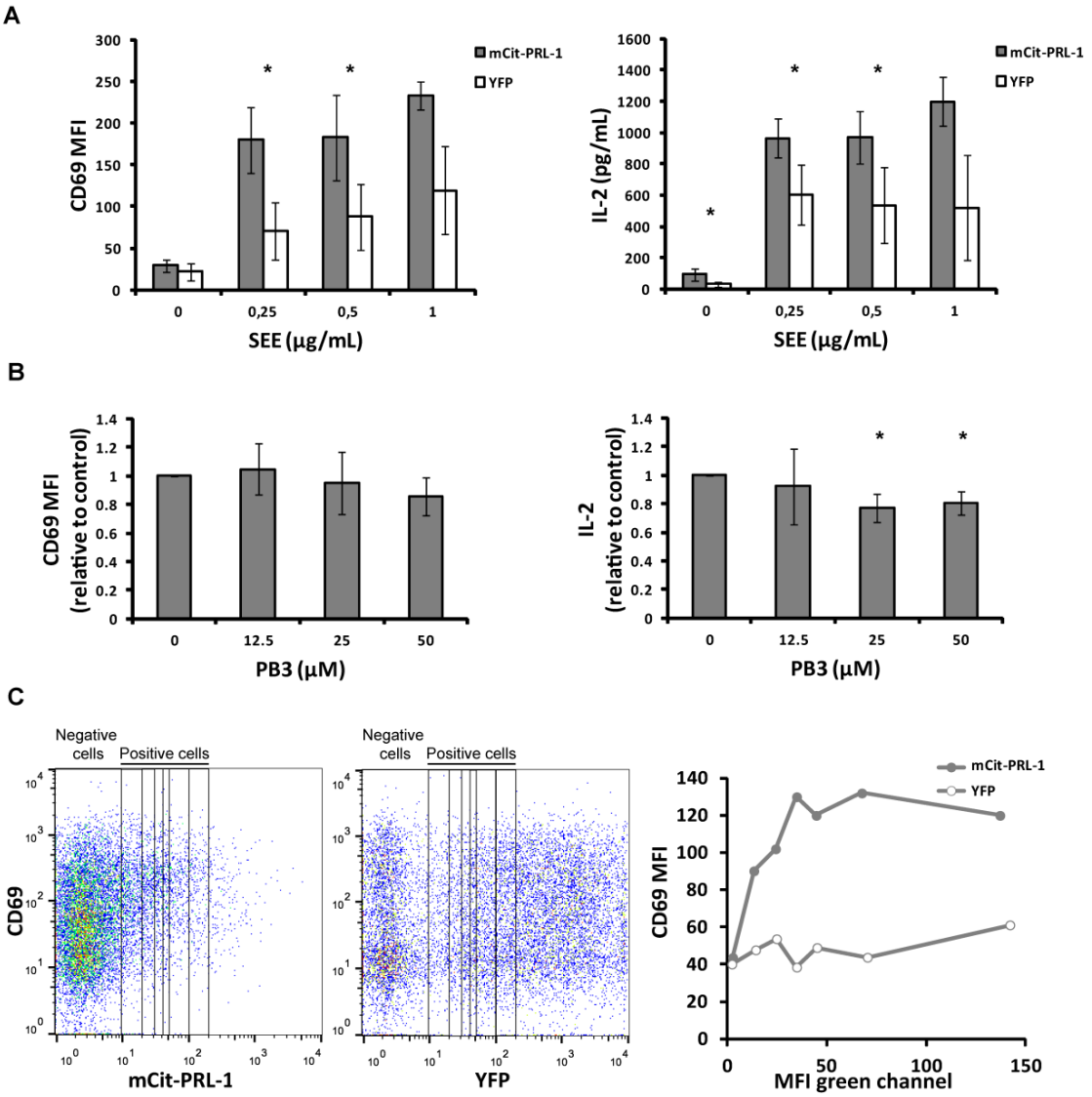

Figure R14. Regulation of T cell activation by PRL-1. CD69 expression was analyzed by flow cytometry and IL-2 production by ELISA. **A.** CD69 expression and IL-2 secretion in J77 cells overexpressing mCit-PRL-1 or YFP alone and stimulated with RAJI cells pulsed with the indicated concentrations of SEE. The means ± SD of three (SEE 0 and 0.5) or two (SEE 0.25 and 1) experiments are shown. Asterisks represent the p-value of a one-tailed paired T-test. **B**. CD69 expression and IL-2 secretion in CD4 T cells stimulated with anti-CD3ε/anti-CD28 coated beads in presence of different concentrations of PB3. Results were normalized to control (PB3 0 µM). The means ± SD of three donors are shown. **A** and **B**. Asterisks represent the p-value of a one-tailed one sample T test. * p≤0.05. **C**. Dot plot showing CD69 expression in CD4 T cells overexpressing mCit-PRL-1 of YFP. The mean fluorescence intensity (MFI) of both channels in each region drawn on the dot plot is represented in the graph on the right. A representative experiment out of three is shown. MFI, mean fluorescence intensity.

6. PRL-1 regulates actin dynamics and PLCγ1 at the IS

To investigate whether PRL-1 was regulating actin rearrangements at the IS, we imaged actin dynamics during IS formation using TIRFM. Initially, we tracked the formation of F-actin by using the LifeAct-RFP probe. An early, transient enrichment of GFP-PRL-1 preceded actin polymerization at contact sites (Figure R15A and Movie 6), suggesting that PRL-1 could participate in this process. Hence, we did GOF and LOF experiments to test this hypothesis.

For GOF experiments, J77 cells were co-transfected with a plasmid expressing mCherry-β-actin and either the plasmid expressing GFP-PRL-1 or GFP alone. This model enabled us to observe the formation of the dSMAC/lamellipodium, which contains the retrograde flow of actin and surrounds a wide central area cleared of actin (15, 186). While cells overexpressing the GFP alone spread normally and showed a typical formation of a dSMAC, cells overexpressing GFP-PRL-1 showed a reduced area of contact and a wider dSMAC surrounding smaller central areas with low actin density (Figure R15B). These experiments suggested a regulatory role of PRL-1 in actin dynamics during IS assembly.

We further studied whether the catalytic activity of PRL-1 regulated F-actin dynamics during T cell activation by doing LOF experiments. Cells were treated with the inhibitor PB3 as described in materials and methods and allowed to interact with latex beads coated with anti-CD3 and anti-CD28 antibodies as in Figure R7. Polymerization of F-actin at the IS was significantly reduced in cells treated with the inhibitor when compared with cells exposed to the vehicle as control (Figure R15C).

These data indicated that the catalytic activity of PRL-1 regulates actin dynamics during the assembly of the IS. Given that actin polymerization at the IS is required for sustained PLCγ1 activation (15), we decided to analyze PLCγ1 phosphorylation when PRL-1 was overexpressed or inhibited as before. We also analyzed ERK1/2 phosphorylation levels, since the PRLs have been shown to induce ERK1/2 activation in cancer cells (139). As shown in Figure R16A, GFP-PRL-1 overexpression increased the activation of PLCγ1, while pharmacological inhibition of PRL-1 in peripheral blood CD4 T cells reduced it. No differences were detected in ERK phosphorylation (Figure R16B) when overexpressing PRL-1 or inhibiting its catalytic activity.

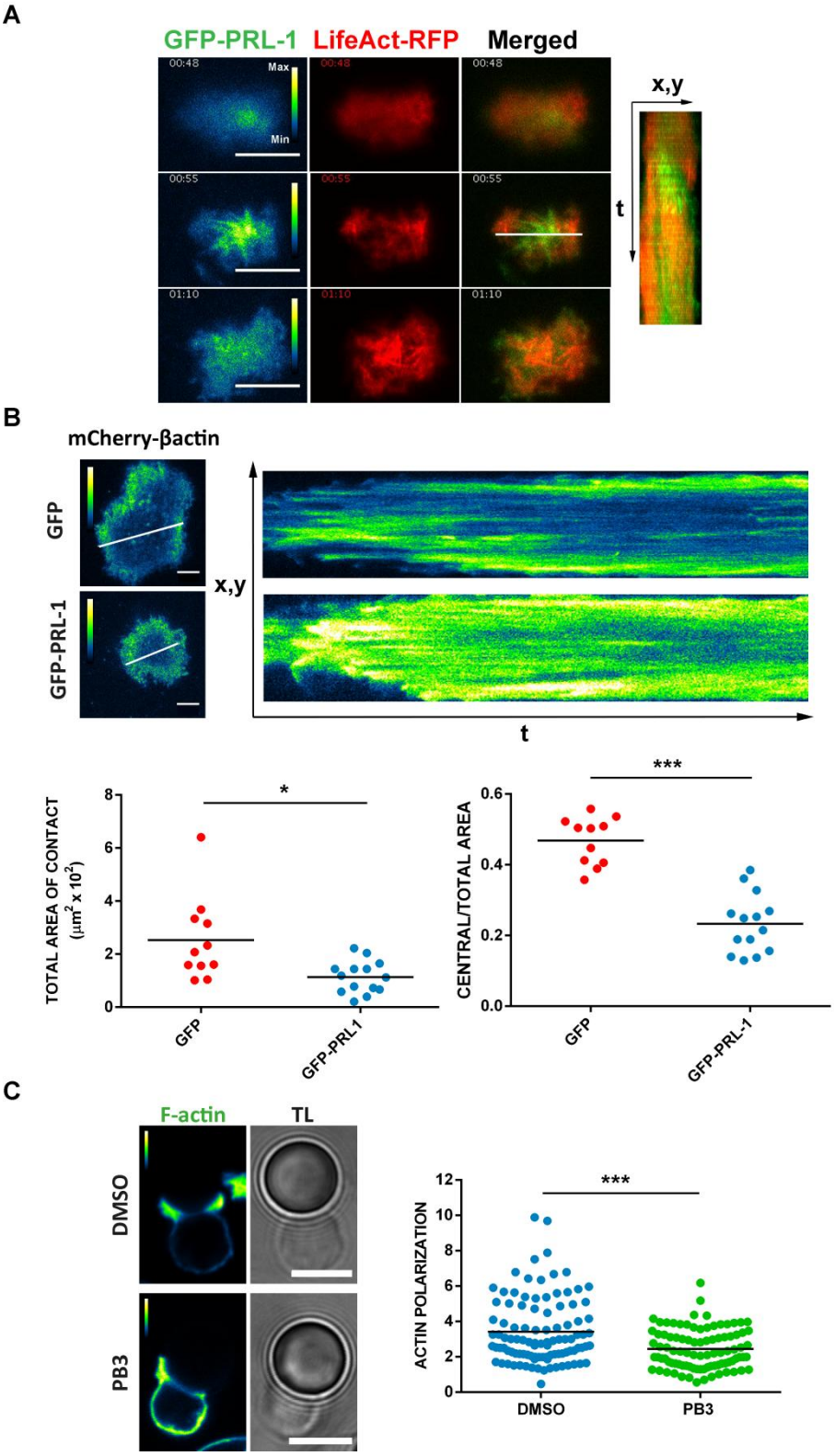

Figure R15. Regulation of actin dynamcs at the IS by PRL-1. A and **B**. Images from TIRFM experiments performed with J77 cells plated on glass bottom dishes coated with ICAM-FC, anti-CD3ε and anti-CD28 antibodies.. **A.** Images from three time frames of the experiment in Movie 6. Time in minutes:seconds is shown. The panel on the right shows the kymograph obtained with the line drawn on the merged image. Scale bar 10 μm. **B.** Representative time frames of two TIRFM experiments performed with cells overexpressing mCherry-β-actin (signal shown in pseudocolor) and GFP-PRL-1 or GFP alone (signal not shown). Kymographs were obtained with lines shown in the

frame. Scale bars 5 µm. Lower graphs represent total area and ratio of central to total area of contacts like the ones shown in the upper images. Each dot represents a single cell. **C.** Immunofluorescence of IS-like structures as in Figure R7. Cells were incubated in presence of PB3 (25 µM) or DMSO as control. Scale bars 5 µm. Graph on the right represents quantification of the actin accumulation at the IS interface. Dots in the graph represent individual cell/bead conjugates from four different donors. Asterisks represent the p-value of unpaired T-tests. * p≤0.05, *** p≤0.001.

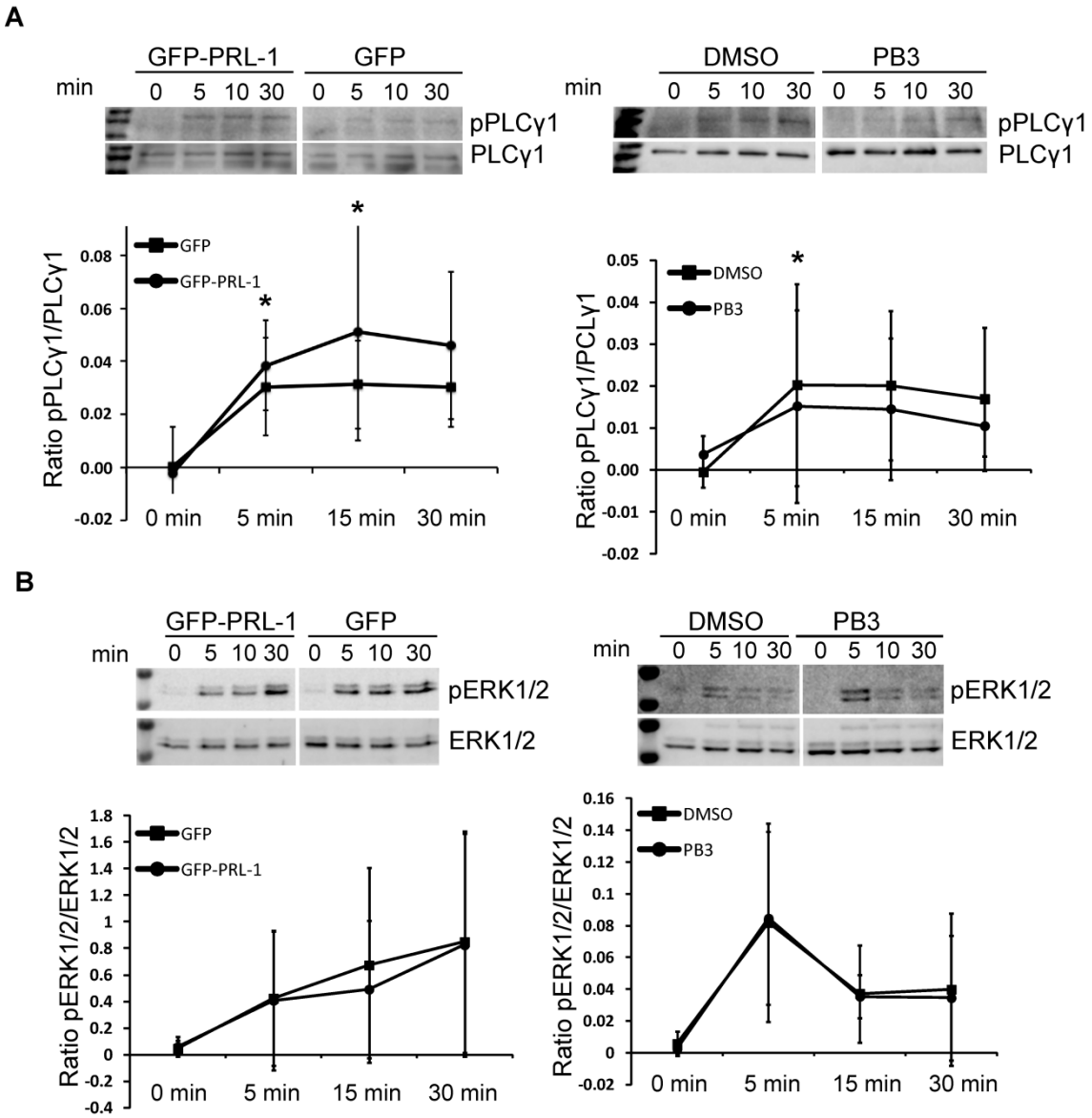

Figure R16. Regulation of early signalling downstream the TCR by PRL-1. Left panel, J77 cells overexpressing GFP-PRL-1 or GFP alone were stimulated with SEE-pulsed RAJI cells for the indicated times. Right panels, peripheral blood CD4 T cells were stimulated with ImmunoCult™ Human CD3/CD28 T Cell Activator for the indicated times in presence of PB3 (25 µM) or DMSO (control). **A.** Phosphorylated (pPLCγ1) and total PLCγ1 were analyzed by WB in J77 (left panel) and CD4 (right panel) cells. **B.** Phosphorylated (pERK1/2) and total ERK1/2 were analyzed by WB in J77 (left panel) and CD4 (right panel) cells. Graphs under the gels represent the mean ± SD of phosphorylated signal normalized to the total protein from three independent experiments. Samples at each time were compared by a paired T-test. Asterisks represent the p-value of the used tests. * p≤0.05.

Movie legends

Movie 1 and Movie 2. Dynamic distribution of GFP-PRL-1 at the IS. Time-lapse confocal microscopy experiments of J77 cells overexpressing CD3ζ-mCherry (red) and GFP-PRL-1 (green) interacting with a SEE-pulsed RAJI cell (blue). In Movie 1 separated channels as well as merged and transmission light images are shown. In Movie 2 merged and transmission light images are shown. Time in seconds (sec) is indicated. Elapsed time 5 seconds in Movie 1 and 10 seconds in Movie 2. Scale bars 10 µm.

Movie 3. Colocalization of GFP-PRL-1 and CD3ζ-mCherry during early adhesion of T cells to activating surfaces. Time-lapse TIRFM experiment showing a J77 cell overexpressing with CD3ζ-mCherry (red) and GFP-PRL-1 (green). Green (left, displayed as pseudolocor) and red (middle) channels as well as the merged image (right) are shown. Time (minutes:seconds) is indicated on the pseudocolored image and scale bar (10 µm) on the merged image. Elapsed time 1 second.

Movie 4 and Movie 5. Dynamic colocalization of GFP-PRL-1 and CD3ζ-mCherry at the IS. Time-lapse TIRFM experiments of J77 cells overexpressing CD3ζ-mCherry (red) and GFP-PRL-1 (green). Red (left) and green (middle) channels as well as the merged image (right) are shown. Time (minutes:seconds) and scale bar are indicated on the merged image. Elapsed time 1 second.

Movie 6. Enrichment of GFP-PRL-1 at sites of actin polymerization during early adhesion of T cells to activating surfaces. Time-lapse TIRFM experiment showing a J77 cell overexpressing GFP-PRL-1 (green) and LifeAct–RFP (red). Green (left) and red (middle) channels as well as the merged image (right) are shown. Time minutes:seconds and scale bar (10 µm) are indicated. Elapsed time 1 second.

DISCUSSION

DISCUSSION

1. Expression profile of NC PTPs during Th1 differentiation and restimulation

PTPs are key regulators of signaling pathways involved in almost every cellular process. More than a hundred genes coding for PTPs have been identified in the human genome (87). Although it is known that T cells express a high number of these enzymes (88), whether they play a role in T cell responses is unknown for the majority of them, especially for NC PTPs. This work aimed to identify NC PTPs that might be potential regulators of T cell activation or differentiation. As an initial approach, we performed expression studies in naïve, Th1 and restimulated Th1 cells.

The systematic analysis performed in this study reveals that several genes coding for PTPs are regulated during Th1 polarization and stimulation of effector cells. Regarding Th1 polarization, the mRNA level of the majority of the regulated genes coding for NC PTPs was increased during this process (Figure R2 and Table R2), suggesting that these PTPs might have a regulatory role in Th1 polarization or effector function.

Th1 restimulation caused both gene up- and downregulation. This might indicate that once an effector cell is recruited to the site of inflammation, it needs to reorganize a wide range of intracellular signaling networks to respond adequately, and that these networks are, at least in part, regulated by PTPs. Taken together, changes in expression levels of genes coding for PTPs during both Th1 polarization and Th1 restimulation might uncover a role of these proteins in T cell responses.

1.1 Regulators of cytokine signaling and secretion

The classical PTPs *PTPN9* (coding for PTP-MEG2) and *PTPN13* (coding for PTP-BAS or PTP-BL), which in T cells regulate cytokine secretion and signaling, respectively, were significantly upregulated during Th1 polarization (Table R2).

PTP-MEG2 regulates the fusion of secretory vesicles and promotes cytokine secretion by dephosphoorylating the N-ethylmaleimide-sensitive factor (NSF) (168). Consistently, it has

been shown that PTP-MEG2-deficient T cells show impaired IL-2 secretion (169). Hence, the upregulation of *PTPN9* found during Th1 polarization might reflect the increased cytokine secretion needed for effector T cell function. *PTPN9* shared cluster with the myotubularin *MTMR2* (Figure R2), a regulator of endosomal trafficking and phosphoinositide phosphorylation (98, 188), which was also upregulated during Th1 polarization (Table R2). Interestingly, PTP-MEG2 is activated by interaction with phosphoinositides (189, 190). Hence, the segregation of both genes in the same cluster might indicate a functional connection between these proteins. Whether MTMR2 is required for proper Th1 polarization and cytokine secretion should also be investigated.

PTP-BL has been shown to dephosphorylate and inhibit STAT4 and STAT6, and its deficiency results in enhanced Th1 and Th2 differentiation (171). Hence, *PTPN13* might be induced during Th1 polarization as a regulatory mechanism to decrease STAT6 signaling in Th1 cells. Interestingly, *PTPN13* was found in the same cluster as *PTPN18*. Both PTPs have been suggested to regulate *(PTPN18)* or associate with *(PTPN13)* the actin cytoskeleton in non-immune cells (191, 192), and they also shared cluster with the DSP *SSH3*, another regulator of the actin cytoskeleton (193). This result sets out the question of whether PTP-BL is also regulating the cytoskeleton dynamics in T cells.

1.2 MAPK regulators

The expression of MAPK regulators (MKPs and atypical DSPs) was regulated in both Th1 polarization and PI treatment (Figures R2 and R3, and Table R2). MKPs are characterized by sharing MAPK substrates. For example, ERK is dephosphorylated by 13 different MKPs. As mentioned in the introduction, the spatial distribution of dephosphorylated MAPKs is regulated by the binding of MKPs (92). For example, the nuclear ERK-specific MKPs DUSP2 DUSP4 and DUSP5 have been described to dephosphorylate ERK in the nucleus and induce its nuclear accumulation in the dephosphorylated (kinase inactive) form (92, 194, 195). On the contrary, the cytoplasmic DUSP6 dephosphorylates and retains ERK in the cytoplasm (92). The subcellular localization of dephosphorylated ERK is of great importance, because it can have functions nondependent on its kinase activity (196). For example, it has been proposed that binding of kinase-inactive ERK to DUSP6 increases the activity of this phosphatase towards p38 (197), and dephosphorylated ERK2 can also regulate gene expression and cell cycle progression

(198, 199). Interestingly, not only MKPs can regulate the subcellular localization of ERK. It has been shown that also the catalytically inactive atypical DSP STYX is a nuclear anchor for both phospho- and dephosphorylated ERK, and that it competes with DUSP4 for ERK binding (200). Thus, more than simply having a role in down-modulating the response of the module, PTPs that regulate MAPKs determine the subcellular localization and crosstalk of MAPKs. In this regard, changes in the protein dose, as may be achieved by regulating their expression levels, may enable MKPs to compete with other molecules for the binding of MAPKs. The comparison of the levels of MAPK regulators in naïve and restimulated Th1 cells (Figure D1A) could then give an idea of the differential spatial distribution of ERK in each situation (Figure D1B). In naïve T cells, the module of MAPK regulators was dominated by the nuclear *DUSP1*, which is not able to bind dephosphorylated ERK, the cytoplasmic *DUSP16*, which has not been reported to retain ERK, and the nuclear *DUSP2*, able to anchor dephosphorylated ERK in the nucleus. By contrast, the MAPK regulators with higher expression in restimulated Th1 cells were the nuclear *DUSP2*, *DUSP4* and *DUSP5*, which bind dephosphorylated ERK, promoting its accumulation in the nucleus, and the cytoplasmic *DUSP6*, able to retain dephosphorylated ERK in the cytoplasm. These data suggest that while in naïve T cells rapid nuclear translocation and transient phosphorylation of ERK should dominate the response, in restimulated effector cells dephosphorylated ERK is accumulated both in the cytoplasm and the nucleus, where it could exert functions nonrelated to its phosphorylation state.

Some MAPK regulators have been proposed to have a role in T cell responses. The most relevant findings in relation to our results will be discussed below.

The expression of DUSP5 was upregulated during Th1 restimulation (Figure R3A). This nuclear MKP has been reported to regulate Th17/Treg cell balance in a mouse model of autoimmune arthritis (201), and to participate in MAPK regulation during IL-2 signaling (181). Our data further points to a role of DUSP5 in regulation of T cell stimulation, although determining the mechanism of such regulation will require further research.

We found that *DUSP7,* the gene coding for MKP-X, was upregulated during Th1 polarization (Table R2). The role of this ERK-selective cytoplasmic phosphatase in T cell activation or differentiation has not been addressed. However, our group has recently found that *DUSP7* expression is reduced in CD4 T cells of patients with rheumatoid arthritis with respect to healthy donors (202). Interestingly, such downregulation was restricted to patients with positive rheumatoid factor and anti-citrullinated protein antibodies, suggesting that MKP-X

could be involved in T/B cooperation. Altogether, our findings point to a requirement of *DUSP7* for proper T cell effector function.

The expression of *DUSP22,* coding for the atypical DSP VHX*,* was upregulated during Th1 polarization (Table R2). VHX has been reported to control TCR signaling through different mechanisms. Initially, it was described as negative regulator of TCR-induced ERK2 activation (203), but recently it has also been shown to inactivate Lck (204). In addition, *DUSP22* knockout mice show exacerbated autoimmunity (204), and T cells of patients with nefritis associated to systemic lupus erythematosus (SLE) have less *DUSP22* expression than SLE patients without nefritis (205). The upregulation during Th1 polarization found in our work suggests that it is involved in Th1 responses. Given the role of Th17 cells in development of autoimmunity, it would be interesting to study the expression and role of *DUSP22* in Th17 polarization.

In this work, the expression of two MAPK regulators, *DUSP8* and *DUSP23*, was significantly regulated during both Th1 polarization and restimulation.

DUSP8 is a JNK/p38-selective MKP that has been identified as an upregulated gene in fungal infections (206), but its role in T cell responses has not been addressed. Interestingly, we found downregulation of *DUSP8* during Th1 polarization (Figure R2) and upregulation during Th1 restimulation (Figure R3A), suggesting that the requirements of this protein are different in N and effector Th1 cells.

DUSP23 is able dephosphorylate ERK *in vitro* (207), but no studies *in vivo* are available. Recently, it has been proposed that DUSP23 dephosphorylates β-catenin in epithelial cells (208). β-catenin is recruited to the IS, where it could anchor dynein (38). This finding, together with its location at the centrosome (209), suggests that DUSP23 could play a role in the assembly of the IS, and, consequently, in T cell activation. Our data showed a significant upregulation of *DUSP23* during both Th1 polarization and restimulation (Figures R2 and R3A). Interestingly, overexpression of DUSP23 in CD4 T cells of patients with systemic lupus erythematosus has been described (210), further pointing to a role of this phosphatase in T cell responses. Hence, studying the distribution and substrates of DUSP23 in T cells would be of great interest.

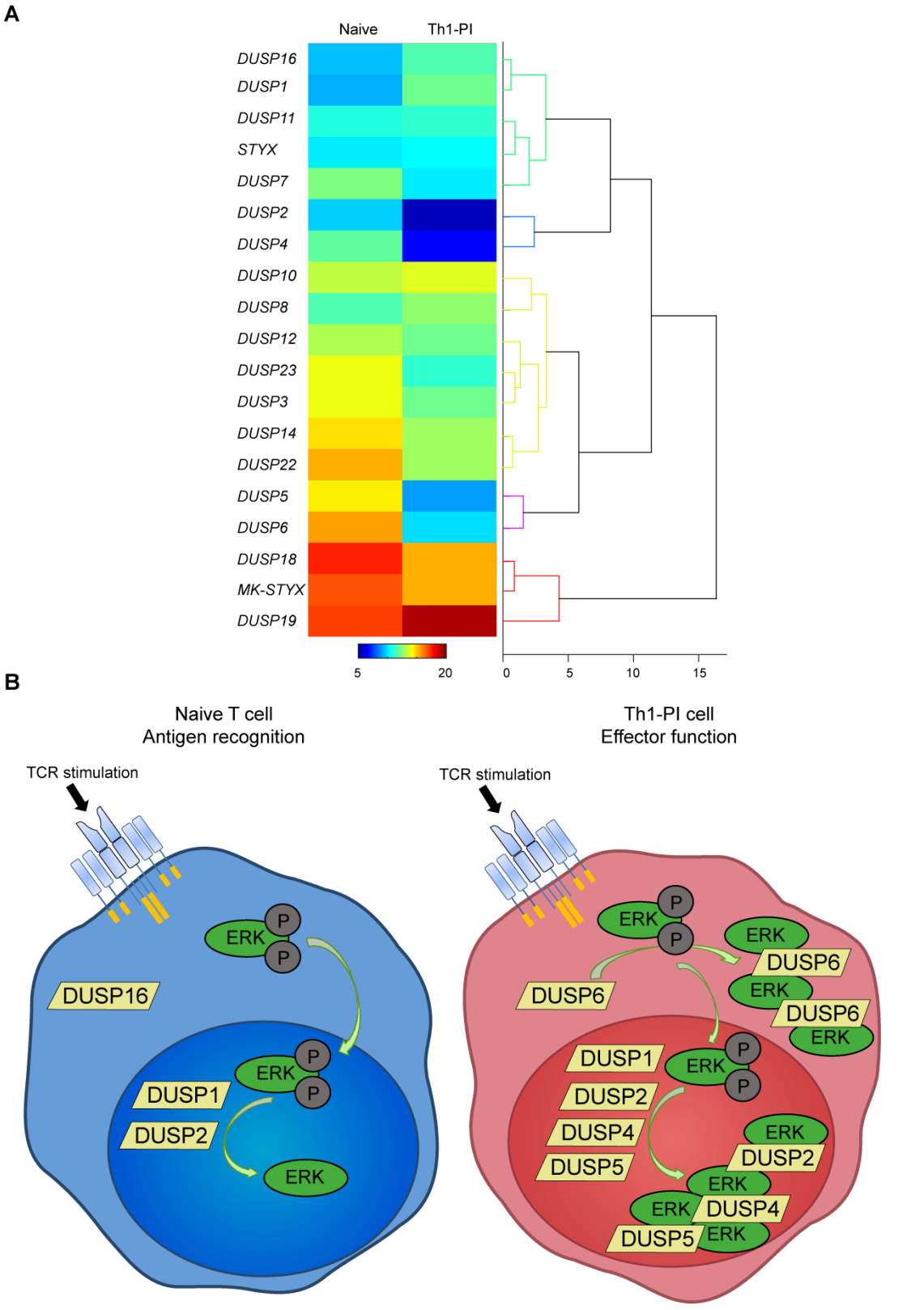

Figure D1. Expression of MAPK regulators in naïve and restimulated Th1 cells. A. Agglomerative hierarchical tree of the expression profile of MAPK regulators naïve and restimulated Th1 (Th1-PI) cells. Numbers under the tree indicate the Euclidean distance among the expression profile. Hitmap represents the average DCT obtained for each gene in four donors. Calibration bar between 5 and 20 DCT is shown. **B.** Schematic representation of the proposed spatial regulation of ERK during CD4 T cell immune responses. Dominance of partners of the dephosphorylated ERK in cytoplasm or nucleus might mediate the accumulation of this MAPK and, consequently, promote ERK functions nonmediated by the kinase activity in restimulated Th1 cells.

1.3 Cell cycle regulators

It should be noted that while naïve cells are quiescent, the effector cells generated in this work were proliferating at the moment of the analysis. Therefore, some of the genes found upregulated in Th1 cells could be promoters of cell cycle progression or mitosis. This is the case for CDC25A and CDC25B, which are known to cooperate to induce mitosis (211). Consistently, it has been shown that PD-1 inhibits T cell proliferation through suppression of CDC25A (212). Regarding CDC25B, recent findings suggest that it may play a role in T cell responses. Our group has recently found that *CDC25B* expression is impaired in CD4 T cells from patients with rheumatoid arthritis (RA) (202) , an autoimmune disease in which T cells play a central role (213). In the present work, we also found downregulation of *CDC25B* during restimulation of Th1 cells (Figure R3B), suggesting that the decreased levels of *CDC25B* found in RA patients could reflect the high inflammatory environment in RA pathology. Consistent with this idea, low levels of CDC25B correlated with the disease activity in RA patients (202). In addition, it has been reported that the CDC25B-specific kinase Aurora A participates in T cell activation sustaining signaling downstream the TCR (214). In this work, we found upregulation of *CDC25B* after Th1 polarization (Table R2). This result further suggests that CDC25B could have a function during T cell responses in addition to its role as a cell cycle regulator.

1.4 Phosphoinositide phosphatases

Among MTMs, two of them, *MTMR2* and *MTMR11* were significantly regulated during both Th1 polarization and Th1 restimulation (Figures 2 and 3C, and Table 2). The role of MTMR2 in immune cells has not been addressed, but it has been reported that it interacts with Disc large-1 (Dlg-1) (215), a protein that has been shown to regulate NFAT activation downstream the TCR through p38 (216). Recently, it has also been proposed that ezrin controls tubulin cytoskeleton dynamics, immunological synapse organization, and NFAT activation by interacting with Dlg-1 (217). Thus, it is conceivable that MTMR2 could also have a regulatory role in IS organization and Th1 cell activation through interaction with Dlg-1. In addition, it has been suggested that MTMR2 sustains Akt signaling by dephosphorylating $PI(3,5)P_2$ to PI5P (218). Hence, MTMR2 could function as a promoter of the Akt/mTOR pathway activated during T cell stimulation. Our results show upregulation of *MTMR2* during both Th1 polarization and Th1 restimulation, supporting a requirement of this enzyme in the response of Th1 cells. Unravel the role of MTMR2 in the context of T cell activation will need further research.

The PD *MTMR11* was induced with Th1 polarization and upregulated during PI treatment. PD MTMs physically interact and increase the catalytic activity of active MTMs (188), playing a key role in the regulation of this group of phosphatases. The binding partners of MTMR11, however, remain unknown. Our results encourage further research on this MTM in T cells.

1.5 SSHs

Among the cofilin regulators SSHs, the expression of *SSH1* did not change during Th1 polarization or restimulation. This might indicate that the reported regulation of SSH1 activity through phosphorylation and interaction with other proteins (219) is enough to provide adequate levels of active SSH1 during Th1 responses. *SSH2* expression was downregulated during both Th1 polarization and Th1 restimulation, while *SSH3* expression was upregulated in the first process and downregulated in the second. The different regulation of SSHs expression in this study points to non-redundant functions of these phosphatases in T cells responses. This could be the case at least for SSH3, which dephosphorylates cofilin weaker than SSH1 and 2, and did not colocalize with F-actin when overexpressed in HeLa cells (59). Recent findings of our group suggest that at least SSH1 regulates actin dynamics at the IS (220), but further investigation will be required to determine the role of each SSH in T cell activation and Th polarization.

2. Regulated expression of PRLs during T cell activation

The group of PRLs showed no regulation during Th1 polarization (Figure R2). Currently there is no information on the role of these phosphatases in T cell activation or Th polarization. The only datum available comes from the screening of a mouse phosphatase shRNA library where PRL-3-knockdown Th1 cells did not lose Tbet expression upon Th2-polarizing conditions (177). Although the authors do not discuss it further, their data suggest that PRL-3 might have a role in Th2 commitment or Th1/Th2 plasticity. Our results do not point to a different requirement in the levels of PRL-3 between naive and Th1 cells in human, but whether this is also the case for Th2 cells will require further research.

Interestingly, each member of the PRL subfamily showed a distinct pattern of expression upon Th1 restimulation (Figure R3E). *PTP4A1* was upregulated, *PTP4A2* downregulated, and *PTP4A3,* the PRL with the lowest expression, did not significantly change. Time-course analysis of PRLs expression in more donors confirmed the initial results in Th1 cells, showing increased levels of *PTP4A1* after 120 minutes of PI stimulation which were maintained until 240 minutes (Figure R4C). In peripheral blood CD4 T cells, however, the induction of *PTP4A1* was more transient and smaller than in Th1 cells, and it was downmodulated from 120 minutes onwards (Figure R4B). Such differences between Th1 and peripheral blood CD4 T cells could be explained by the fact that peripheral blood CD4 T cells were in a resting state at the moment of PI treatment, while Th1 cells had been stimulated previously with anti-CD3ε and CD28 antibodies for several days and were actively proliferating before the experiment. A differential regulation of *PTP4A1* expression in proliferating *versus* quiescent cells could explain our results. Consistent with this idea, PRL-1 is upregulated in mitogen-stimulated cells (106) and participates in mitosis (114). Besides, PRL-1 induction could depend on the activation state of cells. In our results, Th1 cells induced higher levels of both the CD69 and *PTP4A1* than CD4 T cells (Figure R4B, C and D), suggesting that higher activation induces higher PRL-1 function. This idea is further suggested by the positive correlation between PRL-1 and CD3ζ recruitment to the IS shown in Figure R7C. The upregulation of *PTP4A1* expression during T cell stimulation could be driven by the transcription factor Egr-1 (early growth response 1), which has been shown to regulate *PTP4A1* expression (221) and is also induced within the first hour of T cell stimulation (222).

The relative expression of PRLs was similar in peripheral blood CD4 and Th1 cells, with *PTP4A2* being the most abundant, followed by *PTP4A1* and *PTP4A3* (Figure R4A). However, the differential regulation of *PTP4A1* and *PTP4A2* during stimulation with PMA and Ionomycin changed this expression pattern, balancing PTP4A1 and PTP4A2 expression after 120 minutes of stimulation in both Th1 and CD4 T cells (Figure D2). Whether downregulation of PTP4A2 levels is necessary for T cell function after stimulation remains to be determined. Here, we focused in the study of PRL-1 function, since expression data suggested that its function should prevail over PRL-2 function during T cell stimulation.

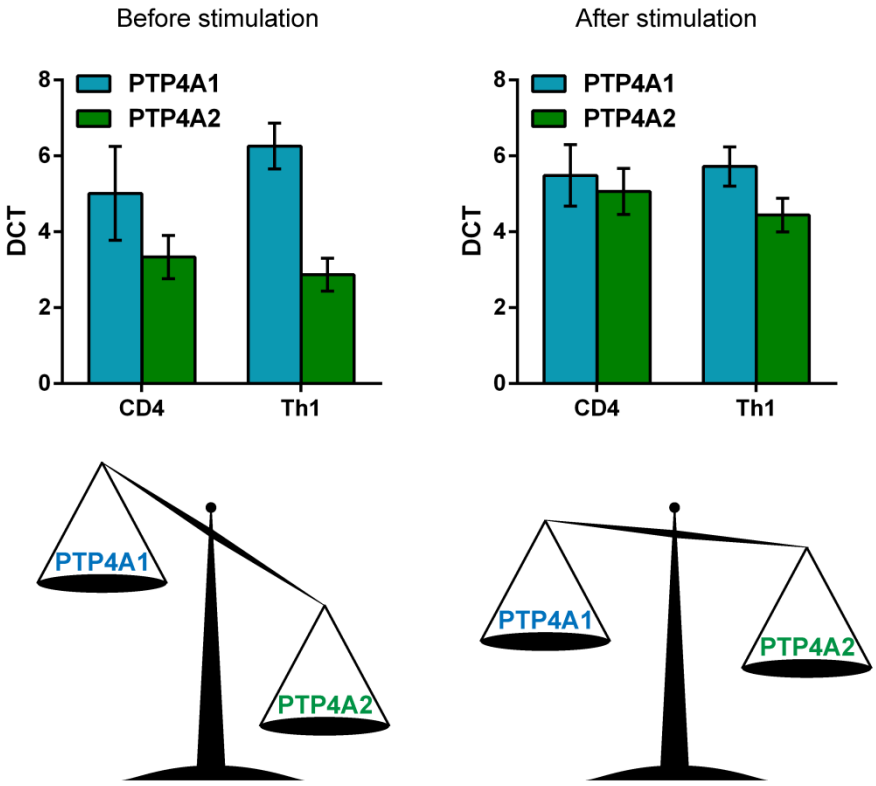

Figure D2. Regulation of the balance between PTP4A1 and PTP4A2 expression upon T cell stimulation. DCT of *PTP4A1* and *PTP4A2* in CD4 T cells before (left graph) and after (right graph) stimulation with PMA and Ionomycin. The higher levels of PTP4A2 before stimulation and the balanced expression of both genes after stimulation are represented by weighing scales.

3. Recruitment of PRL-1 to the IS

Taken together, our data show that PRL-1, which in unstimulated cells is located around the MTOC and at the plasma membrane, is polarized to the IS, suggesting a regulatory role of this protein in IS assembly or in signaling following antigenic stimulation (Figure D3). In our model, PRL-1 was delivered to the IS in two waves: an initial delivery to the plasma membrane contacting the APC, where PRL-1 could regulate actin dynamics, and a later delivery together with the MTOC where it showed localization at CD3ζ sites. PRL-1 was also present at the plasma membrane at the mature IS, where it also showed partial colocalization with LFA-I and surface CD3ε.

Localization of PRL-1 at scanning membranes was fast and transient (Figure R10A, see white arrows, and Movie 1), suggesting that there is a pool of protein able to rapidly diffuse from the

cytosol to sites where actin polymerization must take place. The regulatory role of PRL-1 in actin dynamics and lamellipodium formation will be discussed further in the next section.

The endosomal localization of PRL-1 reported in this work is consistent with previous observation of this protein at the early endosomal compartment in chinese hamster ovary (CHO) cells (115). The endosomal compartment is organized around the MTOC, from which microvesicles are directed to the IS through the microtubular network (223). This compartment plays an important role during every stage of T cell stimulation. Polarized recycling from the endosomal compartment has been proposed to be a mechanism for TCR accumulation at the IS (224), contributing to mature IS formation. Dynamic interaction between signaling complexes at the plasma membrane and intracellular vesicles carrying signaling molecules like LAT seems to contribute to the signaling process (225), and endocytosis of signaling complexes to the endosomal compartment has been suggested to mediate TCR signal extinction at the cSMAC (226, 227). Hence, localization of PRL-1 at the pericentriolar area suggests a role of the protein in controlling the microtubule dynamics, the endosomal traffic and potentially the IS organization. In fact, trafficking of the GTPase Rac-1, which is also localized at the pericentrosomal compartment, has been shown to regulate IS assembly and IL-2 secretion (228), and molecules involved in early signalling downstream the TCR, such as Lck and LAT, are also located at pericentrosomal vesicles (229). In the case of PRL-1, the reported binding to tubulin in vitro and the localization to the mitotic spindle during mitosis (114) suggest that it could regulate endosomal dynamics through rearrangement of microtubules. In addition, presence of PRL-1 in vesicles containing CD3ζ (Figures R10B, R11A, R13B, and Movies 2 and 4) suggests that PRL-1 could be regulating TCR recruitment to the IS or sustained signaling for full T cell activation. Further characterization of the endosomes where PRL-1 is localized during IS formation would be useful to determine the role of PRL-1 in TCR recruitment to the IS or in sustaining signaling. Of note, recent data in epithelial cells show that PRL-3 enhances clathrin-mediated endocytosis through dephosphorylation of $PI(4,5)P_2$, which might promote intracellular trafficking of transmembrane proteins (Mäja Kohn group, oral communication at the EMBO meeting "Europhosphatase 2017", Paris). Given the high identity between both proteins, it is conceivable that PRL-1 could also regulate endocytosis, and, therefore, play a role in traffic of TCR complexes during T cell stimulation.

The presence of PRL-1 at the plasma membrane contacting the APC, where it partially colocalized with CD3ζ (Figure R10B) and CD3ε (Figure R12), and the positive correlation found between PRL-1 and CD3ζ polarization at the IS (Figure R7C) suggested that PRL-1 substrates are

present in TCR signaling complexes, or that PRL-1 participates in TCR recruitment to the IS, or both. As will be discussed in section 5 of this Discussion, in this work we provide evidences that PRL-1 regulates actin dynamics at the IS. Hence, PRL-1 might link signalling downstream the TCR and actin rearrangements during IS assembly through a mechanism that remains to be determined.

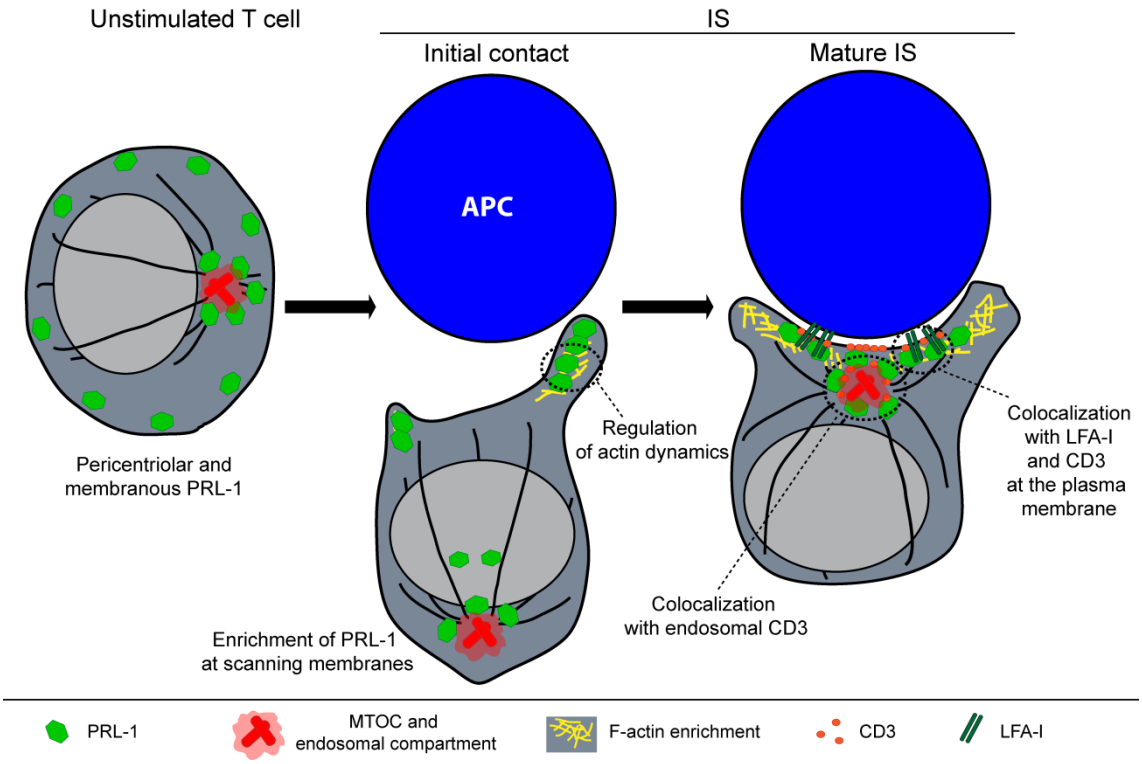

Figure D3. Model for PRL-1 distribution of PRL-1 at the IS. The recruitment of PRL-1 to the IS in two waves is schematized

The observed recruitment of PRL-1 to the IS and to vesicles containing CD3ζ was dependent on the presence of the CAAX motif (CCIQ in PRL-1), as shown by the overexpression of a mutant lacking this sequence (Figure R11B). Our finding is consistent with previous works which showed that either deletion of the whole CAAX motif, mutation of the first cysteine or treatment with farnesyltransferase inhibitors delocalized PRL-1 from plasma and endomembranes and localized it in the nucleus and the cytosol (112, 114-116). Since the mutant used in this work lacked the complete CAAX motif, we cannot determine if delocalization of the ΔCAAX mutant was due only to absence of farnesylation of the first Cys or if palmitoylation of the second Cys, as proposed for PRL-3 (117), was also involved. Our data

also point to the notion that in absence of farnesylation the polybasic region is not sufficient for membrane and endosomal targeting of PRL-1, but whether this region contributes to the enrichment of the farnesylated protein to the membrane and the IS has not been addressed in our work. Data from other groups has shown that in HEK293 cells the polybasic region is indeed necessary for proper localization of PRL-1 at the inner face of the plasma membrane (112). Hence, it would be interesting to study the distribution of a mutant lacking the polybasic region during IS formation. Besides, PRL-1 has been shown to form trimers and dimers *in vivo*, a condition that is proposed to stabilize PRL-1 at membranes and to be necessary to its cellular function (112, 120). In fact, inhibitors of PRL-1 trimerization have been shown to decrease PRL-1-mediated cell proliferation and invasion (230). It would be interesting to investigate the effect of the inhibition of PRL-1 oligomerization on PRL-1 delivery to the IS and on T cell activation.

4. Contribution of PRL-1 to T cell activation

In the present work, we show that specific inhibition of the catalytic activity of PRLs with TP results in decreased CD69 induction and IL-2 secretion upon T cell stimulation (Figure R5), indicating that PRLs are active enzymes *in vivo* and that their catalytic activity is required for full T cell activation. This is consistent with previous works showing that the oncogenic activities of PRLs require their catalytic activity (116, 147, 231). The use of the PRL-1-specific inhibitor PB3 revealed that PRL-1 phosphatase activity contributes to IL-2 secretion during T cell stimulation (Figure R15B, right panel). The effect of PRL-1 inhibition was, however, smaller than the effect of inhibiting the three PRLs, suggesting that these proteins might have overlapping functions in regulation of T cell activation. This is conceivable, given the high identity between PRLs (95), and given that PRL-1, PRL-2 and PRL-3 show similar subcellular distribution in J77 cells and the three of them are recruited to the IS (data not shown). Remarkably, PRL-1 inhibition decreased CD69 induction only slightly, not reaching statistical significance (Figure R14B, left panel). Hence, our data might indicate that PRL-2 and PRL-3 catalytic activity would also participate in T cell activation, being the main contributors to CD69 induction. It would be interesting to study the function of each member of the PRL family during T cell stimulation, in order to determine whether they have or not overlapping functions in T cell signalling. Regarding PRL-2, it has recently been shown that it is involved in T

cell development (146), but whether it also regulates mature T cell responses has not been addressed. Regarding PRL-3, the proposed substrates ezrin (125) and $PI(4,5)P_2$ (126) in non-immune cell types strongly encourages further research in T cells.

PRL-1 overexpression led to a clear increase in CD69 surface expression upon T cell stimulation, while inhibition of PRL-1 catalytic activity decreased CD69 induction only weakly (Figure R14). Such discrepancy could be explained by the fact that when PRL-1 is overexpressed, both phosphatase dependent and independent activities are enhanced, while when using an inhibitor, phosphatase activity is decreased, but functions independent on dephosphorylation remain intact. Hence, increased CD69 induction observed when overexpressing PRL-1 could be mediated, at least in part, by a mechanism independent of PRL-1 catalytic activity. To address this issue, it would be useful to study the effect of interfering PRL-1 expression, or the effect of overexpressing a catalytically inactive mutant. Of note, it has been proposed that PRL-1 promotes ERK-1/2 activation by binding and displacing the MEKK1 inhibitor p115RhoGAP (141). Binding to p115RhoGAP does not take place through the catalytic region of PRL-1, but whether this mechanism indirectly requires phosphatase activity remains to be determined. Although p115RhoGAP is expressed by T cells (232), we have not detected enhanced ERK-1/2 phosphorylation when overexpressing or inhibiting PRL-1 (Figure R16B). Hence, an alternative mechanism should be behind PRL-1-mediated upregulation of CD69. Such mechanism could be mediated by the actin rearrangements and PLCγ1 activation, as will be discussed in the next section. It is also conceivable that PRL-1 regulates T cell signalling by a mechanism involving its catalytic activity, but independent on actin dynamics. Until date, the only substrate proposed for PRL-1 is ATF-7 (124). This activating transcription factor belongs to the AP-1 family (233). Hence, it might be involved in regulation of IL-2 expression during T cell activation. In fact, the related ATF-2 has been shown to induce IFNγ expression in T cells (234). It would be interesting to determine if the enhanced IL-2 secretion we found is a result of enhanced gene expression or increased exocytosis. Besides, our work suggests the existence of yet unknown substrates of PRL-1 at the IS, specially at sites enriched in CD3 and LFA-I, and at the pericentriolar compartment. Further research will be needed to identify such substrates.

5. PRL-1 regulates actin dynamics at the IS

In this work, we show that PRL-1 is rapidly recruited to membrane protrusions during the scanning phase of IS formation (Figure R10A and Movie 1) and to sites of actin polymerization during early contact with activating surfaces (Figure R14A and Movie 6). These observations suggested that PRL-1 was regulating actin dynamics during initial steps of IS formation.

Initial scanning of the APC by the moving T cell leads to TCR and LFA-I engagement at the leading lamellipodium. TCR and LFA-I engagement induces a stable contact between the APC and the T cell (9). Actin polymerizes at the leading edge of moving cells, and the formation of the lamellipodium is regulated by the actin nucleation factor Wave2, as demonstrated by the fact that knockdown of Wave2 in Jurkat T cells impairs cell spreading on anti-CD3 coated coverslips (52). Interestingly, we observed that PRL-1 overexpression in J77 cells also led to impaired cell spreading on activating surfaces (Figure R15B), showing a similar, although less dramatic effect than Wave2 knockdown. This result suggested that PRL-1 could be inhibiting Wave2 function. Wave2 is activated by the Rho family GTPase Rac1 (235), which is transiently activated upon TCR and LFA-I stimulation (48, 236). Interestingly, two different groups have shown that overexpression of PRL-1 in epithelial cells leads to decreased GTP-Rac (active) levels, without altering total Rac (116, 147). This effect seems to be independent on the phosphatase activity, since overexpression of catalytically inactive mutants of PRL-1 also decrease Rac activation (147). Hence, the impaired cell spreading reported in our work could be due to a defective Wave2 activation, caused by PRL-1-mediated inhibition of Rac1. It would be interesting to analyze GTP-Rac1 levels in T cells overexpressing PRL-1 to determine if this regulatory pathway is indeed taking place in our system, and to confirm if this effect is independent of PRL-1 catalytic activity, as previously reported (147).

During cell spreading, actin is polymerized at the periphery of the interaction and depolymerized at the central area, leading to the formation of a dynamic actin ring (186). As mentioned in the introduction, actin depolymerization at the IS is promoted by cofilin, an actin severing protein that is activated during TCR/CD28 signaling (58) and inactivated downstream RhoA/ROCK/LIMK pathway (61, 62). In this work, we observed that PRL-1 overexpression impaired actin clearance during IS assembly (Figure R15B), suggesting that actin depolymerization could be regulated by PRL-1. Interestingly, PRL-1 has been shown to activate

RhoA in a manner that requires its catalytic activity (116, 147). Hence, overexpression of PRL-1 in J77 cells might enhance RhoA activation, leading to an increase in LIMK activity that would result in augmented cofilin inhibition and, as a consequence, defective actin depolymerization at the IS (Figure D4A).

In the present work, we also observed that inhibition of the catalytic activity of PRL-1 resulted in decreased F-actin accumulation at the IS (Figure R15C). This phenotype could be due to increased actin depolymerization. As mentioned before, actin depolymerization is induced by the RhoA/ROCK/LIMK pathway (61, 62), and PRL-1 has been shown to activate RhoA by a mechanism that requires its catalytic activity (116, 147). Although the cited works were performed overexpressing WT or catalyticallt inactive mutants of PRL-1, it is conceivable that endogenous PRL-1 might also be maintaining basal levels of active RhoA through its enzymatic activity. Hence, inhibition of PRL-1 catalytic activity would result in impaired RhoA activation, leading to accumulation of active cofilin and, a consequence, enhanced actin depolymerization and less F-actin at the IS (Figure D4B). Interestingly, crosstalk between RhoA and signaling through LFA-I has been reported. It has been proposed that RhoA is activated by the cytoplasmic protein cytohesin-1 (237), which binds to and activates LFA-I in Jurkat cells (238). Besides, it has been shown that in lymphocytes RhoA enhances LFA-I adhesion to ICAM-I by inducing LFA-I high affinity state (239). The high colocalization found between GFP-PRL-1 and LFA-I at the mature IS in this work (Figure R12) suggests that PRL-1 could be involved in the crosstalk between LFA-I and RhoA, linking integrin signaling and regulation of actin dynamics at the IS.

Proper actin flow is required for sustaining T cell signalling, including PLCγ1 activation (15). In this work, we found decreased PLCγ1 activation when PRL-1 was inhibited, and enhanced PLCγ1 phosphorylation when PRL-1 was overexpressed (Figure R16A). Hence, in our system, defective actin phosphorylation upon PRL-1 activation could result in defective formation of signaling clusters, leading to decreased PLCγ1 activation and, as a consequence, less IL-2 secretion and CD69 expression. By contrast, increased actin polymerization at the area of contact induced by PRL-1 overexpression could maintain signaling clusters at the interaction for longer times, sustaining early signaling. This would lead to enhanced PLCγ1 activation, and consequently to increased IL-2 secretion and CD69 induction.

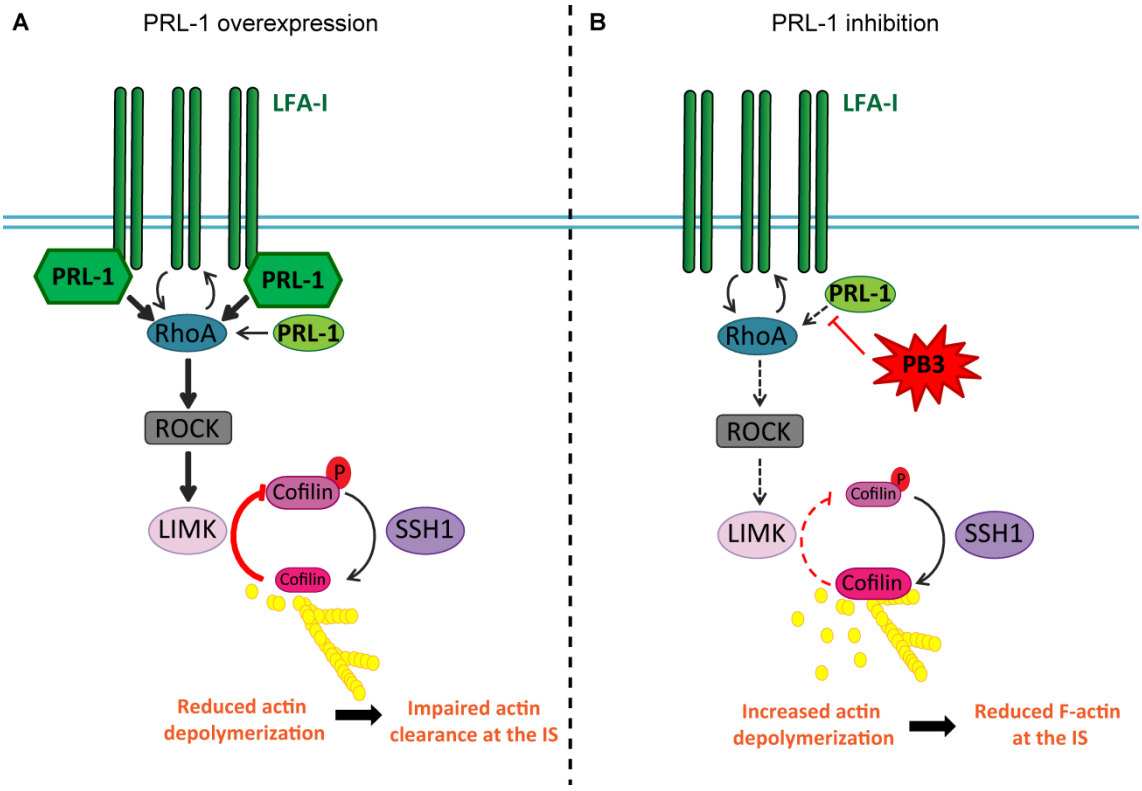

Figure D4. Regulation of actin dynamics by PRL-1 through activation of RhoA. A. Effect of PRL-1 overexpression in regulation of actin dynamics. GFP-PRL-1 is represented as a green hexagon, and endogenous PRL-1 as a light green ellipse. **B.** Effect of endogenous PRL-1 inhibition by PB3. Grey arrows indicate activation. Red line indicates inhibition. Orange arrows indicate dynamics of actin.

Altogether, our data point to a role of PRL-1 in regulating actin polymerization during IS assembly, and consequently T cell signaling required for full T cell activation. This is consistent with previous findings in cancer models, and provides the first evidence of a role of PRL-1 in cytoskeletal rearrangements and T cell activation

CONCLUSIONS

CONCLUSIONS

1. Th1 polarization induces upregulation of the expression levels of several NC PTPs, suggesting a different requirement of these enzimes in naïve versus effector cells.

2. The expression of several NC PTPs is regulated upon stimulation of Th1 cells, suggesting that some of these enzimes could be novel regulators of T cell effector function in responses at sites of inflammation.

3. PRLs might regulate T cell activation, as suggested by the fact that (i) their expression levels in CD4 T cells are comparable to that of PTPs known to regulate T cell activation, (ii) the expression of PTP4A1 and PTP4A2 is regulated during T cell activation, resulting in a balanced expression of both genes, and (iii) the catalytic activity of PRLs is required for T cell activation

4. PRL-1 participates in IS assembly and signaling, as suggested by its recruitment to the IS in two waves: an initial recruitment to scanning membranes and a later delivery in the endosomal compartment at the stablished IS, where it colocalizes with LFA-I and CD3

5. PRL-1 regulates actin rearrangements during IS assembly and positively regulates PLCγ-1 activation and IL-2 secretion during T cell stimulation through a mechanism involving its catalytic activity.

Altogether, our data encourage further research on the role of NC PTPs in T cell responses and provides evidences that PRL-1 is a positive regulator of T cell stimulation

REFERENCES

REFERENCES

1. Sallusto F, Lanzavecchia A. Heterogeneity of CD4+ memory T cells: functional modules for tailored immunity. Eur J Immunol. 2009;39(8):2076-82.
2. Raphael I, Nalawade S, Eagar TN, Forsthuber TG. T cell subsets and their signature cytokines in autoimmune and inflammatory diseases. Cytokine. 2015;74(1):5-17.
3. Starr TK, Jameson SC, Hogquist KA. Positive and negative selection of T cells. Annu Rev Immunol. 2003;21:139-76.
4. Berard M, Tough DF. Qualitative differences between naive and memory T cells. Immunology. 2002;106(2):127-38.
5. Miller MJ, Hejazi AS, Wei SH, Cahalan MD, Parker I. T cell repertoire scanning is promoted by dynamic dendritic cell behavior and random T cell motility in the lymph node. Proc Natl Acad Sci U S A. 2004;101(4):998-1003.
6. Mempel TR, Henrickson SE, Von Andrian UH. T-cell priming by dendritic cells in lymph nodes occurs in three distinct phases. Nature. 2004;427(6970):154-9.
7. Zhu J, Paul WE. CD4 T cells: fates, functions, and faults. Blood. 2008;112(5):1557-69.
8. Dustin ML, Olszowy MW, Holdorf AD, Li J, Bromley S, Desai N, et al. A novel adaptor protein orchestrates receptor patterning and cytoskeletal polarity in T-cell contacts. Cell. 1998;94(5):667-77.
9. Dustin ML, Bromley SK, Kan Z, Peterson DA, Unanue ER. Antigen receptor engagement delivers a stop signal to migrating T lymphocytes. Proc Natl Acad Sci U S A. 1997;94(8):3909-13.
10. Bunnell SC, Kapoor V, Trible RP, Zhang W, Samelson LE. Dynamic actin polymerization drives T cell receptor-induced spreading: a role for the signal transduction adaptor LAT. Immunity. 2001;14(3):315-29.
11. Yokosuka T, Sakata-Sogawa K, Kobayashi W, Hiroshima M, Hashimoto-Tane A, Tokunaga M, et al. Newly generated T cell receptor microclusters initiate and sustain T cell activation by recruitment of Zap70 and SLP-76. Nat Immunol. 2005;6(12):1253-62.
12. Yi J, Wu XS, Crites T, Hammer JA, 3rd. Actin retrograde flow and actomyosin II arc contraction drive receptor cluster dynamics at the immunological synapse in Jurkat T cells. Mol Biol Cell. 2012;23(5):834-52.
13. Kaizuka Y, Douglass AD, Varma R, Dustin ML, Vale RD. Mechanisms for segregating T cell receptor and adhesion molecules during immunological synapse formation in Jurkat T cells. Proc Natl Acad Sci U S A. 2007;104(51):20296-301.
14. Varma R, Campi G, Yokosuka T, Saito T, Dustin ML. T cell receptor-proximal signals are sustained in peripheral microclusters and terminated in the central supramolecular activation cluster. Immunity. 2006;25(1):117-27.
15. Babich A, Li S, O'Connor RS, Milone MC, Freedman BD, Burkhardt JK. F-actin polymerization and retrograde flow drive sustained PLCgamma1 signaling during T cell activation. J Cell Biol. 2012;197(6):775-87.
16. Kupfer A, Dennert G, Singer SJ. Polarization of the Golgi apparatus and the microtubule-organizing center within cloned natural killer cells bound to their targets. Proc Natl Acad Sci U S A. 1983;80(23):7224-8.
17. Stinchcombe JC, Majorovits E, Bossi G, Fuller S, Griffiths GM. Centrosome polarization delivers secretory granules to the immunological synapse. Nature. 2006;443(7110):462-5.
18. Martin-Cofreces NB, Robles-Valero J, Cabrero JR, Mittelbrunn M, Gordon-Alonso M, Sung CH, et al. MTOC translocation modulates IS formation and controls sustained T cell signaling. J Cell Biol. 2008;182(5):951-62.

19. Martin-Cofreces NB, Baixauli F, Lopez MJ, Gil D, Monjas A, Alarcon B, et al. End-binding protein 1 controls signal propagation from the T cell receptor. EMBO J. 2012;31(21):4140-52.
20. Hashimoto-Tane A, Yokosuka T, Sakata-Sogawa K, Sakuma M, Ishihara C, Tokunaga M, et al. Dynein-driven transport of T cell receptor microclusters regulates immune synapse formation and T cell activation. Immunity. 2011;34(6):919-31.
21. Monks CR, Freiberg BA, Kupfer H, Sciaky N, Kupfer A. Three-dimensional segregation of supramolecular activation clusters in T cells. Nature. 1998;395(6697):82-6.
22. Lee KH, Dinner AR, Tu C, Campi G, Raychaudhuri S, Varma R, et al. The immunological synapse balances T cell receptor signaling and degradation. Science. 2003;302(5648):1218-22.
23. Yokosuka T, Kobayashi W, Sakata-Sogawa K, Takamatsu M, Hashimoto-Tane A, Dustin ML, et al. Spatiotemporal regulation of T cell costimulation by TCR-CD28 microclusters and protein kinase C theta translocation. Immunity. 2008;29(4):589-601.
24. Hashimoto-Tane A, Saito T. Dynamic Regulation of TCR-Microclusters and the Microsynapse for T Cell Activation. Front Immunol. 2016;7:255.
25. Sperling AI, Sedy JR, Manjunath N, Kupfer A, Ardman B, Burkhardt JK. TCR signaling induces selective exclusion of CD43 from the T cell-antigen-presenting cell contact site. J Immunol. 1998;161(12):6459-62.
26. Comrie WA, Burkhardt JK. Action and Traction: Cytoskeletal Control of Receptor Triggering at the Immunological Synapse. Front Immunol. 2016;7:68.
27. Alarcon B, Mestre D, Martinez-Martin N. The immunological synapse: a cause or consequence of T-cell receptor triggering? Immunology. 2011;133(4):420-5.
28. Gil D, Schamel WW, Montoya M, Sanchez-Madrid F, Alarcon B. Recruitment of Nck by CD3 epsilon reveals a ligand-induced conformational change essential for T cell receptor signaling and synapse formation. Cell. 2002;109(7):901-12.
29. Risueno RM, Schamel WW, Alarcon B. T cell receptor engagement triggers its CD3epsilon and CD3zeta subunits to adopt a compact, locked conformation. PLoS One. 2008;3(3):e1747.
30. Palacios EH, Weiss A. Function of the Src-family kinases, Lck and Fyn, in T-cell development and activation. Oncogene. 2004;23(48):7990-8000.
31. Chan AC, Iwashima M, Turck CW, Weiss A. ZAP-70: a 70 kd protein-tyrosine kinase that associates with the TCR zeta chain. Cell. 1992;71(4):649-62.
32. Dennehy KM, Elias F, Na SY, Fischer KD, Hunig T, Luhder F. Mitogenic CD28 signals require the exchange factor Vav1 to enhance TCR signaling at the SLP-76-Vav-Itk signalosome. J Immunol. 2007;178(3):1363-71.
33. Pages F, Ragueneau M, Rottapel R, Truneh A, Nunes J, Imbert J, et al. Binding of phosphatidylinositol-3-OH kinase to CD28 is required for T-cell signalling. Nature. 1994;369(6478):327-9.
34. Heyeck SD, Wilcox HM, Bunnell SC, Berg LJ. Lck phosphorylates the activation loop tyrosine of the Itk kinase domain and activates Itk kinase activity. J Biol Chem. 1997;272(40):25401-8.
35. Feske S, Giltnane J, Dolmetsch R, Staudt LM, Rao A. Gene regulation mediated by calcium signals in T lymphocytes. Nat Immunol. 2001;2(4):316-24.
36. Macian F, Lopez-Rodriguez C, Rao A. Partners in transcription: NFAT and AP-1. Oncogene. 2001;20(19):2476-89.
37. Quann EJ, Liu X, Altan-Bonnet G, Huse M. A cascade of protein kinase C isozymes promotes cytoskeletal polarization in T cells. Nat Immunol. 2011;12(7):647-54.
38. Combs J, Kim SJ, Tan S, Ligon LA, Holzbaur EL, Kuhn J, et al. Recruitment of dynein to the Jurkat immunological synapse. Proc Natl Acad Sci U S A. 2006;103(40):14883-8.

39. Jun JE, Yang M, Chen H, Chakraborty AK, Roose JP. Activation of extracellular signal-regulated kinase but not of p38 mitogen-activated protein kinase pathways in lymphocytes requires allosteric activation of SOS. Mol Cell Biol. 2013;33(12):2470-84.
40. Salojin KV, Zhang J, Delovitch TL. TCR and CD28 are coupled via ZAP-70 to the activation of the Vav/Rac-1-/PAK-1/p38 MAPK signaling pathway. J Immunol. 1999;163(2):844-53.
41. Salvador JM, Mittelstadt PR, Guszczynski T, Copeland TD, Yamaguchi H, Appella E, et al. Alternative p38 activation pathway mediated by T cell receptor-proximal tyrosine kinases. Nat Immunol. 2005;6(4):390-5.
42. Ashwell JD. The many paths to p38 mitogen-activated protein kinase activation in the immune system. Nat Rev Immunol. 2006;6(7):532-40.
43. Su B, Jacinto E, Hibi M, Kallunki T, Karin M, Ben-Neriah Y. JNK is involved in signal integration during costimulation of T lymphocytes. Cell. 1994;77(5):727-36.
44. Jacinto E, Werlen G, Karin M. Cooperation between Syk and Rac1 leads to synergistic JNK activation in T lymphocytes. Immunity. 1998;8(1):31-41.
45. Blonska M, Pappu BP, Matsumoto R, Li H, Su B, Wang D, et al. The CARMA1-Bcl10 signaling complex selectively regulates JNK2 kinase in the T cell receptor-signaling pathway. Immunity. 2007;26(1):55-66.
46. Baker RG, Hsu CJ, Lee D, Jordan MS, Maltzman JS, Hammer DA, et al. The adapter protein SLP-76 mediates "outside-in" integrin signaling and function in T cells. Mol Cell Biol. 2009;29(20):5578-89.
47. Perez OD, Mitchell D, Jager GC, South S, Murriel C, McBride J, et al. Leukocyte functional antigen 1 lowers T cell activation thresholds and signaling through cytohesin-1 and Jun-activating binding protein 1. Nat Immunol. 2003;4(11):1083-92.
48. Sanchez-Martin L, Sanchez-Sanchez N, Gutierrez-Lopez MD, Rojo AI, Vicente-Manzanares M, Perez-Alvarez MJ, et al. Signaling through the leukocyte integrin LFA-1 in T cells induces a transient activation of Rac-1 that is regulated by Vav and PI3K/Akt-1. J Biol Chem. 2004;279(16):16194-205.
49. Bianchi E, Denti S, Granata A, Bossi G, Geginat J, Villa A, et al. Integrin LFA-1 interacts with the transcriptional co-activator JAB1 to modulate AP-1 activity. Nature. 2000;404(6778):617-21.
50. Labno CM, Lewis CM, You D, Leung DW, Takesono A, Kamberos N, et al. Itk functions to control actin polymerization at the immune synapse through localized activation of Cdc42 and WASP. Curr Biol. 2003;13(18):1619-24.
51. Pauker MH, Reicher B, Joseph N, Wortzel I, Jakubowicz S, Noy E, et al. WASp family verprolin-homologous protein-2 (WAVE2) and Wiskott-Aldrich syndrome protein (WASp) engage in distinct downstream signaling interactions at the T cell antigen receptor site. J Biol Chem. 2014;289(50):34503-19.
52. Nolz JC, Gomez TS, Zhu P, Li S, Medeiros RB, Shimizu Y, et al. The WAVE2 complex regulates actin cytoskeletal reorganization and CRAC-mediated calcium entry during T cell activation. Curr Biol. 2006;16(1):24-34.
53. Gomez TS, McCarney SD, Carrizosa E, Labno CM, Comiskey EO, Nolz JC, et al. HS1 functions as an essential actin-regulatory adaptor protein at the immune synapse. Immunity. 2006;24(6):741-52.
54. Goley ED, Welch MD. The ARP2/3 complex: an actin nucleator comes of age. Nat Rev Mol Cell Biol. 2006;7(10):713-26.
55. Uruno T, Zhang P, Liu J, Hao JJ, Zhan X. Haematopoietic lineage cell-specific protein 1 (HS1) promotes actin-related protein (Arp) 2/3 complex-mediated actin polymerization. Biochem J. 2003;371(Pt 2):485-93.
56. Pavlov D, Muhlrad A, Cooper J, Wear M, Reisler E. Actin filament severing by cofilin. J Mol Biol. 2007;365(5):1350-8.

57. Eibert SM, Lee KH, Pipkorn R, Sester U, Wabnitz GH, Giese T, et al. Cofilin peptide homologs interfere with immunological synapse formation and T cell activation. Proc Natl Acad Sci U S A. 2004;101(7):1957-62.
58. Wabnitz GH, Nebl G, Klemke M, Schroder AJ, Samstag Y. Phosphatidylinositol 3-kinase functions as a Ras effector in the signaling cascade that regulates dephosphorylation of the actin-remodeling protein cofilin after costimulation of untransformed human T lymphocytes. J Immunol. 2006;176(3):1668-74.
59. Ohta Y, Kousaka K, Nagata-Ohashi K, Ohashi K, Muramoto A, Shima Y, et al. Differential activities, subcellular distribution and tissue expression patterns of three members of Slingshot family phosphatases that dephosphorylate cofilin. Genes Cells. 2003;8(10):811-24.
60. Nishita M, Tomizawa C, Yamamoto M, Horita Y, Ohashi K, Mizuno K. Spatial and temporal regulation of cofilin activity by LIM kinase and Slingshot is critical for directional cell migration. J Cell Biol. 2005;171(2):349-59.
61. Amano M, Nakayama M, Kaibuchi K. Rho-kinase/ROCK: A key regulator of the cytoskeleton and cell polarity. Cytoskeleton (Hoboken). 2010;67(9):545-54.
62. Maekawa M, Ishizaki T, Boku S, Watanabe N, Fujita A, Iwamatsu A, et al. Signaling from Rho to the actin cytoskeleton through protein kinases ROCK and LIM-kinase. Science. 1999;285(5429):895-8.
63. Szabo SJ, Kim ST, Costa GL, Zhang X, Fathman CG, Glimcher LH. A novel transcription factor, T-bet, directs Th1 lineage commitment. Cell. 2000;100(6):655-69.
64. Lighvani AA, Frucht DM, Jankovic D, Yamane H, Aliberti J, Hissong BD, et al. T-bet is rapidly induced by interferon-gamma in lymphoid and myeloid cells. Proc Natl Acad Sci U S A. 2001;98(26):15137-42.
65. Abbas AK, Murphy KM, Sher A. Functional diversity of helper T lymphocytes. Nature. 1996;383(6603):787-93.
66. Kaplan MH, Schindler U, Smiley ST, Grusby MJ. Stat6 is required for mediating responses to IL-4 and for development of Th2 cells. Immunity. 1996;4(3):313-9.
67. Zheng W, Flavell RA. The transcription factor GATA-3 is necessary and sufficient for Th2 cytokine gene expression in CD4 T cells. Cell. 1997;89(4):587-96.
68. Jorritsma PJ, Brogdon JL, Bottomly K. Role of TCR-induced extracellular signal-regulated kinase activation in the regulation of early IL-4 expression in naive CD4+ T cells. J Immunol. 2003;170(5):2427-34.
69. Yamane H, Zhu J, Paul WE. Independent roles for IL-2 and GATA-3 in stimulating naive CD4+ T cells to generate a Th2-inducing cytokine environment. J Exp Med. 2005;202(6):793-804.
70. Maldonado RA, Irvine DJ, Schreiber R, Glimcher LH. A role for the immunological synapse in lineage commitment of CD4 lymphocytes. Nature. 2004;431(7008):527-32.
71. Maldonado RA, Soriano MA, Perdomo LC, Sigrist K, Irvine DJ, Decker T, et al. Control of T helper cell differentiation through cytokine receptor inclusion in the immunological synapse. J Exp Med. 2009;206(4):877-92.
72. Ariga H, Shimohakamada Y, Nakada M, Tokunaga T, Kikuchi T, Kariyone A, et al. Instruction of naive CD4+ T-cell fate to T-bet expression and T helper 1 development: roles of T-cell receptor-mediated signals. Immunology. 2007;122(2):210-21.
73. Gu C, Wu L, Li X. IL-17 family: cytokines, receptors and signaling. Cytokine. 2013;64(2):477-85.
74. Acosta-Rodriguez EV, Napolitani G, Lanzavecchia A, Sallusto F. Interleukins 1beta and 6 but not transforming growth factor-beta are essential for the differentiation of interleukin 17-producing human T helper cells. Nat Immunol. 2007;8(9):942-9.

75. Harris TJ, Grosso JF, Yen HR, Xin H, Kortylewski M, Albesiano E, et al. Cutting edge: An in vivo requirement for STAT3 signaling in TH17 development and TH17-dependent autoimmunity. J Immunol. 2007;179(7):4313-7.
76. Volpe E, Servant N, Zollinger R, Bogiatzi SI, Hupe P, Barillot E, et al. A critical function for transforming growth factor-beta, interleukin 23 and proinflammatory cytokines in driving and modulating human T(H)-17 responses. Nat Immunol. 2008;9(6):650-7.
77. Ivanov, II, McKenzie BS, Zhou L, Tadokoro CE, Lepelley A, Lafaille JJ, et al. The orphan nuclear receptor RORgammat directs the differentiation program of proinflammatory IL-17+ T helper cells. Cell. 2006;126(6):1121-33.
78. Chaudhry A, Samstein RM, Treuting P, Liang Y, Pils MC, Heinrich JM, et al. Interleukin-10 signaling in regulatory T cells is required for suppression of Th17 cell-mediated inflammation. Immunity. 2011;34(4):566-78.
79. Chen W, Jin W, Hardegen N, Lei KJ, Li L, Marinos N, et al. Conversion of peripheral CD4+CD25- naive T cells to CD4+CD25+ regulatory T cells by TGF-beta induction of transcription factor Foxp3. J Exp Med. 2003;198(12):1875-86.
80. Fontenot JD, Gavin MA, Rudensky AY. Foxp3 programs the development and function of CD4+CD25+ regulatory T cells. Nat Immunol. 2003;4(4):330-6.
81. Burchill MA, Yang J, Vang KB, Moon JJ, Chu HH, Lio CW, et al. Linked T cell receptor and cytokine signaling govern the development of the regulatory T cell repertoire. Immunity. 2008;28(1):112-21.
82. Molinero LL, Miller ML, Evaristo C, Alegre ML. High TCR stimuli prevent induced regulatory T cell differentiation in a NF-kappaB-dependent manner. J Immunol. 2011;186(8):4609-17.
83. Heffetz D, Bushkin I, Dror R, Zick Y. The insulinomimetic agents H2O2 and vanadate stimulate protein tyrosine phosphorylation in intact cells. J Biol Chem. 1990;265(5):2896-902.
84. Secrist JP, Burns LA, Karnitz L, Koretzky GA, Abraham RT. Stimulatory effects of the protein tyrosine phosphatase inhibitor, pervanadate, on T-cell activation events. J Biol Chem. 1993;268(8):5886-93.
85. Koretzky GA, Picus J, Schultz T, Weiss A. Tyrosine phosphatase CD45 is required for T-cell antigen receptor and CD2-mediated activation of a protein tyrosine kinase and interleukin 2 production. Proc Natl Acad Sci U S A. 1991;88(6):2037-41.
86. Bottini N, Stefanini L, Williams S, Alonso A, Jascur T, Abraham RT, et al. Activation of ZAP-70 through specific dephosphorylation at the inhibitory Tyr-292 by the low molecular weight phosphotyrosine phosphatase (LMPTP). J Biol Chem. 2002;277(27):24220-4.
87. Alonso A, Sasin J, Bottini N, Friedberg I, Friedberg I, Osterman A, et al. Protein tyrosine phosphatases in the human genome. Cell. 2004;117(6):699-711.
88. Mustelin T, Vang T, Bottini N. Protein tyrosine phosphatases and the immune response. Nat Rev Immunol. 2005;5(1):43-57.
89. Niemi NM, Lanning NJ, Klomp JA, Tait SW, Xu Y, Dykema KJ, et al. MK-STYX, a catalytically inactive phosphatase regulating mitochondrially dependent apoptosis. Mol Cell Biol. 2011;31(7):1357-68.
90. Niemi NM, Sacoman JL, Westrate LM, Gaither LA, Lanning NJ, Martin KR, et al. The pseudophosphatase MK-STYX physically and genetically interacts with the mitochondrial phosphatase PTPMT1. PLoS One. 2014;9(4):e93896.
91. Robinson FL, Dixon JE. Myotubularin phosphatases: policing 3-phosphoinositides. Trends Cell Biol. 2006;16(8):403-12.
92. Caunt CJ, Keyse SM. Dual-specificity MAP kinase phosphatases (MKPs): shaping the outcome of MAP kinase signalling. FEBS J. 2013;280(2):489-504.
93. Deshpande T, Takagi T, Hao L, Buratowski S, Charbonneau H. Human PIR1 of the protein-tyrosine phosphatase superfamily has RNA 5'-triphosphatase and diphosphatase activities. J Biol Chem. 1999;274(23):16590-4.

94. Gentry MS, Roma-Mateo C, Sanz P. Laforin, a protein with many faces: glucan phosphatase, adapter protein, et alii. FEBS J. 2013;280(2):525-37.
95. Rios P, Li X, Kohn M. Molecular mechanisms of the PRL phosphatases. FEBS J. 2013;280(2):505-24.
96. Visintin R, Craig K, Hwang ES, Prinz S, Tyers M, Amon A. The phosphatase Cdc14 triggers mitotic exit by reversal of Cdk-dependent phosphorylation. Mol Cell. 1998;2(6):709-18.
97. Stegmeier F, Amon A. Closing mitosis: the functions of the Cdc14 phosphatase and its regulation. Annu Rev Genet. 2004;38:203-32.
98. Hsu F, Mao Y. The structure of phosphoinositide phosphatases: Insights into substrate specificity and catalysis. Biochim Biophys Acta. 2015;1851(6):698-710.
99. Chernoff J, Li HC. A major phosphotyrosyl-protein phosphatase from bovine heart is associated with a low-molecular-weight acid phosphatase. Arch Biochem Biophys. 1985;240(1):135-45.
100. Giannoni E, Chiarugi P, Cozzi G, Magnelli L, Taddei ML, Fiaschi T, et al. Lymphocyte function-associated antigen-1-mediated T cell adhesion is impaired by low molecular weight phosphotyrosine phosphatase-dependent inhibition of FAK activity. J Biol Chem. 2003;278(38):36763-76.
101. Sur S, Agrawal DK. Phosphatases and kinases regulating CDC25 activity in the cell cycle: clinical implications of CDC25 overexpression and potential treatment strategies. Mol Cell Biochem. 2016;416(1-2):33-46.
102. Rayapureddi JP, Kattamuri C, Steinmetz BD, Frankfort BJ, Ostrin EJ, Mardon G, et al. Eyes absent represents a class of protein tyrosine phosphatases. Nature. 2003;426(6964):295-8.
103. Tootle TL, Silver SJ, Davies EL, Newman V, Latek RR, Mills IA, et al. The transcription factor Eyes absent is a protein tyrosine phosphatase. Nature. 2003;426(6964):299-302.
104. Li X, Oghi KA, Zhang J, Krones A, Bush KT, Glass CK, et al. Eya protein phosphatase activity regulates Six1-Dach-Eya transcriptional effects in mammalian organogenesis. Nature. 2003;426(6964):247-54.
105. Mohn KL, Laz TM, Hsu JC, Melby AE, Bravo R, Taub R. The immediate-early growth response in regenerating liver and insulin-stimulated H-35 cells: comparison with serum-stimulated 3T3 cells and identification of 41 novel immediate-early genes. Mol Cell Biol. 1991;11(1):381-90.
106. Diamond RH, Cressman DE, Laz TM, Abrams CS, Taub R. PRL-1, a unique nuclear protein tyrosine phosphatase, affects cell growth. Mol Cell Biol. 1994;14(6):3752-62.
107. Zeng Q, Hong W, Tan YH. Mouse PRL-2 and PRL-3, two potentially prenylated protein tyrosine phosphatases homologous to PRL-1. Biochem Biophys Res Commun. 1998;244(2):421-7.
108. Tonks NK. Protein tyrosine phosphatases--from housekeeping enzymes to master regulators of signal transduction. FEBS J. 2013;280(2):346-78.
109. Pannifer AD, Flint AJ, Tonks NK, Barford D. Visualization of the cysteinyl-phosphate intermediate of a protein-tyrosine phosphatase by x-ray crystallography. J Biol Chem. 1998;273(17):10454-62.
110. Kozlov G, Cheng J, Ziomek E, Banville D, Gehring K, Ekiel I. Structural insights into molecular function of the metastasis-associated phosphatase PRL-3. J Biol Chem. 2004;279(12):11882-9.
111. Sun JP, Wang WQ, Yang H, Liu S, Liang F, Fedorov AA, et al. Structure and biochemical properties of PRL-1, a phosphatase implicated in cell growth, differentiation, and tumor invasion. Biochemistry. 2005;44(36):12009-21.

112. Sun JP, Luo Y, Yu X, Wang WQ, Zhou B, Liang F, et al. Phosphatase activity, trimerization, and the C-terminal polybasic region are all required for PRL1-mediated cell growth and migration. J Biol Chem. 2007;282(39):29043-51.
113. Cates CA, Michael RL, Stayrook KR, Harvey KA, Burke YD, Randall SK, et al. Prenylation of oncogenic human PTP(CAAX) protein tyrosine phosphatases. Cancer Lett. 1996;110(1-2):49-55.
114. Wang J, Kirby CE, Herbst R. The tyrosine phosphatase PRL-1 localizes to the endoplasmic reticulum and the mitotic spindle and is required for normal mitosis. J Biol Chem. 2002;277(48):46659-68.
115. Zeng Q, Si X, Horstmann H, Xu Y, Hong W, Pallen CJ. Prenylation-dependent association of protein-tyrosine phosphatases PRL-1, -2, and -3 with the plasma membrane and the early endosome. J Biol Chem. 2000;275(28):21444-52.
116. Fiordalisi JJ, Keller PJ, Cox AD. PRL tyrosine phosphatases regulate rho family GTPases to promote invasion and motility. Cancer Res. 2006;66(6):3153-61.
117. Nishimura A, Linder ME. Identification of a novel prenyl and palmitoyl modification at the CaaX motif of Cdc42 that regulates RhoGDI binding. Mol Cell Biol. 2013;33(7):1417-29.
118. Funato Y, Miki H. Reversible oxidation of PRL family protein-tyrosine phosphatases. Methods. 2014;65(2):184-9.
119. Yu L, Kelly U, Ebright JN, Malek G, Saloupis P, Rickman DW, et al. Oxidative stress-induced expression and modulation of Phosphatase of Regenerating Liver-1 (PRL-1) in mammalian retina. Biochim Biophys Acta. 2007;1773(9):1473-82.
120. Jeong DG, Kim SJ, Kim JH, Son JH, Park MR, Lim SM, et al. Trimeric structure of PRL-1 phosphatase reveals an active enzyme conformation and regulation mechanisms. J Mol Biol. 2005;345(2):401-13.
121. Hoyt R, Zhu W, Cerignoli F, Alonso A, Mustelin T, David M. Cutting edge: selective tyrosine dephosphorylation of interferon-activated nuclear STAT5 by the VHR phosphatase. J Immunol. 2007;179(6):3402-6.
122. Li L, Ljungman M, Dixon JE. The human Cdc14 phosphatases interact with and dephosphorylate the tumor suppressor protein p53. J Biol Chem. 2000;275(4):2410-4.
123. Poon RY, Hunter T. Dephosphorylation of Cdk2 Thr160 by the cyclin-dependent kinase-interacting phosphatase KAP in the absence of cyclin. Science. 1995;270(5233):90-3.
124. Peters CS, Liang X, Li S, Kannan S, Peng Y, Taub R, et al. ATF-7, a novel bZIP protein, interacts with the PRL-1 protein-tyrosine phosphatase. J Biol Chem. 2001;276(17):13718-26.
125. Forte E, Orsatti L, Talamo F, Barbato G, De Francesco R, Tomei L. Ezrin is a specific and direct target of protein tyrosine phosphatase PRL-3. Biochim Biophys Acta. 2008;1783(2):334-44.
126. McParland V, Varsano G, Li X, Thornton J, Baby J, Aravind A, et al. The metastasis-promoting phosphatase PRL-3 shows activity toward phosphoinositides. Biochemistry. 2011;50(35):7579-90.
127. Dumaual CM, Sandusky GE, Crowell PL, Randall SK. Cellular localization of PRL-1 and PRL-2 gene expression in normal adult human tissues. J Histochem Cytochem. 2006;54(12):1401-12.
128. Gjorloff-Wingren A, Saxena M, Han S, Wang X, Alonso A, Renedo M, et al. Subcellular localization of intracellular protein tyrosine phosphatases in T cells. Eur J Immunol. 2000;30(8):2412-21.
129. Matter WF, Estridge T, Zhang C, Belagaje R, Stancato L, Dixon J, et al. Role of PRL-3, a human muscle-specific tyrosine phosphatase, in angiotensin-II signaling. Biochem Biophys Res Commun. 2001;283(5):1061-8.
130. Guo K, Li J, Wang H, Osato M, Tang JP, Quah SY, et al. PRL-3 initiates tumor angiogenesis by recruiting endothelial cells in vitro and in vivo. Cancer Res. 2006;66(19):9625-35.

131. Kobayashi M, Chen S, Gao R, Bai Y, Zhang ZY, Liu Y. Phosphatase of regenerating liver in hematopoietic stem cells and hematological malignancies. Cell Cycle. 2014;13(18):2827-35.
132. Wang Y, Lazo JS. Metastasis-associated phosphatase PRL-2 regulates tumor cell migration and invasion. Oncogene. 2012;31(7):818-27.
133. Wang L, Peng L, Dong B, Kong L, Meng L, Yan L, et al. Overexpression of phosphatase of regenerating liver-3 in breast cancer: association with a poor clinical outcome. Ann Oncol. 2006;17(10):1517-22.
134. Miskad UA, Semba S, Kato H, Yokozaki H. Expression of PRL-3 phosphatase in human gastric carcinomas: close correlation with invasion and metastasis. Pathobiology. 2004;71(4):176-84.
135. Polato F, Codegoni A, Fruscio R, Perego P, Mangioni C, Saha S, et al. PRL-3 phosphatase is implicated in ovarian cancer growth. Clin Cancer Res. 2005;11(19 Pt 1):6835-9.
136. Bessette DC, Qiu D, Pallen CJ. PRL PTPs: mediators and markers of cancer progression. Cancer Metastasis Rev. 2008;27(2):231-52.
137. Daouti S, Li WH, Qian H, Huang KS, Holmgren J, Levin W, et al. A selective phosphatase of regenerating liver phosphatase inhibitor suppresses tumor cell anchorage-independent growth by a novel mechanism involving p130Cas cleavage. Cancer Res. 2008;68(4):1162-9.
138. Defilippi P, Di Stefano P, Cabodi S. p130Cas: a versatile scaffold in signaling networks. Trends Cell Biol. 2006;16(5):257-63.
139. Luo Y, Liang F, Zhang ZY. PRL1 promotes cell migration and invasion by increasing MMP2 and MMP9 expression through Src and ERK1/2 pathways. Biochemistry. 2009;48(8):1838-46.
140. Peng L, Xing X, Li W, Qu L, Meng L, Lian S, et al. PRL-3 promotes the motility, invasion, and metastasis of LoVo colon cancer cells through PRL-3-integrin beta1-ERK1/2 and-MMP2 signaling. Mol Cancer. 2009;8:110.
141. Bai Y, Luo Y, Liu S, Zhang L, Shen K, Dong Y, et al. PRL-1 protein promotes ERK1/2 and RhoA protein activation through a non-canonical interaction with the Src homology 3 domain of p115 Rho GTPase-activating protein. J Biol Chem. 2011;286(49):42316-24.
142. Lee SK, Han YM, Yun J, Lee CW, Shin DS, Ha YR, et al. Phosphatase of regenerating liver-3 promotes migration and invasion by upregulating matrix metalloproteinases-7 in human colorectal cancer cells. Int J Cancer. 2012;131(3):E190-203.
143. Wang H, Quah SY, Dong JM, Manser E, Tang JP, Zeng Q. PRL-3 down-regulates PTEN expression and signals through PI3K to promote epithelial-mesenchymal transition. Cancer Res. 2007;67(7):2922-6.
144. Dong Y, Zhang L, Zhang S, Bai Y, Chen H, Sun X, et al. Phosphatase of regenerating liver 2 (PRL2) is essential for placental development by down-regulating PTEN (Phosphatase and Tensin Homologue Deleted on Chromosome 10) and activating Akt protein. J Biol Chem. 2012;287(38):32172-9.
145. Kobayashi M, Bai Y, Dong Y, Yu H, Chen S, Gao R, et al. PRL2/PTP4A2 phosphatase is important for hematopoietic stem cell self-renewal. Stem Cells. 2014;32(7):1956-67.
146. Kobayashi M, Nabinger SC, Bai Y, Yoshimoto M, Gao R, Chen S, et al. Protein Tyrosine Phosphatase PRL2 Mediates Notch and Kit Signals in Early T Cell Progenitors. Stem Cells. 2017;35(4):1053-64.
147. Nakashima M, Lazo JS. Phosphatase of regenerating liver-1 promotes cell migration and invasion and regulates filamentous actin dynamics. J Pharmacol Exp Ther. 2010;334(2):627-33.
148. Achiwa H, Lazo JS. PRL-1 tyrosine phosphatase regulates c-Src levels, adherence, and invasion in human lung cancer cells. Cancer Res. 2007;67(2):643-50.

149. Niedergang F, Dautry-Varsat A, Alcover A. Peptide antigen or superantigen-induced down-regulation of TCRs involves both stimulated and unstimulated receptors. J Immunol. 1997;159(4):1703-10.
150. Jinek M, Chylinski K, Fonfara I, Hauer M, Doudna JA, Charpentier E. A programmable dual-RNA-guided DNA endonuclease in adaptive bacterial immunity. Science. 2012;337(6096):816-21.
151. Cong L, Ran FA, Cox D, Lin S, Barretto R, Habib N, et al. Multiplex genome engineering using CRISPR/Cas systems. Science. 2013;339(6121):819-23.
152. Mojica FJ, Rodriguez-Valera F. The discovery of CRISPR in archaea and bacteria. FEBS J. 2016;283(17):3162-9.
153. Calabia-Linares C, Robles-Valero J, de la Fuente H, Perez-Martinez M, Martin-Cofreces N, Alfonso-Perez M, et al. Endosomal clathrin drives actin accumulation at the immunological synapse. J Cell Sci. 2011;124(Pt 5):820-30.
154. Livak KJ, Schmittgen TD. Analysis of relative gene expression data using real-time quantitative PCR and the 2(-Delta Delta C(T)) Method. Methods. 2001;25(4):402-8.
155. Maksumova L, Wang YN, Wong NKY, Le HT, Pallen CJ, Johnson P. Differential function of PTP alpha and PTP alpha Y789F in T cells and regulation of PTP alpha phosphorylation at tyr-789 by CD45. Journal of Biological Chemistry. 2007;282(29):20925-32.
156. Mustelin T, Coggeshall KM, Altman A. Rapid Activation of the T-Cell Tyrosine Protein-Kinase Pp56lck by the Cd45 Phosphotyrosine Phosphatase. P Natl Acad Sci USA. 1989;86(16):6302-6.
157. Lin J, Weiss A. The tyrosine phosphatase CD148 is excluded from the immunologic synapse and down-regulates prolonged T cell signaling. J Cell Biol. 2003;162(4):673-82.
158. Baker JE, Majeti R, Tangye SG, Weiss A. Protein tyrosine phosphatase CD148-mediated inhibition of T-cell receptor signal transduction is associated with reduced LAT and phospholipase Cgamma1 phosphorylation. Mol Cell Biol. 2001;21(7):2393-403.
159. Erdenebayar N, Maekawa Y, Nishida J, Kitamura A, Yasutomo K. Protein-tyrosine phosphatase-kappa regulates CD4+ T cell development through ERK1/2-mediated signaling. Biochemical and biophysical research communications. 2009;390(3):489-93.
160. Iwata R, Sasaki N, Agui T. Contiguous gene deletion of Ptprk and Themis causes T-helper immunodeficiency (thid) in the LEC rat. Biomedical research. 2010;31(1):83-7.
161. Lu XQ, Malumbres R, Shields B, Jiang XY, Sarosiek KA, Natkunam Y, et al. PTP1B is a negative regulator of interleukin 4-induced STAT6 signaling. Blood. 2008;112(10):4098-108.
162. Wiede F, Shields BJ, Chew SH, Kyparissoudis K, van Vliet C, Galic S, et al. T cell protein tyrosine phosphatase attenuates T cell signaling to maintain tolerance in mice. Journal of Clinical Investigation. 2011;121(12):4758-74.
163. Simoncic PD, Lee-Loy A, Barber DL, Tremblay ML, McGlade CJ. The T cell protein tyrosine phosphatase is a negative regulator of janus family kinases 1 and 3. Current Biology. 2002;12(6):446-53.
164. Young JA, Becker AM, Medeiros JJ, Shapiro VS, Wang A, Farrara JD, et al. The protein tyrosine phosphatase PTPN4/PTP-MEG1, an enzyme capable of dephosphorylating the TCR ITAMs and regulating NF-kappa B, is dispensable for T cell development and/or T cell effector functions. Molecular Immunology. 2008;45(14):3756-66.
165. Brockdorff J, Williams S, Couture C, Mustelin T. Dephosphorylation of ZAP-70 and inhibition of T cell activation by activated SHP1. Eur J Immunol. 1999;29(8):2539-50.
166. Nika K, Charvet C, Williams S, Tautz L, Bruckner S, Rahmouni S, et al. Lipid raft targeting of hematopoietic protein tyrosine phosphatase by protein kinase C theta-mediated phosphorylation. Mol Cell Biol. 2006;26(5):1806-16.
167. Saxena M, Williams S, Brockdorff J, Gilman J, Mustelin T. Inhibition of T cell signaling by mitogen-activated protein kinase-targeted hematopoietic tyrosine phosphatase (HePTP). Journal of Biological Chemistry. 1999;274(17):11693-700.

168. Huynh H, Bottini N, Williams S, Cherepanov V, Musumeci L, Saito K, et al. Control of vesicle fusion by a tyrosine phosphatase. Nat Cell Biol. 2004;6(9):831-9.
169. Wang Y, Vachon E, Zhang J, Cherepanov V, Kruger J, Li J, et al. Tyrosine phosphatase MEG2 modulates murine development and platelet and lymphocyte activation through secretory vesicle function. J Exp Med. 2005;202(11):1587-97.
170. Davidson D, Shi X, Zhong MC, Rhee I, Veillette A. The Phosphatase PTP-PEST Promotes Secondary T Cell Responses by Dephosphorylating the Protein Tyrosine Kinase Pyk2. Immunity. 2010;33(2):167-80.
171. Nakahira M, Tanaka T, Robson BE, Mizgerd JP, Grusby MJ. Regulation of signal transducer and activator of transcription signaling by the tyrosine phosphatase PTP-BL. Immunity. 2007;26(2):163-76.
172. Wang HM, Xu YF, Ning SL, Yang DX, Li Y, Du YJ, et al. The catalytic region and PEST domain of PTPN18 distinctly regulate the HER2 phosphorylation and ubiquitination barcodes. Cell Res. 2014;24(9):1067-90.
173. Wu JS, Katrekar A, Honigberg LA, Smith AM, Conn MT, Tang J, et al. Identification of substrates of human protein-tyrosine phosphatase PTPN22. Journal of Biological Chemistry. 2006;281(16):11002-10.
174. Stanford SM, Bottini N. PTPN22: the archetypal non-HLA autoimmunity gene. Nat Rev Rheumatol. 2014;10(10):602-11.
175. Mustelin T, Coggeshall KM, Altman A. Rapid activation of the T-cell tyrosine protein kinase pp56lck by the CD45 phosphotyrosine phosphatase. Proc Natl Acad Sci U S A. 1989;86(16):6302-6.
176. Arimura Y, Yagi J. Comprehensive expression profiles of genes for protein tyrosine phosphatases in immune cells. Sci Signal. 2010;3(137):rs1.
177. Guo L, Martens C, Bruno D, Porcella SF, Yamane H, Caucheteux SM, et al. Lipid phosphatases identified by screening a mouse phosphatase shRNA library regulate T-cell differentiation and protein kinase B AKT signaling. Proc Natl Acad Sci U S A. 2013;110(20):E1849-56.
178. Bertolotto C, Maulon L, Filippa N, Baier G, Auberger P. Protein kinase C theta and epsilon promote T-cell survival by a rsk-dependent phosphorylation and inactivation of BAD. J Biol Chem. 2000;275(47):37246-50.
179. Jun JE, Rubio I, Roose JP. Regulation of ras exchange factors and cellular localization of ras activation by lipid messengers in T cells. Front Immunol. 2013;4:239.
180. Liu CM, Hermann TE. Characterization of Ionomycin as a Calcium Ionophore. Journal of Biological Chemistry. 1978;253(17):5892-4.
181. Kovanen PE, Rosenwald A, Fu J, Hurt EM, Lam LT, Giltnane JM, et al. Analysis of gamma c-family cytokine target genes. Identification of dual-specificity phosphatase 5 (DUSP5) as a regulator of mitogen-activated protein kinase activity in interleukin-2 signaling. J Biol Chem. 2003;278(7):5205-13.
182. Nunes-Xavier CE, Tarrega C, Cejudo-Marin R, Frijhoff J, Sandin A, Ostman A, et al. Differential up-regulation of MAP kinase phosphatases MKP3/DUSP6 and DUSP5 by Ets2 and c-Jun converge in the control of the growth arrest versus proliferation response of MCF-7 breast cancer cells to phorbol ester. J Biol Chem. 2010;285(34):26417-30.
183. Johnson TR, Biggs JR, Winbourn SE, Kraft AS. Regulation of dual-specificity phosphatases M3/6 and hVH5 by phorbol esters. Analysis of a delta-like domain. J Biol Chem. 2000;275(41):31755-62.
184. Lopez-Cabrera M, Santis AG, Fernandez-Ruiz E, Blacher R, Esch F, Sanchez-Mateos P, et al. Molecular cloning, expression, and chromosomal localization of the human earliest lymphocyte activation antigen AIM/CD69, a new member of the C-type animal lectin superfamily of signal-transmitting receptors. J Exp Med. 1993;178(2):537-47.

185. Hoeger B, Diether M, Ballester PJ, Kohn M. Biochemical evaluation of virtual screening methods reveals a cell-active inhibitor of the cancer-promoting phosphatases of regenerating liver. European journal of medicinal chemistry. 2014;88:89-100.
186. Bunnell SC, Hong DI, Kardon JR, Yamazaki T, McGlade CJ, Barr VA, et al. T cell receptor ligation induces the formation of dynamically regulated signaling assemblies. J Cell Biol. 2002;158(7):1263-75.
187. Stadlbauer S, Rios P, Ohmori K, Suzuki K, Kohn M. Procyanidins Negatively Affect the Activity of the Phosphatases of Regenerating Liver. PLoS One. 2015;10(7):e0134336.
188. Hnia K, Vaccari I, Bolino A, Laporte J. Myotubularin phosphoinositide phosphatases: cellular functions and disease pathophysiology. Trends Mol Med. 2012;18(6):317-27.
189. Kruger JM, Fukushima T, Cherepanov V, Borregaard N, Loeve C, Shek C, et al. Protein-tyrosine phosphatase MEG2 is expressed by human neutrophils. Localization to the phagosome and activation by polyphosphoinositides. J Biol Chem. 2002;277(4):2620-8.
190. Huynh H, Wang X, Li W, Bottini N, Williams S, Nika K, et al. Homotypic secretory vesicle fusion induced by the protein tyrosine phosphatase MEG2 depends on polyphosphoinositides in T cells. J Immunol. 2003;171(12):6661-71.
191. Shiota M, Tanihiro T, Nakagawa Y, Aoki N, Ishida N, Miyazaki K, et al. Protein tyrosine phosphatase PTP20 induces actin cytoskeleton reorganization by dephosphorylating p190 RhoGAP in rat ovarian granulosa cells stimulated with follicle-stimulating hormone. Mol Endocrinol. 2003;17(4):534-49.
192. van Ham M, Kemperman L, Wijers M, Fransen J, Hendriks W. Subcellular localization and differentiation-induced redistribution of the protein tyrosine phosphatase PTP-BL in Neuroblastoma cells. Cell Mol Neurobiol. 2005;25(8):1225-44.
193. Niwa R, Nagata-Ohashi K, Takeichi M, Mizuno K, Uemura T. Control of actin reorganization by Slingshot, a family of phosphatases that dephosphorylate ADF/cofilin. Cell. 2002;108(2):233-46.
194. Caunt CJ, Armstrong SP, Rivers CA, Norman MR, McArdle CA. Spatiotemporal regulation of ERK2 by dual specificity phosphatases. J Biol Chem. 2008;283(39):26612-23.
195. Mandl M, Slack DN, Keyse SM. Specific inactivation and nuclear anchoring of extracellular signal-regulated kinase 2 by the inducible dual-specificity protein phosphatase DUSP5. Mol Cell Biol. 2005;25(5):1830-45.
196. Rauch J, Volinsky N, Romano D, Kolch W. The secret life of kinases: functions beyond catalysis. Cell Commun Signal. 2011;9(1):23.
197. Zhang YY, Wu JW, Wang ZX. Mitogen-activated protein kinase (MAPK) phosphatase 3-mediated cross-talk between MAPKs ERK2 and p38alpha. J Biol Chem. 2011;286(18):16150-62.
198. Hu S, Xie Z, Onishi A, Yu X, Jiang L, Lin J, et al. Profiling the human protein-DNA interactome reveals ERK2 as a transcriptional repressor of interferon signaling. Cell. 2009;139(3):610-22.
199. Rodriguez J, Calvo F, Gonzalez JM, Casar B, Andres V, Crespo P. ERK1/2 MAP kinases promote cell cycle entry by rapid, kinase-independent disruption of retinoblastoma-lamin A complexes. J Cell Biol. 2010;191(5):967-79.
200. Reiterer V, Fey D, Kolch W, Kholodenko BN, Farhan H. Pseudophosphatase STYX modulates cell-fate decisions and cell migration by spatiotemporal regulation of ERK1/2. Proc Natl Acad Sci U S A. 2013;110(31):E2934-43.
201. Moon SJ, Lim MA, Park JS, Byun JK, Kim SM, Park MK, et al. Dual-specificity phosphatase 5 attenuates autoimmune arthritis in mice via reciprocal regulation of the Th17/Treg cell balance and inhibition of osteoclastogenesis. Arthritis Rheumatol. 2014;66(11):3083-95.
202. Castro-Sanchez P, Ramirez-Munoz R, Lamana A, Ortiz A, Gonzalez-Alvaro I, Roda-Navarro P. mRNA profilin identifies low levels of phosphatases dual-specific phosphatase-7 (DUSP7) and cell division cycle-25B (CDC25B) in patients with early arthritis. Clin Exp Immunol. 2017;189(1):113-9.

203. Alonso A, Merlo JJ, Na S, Kholod N, Jaroszewski L, Kharitonenkov A, et al. Inhibition of T cell antigen receptor signaling by VHR-related MKPX (VHX), a new dual specificity phosphatase related to VH1 related (VHR). J Biol Chem. 2002;277(7):5524-8.
204. Li JP, Yang CY, Chuang HC, Lan JL, Chen DY, Chen YM, et al. The phosphatase JKAP/DUSP22 inhibits T-cell receptor signalling and autoimmunity by inactivating Lck. Nat Commun. 2014;5:3618.
205. Chuang HC, Chen YM, Hung WT, Li JP, Chen DY, Lan JL, et al. Downregulation of the phosphatase JKAP/DUSP22 in T cells as a potential new biomarker of systemic lupus erythematosus nephritis. Oncotarget. 2016;7(36):57593-605.
206. Kidane YH, Lawrence C, Murali TM. Computational approaches for discovery of common immunomodulators in fungal infections: towards broad-spectrum immunotherapeutic interventions. BMC Microbiol. 2013;13:224.
207. Agarwal R, Burley SK, Swaminathan S. Structure of human dual specificity protein phosphatase 23, VHZ, enzyme-substrate/product complex. J Biol Chem. 2008;283(14):8946-53.
208. Gallegos LL, Ng MR, Sowa ME, Selfors LM, White A, Zervantonakis IK, et al. A protein interaction map for cell-cell adhesion regulators identifies DUSP23 as a novel phosphatase for beta-catenin. Sci Rep. 2016;6:27114.
209. Tang JP, Tan CP, Li J, Siddique MM, Guo K, Chan SW, et al. VHZ is a novel centrosomal phosphatase associated with cell growth and human primary cancers. Mol Cancer. 2010;9:128.
210. Balada E, Felip L, Ordi-Ros J, Vilardell-Tarres M. DUSP23 is over-expressed and linked to the expression of DNMTs in CD4+ T cells from systemic lupus erythematosus patients. Clin Exp Immunol. 2017;187(2):242-50.
211. Lindqvist A, Kallstrom H, Lundgren A, Barsoum E, Rosenthal CK. Cdc25B cooperates with Cdc25A to induce mitosis but has a unique role in activating cyclin B1-Cdk1 at the centrosome. J Cell Biol. 2005;171(1):35-45.
212. Patsoukis N, Sari D, Boussiotis VA. PD-1 inhibits T cell proliferation by upregulating p27 and p15 and suppressing Cdc25A. Cell Cycle. 2012;11(23):4305-9.
213. P C-SPaR-N. Physiology and Pathology of Autoimmune Diseases: Role of CD4+ T-cells in Rheumatoid Arthritis. In: Books IO, editor. Physiology and Pathology of Immunology2017.
214. Blas-Rus N, Bustos-Moran E, Perez de Castro I, de Carcer G, Borroto A, Camafeita E, et al. Aurora A drives early signalling and vesicle dynamics during T-cell activation. Nat Commun. 2016;7:11389.
215. Bolino A, Bolis A, Previtali SC, Dina G, Bussini S, Dati G, et al. Disruption of Mtmr2 produces CMT4B1-like neuropathy with myelin outfolding and impaired spermatogenesis. J Cell Biol. 2004;167(4):711-21.
216. Round JL, Humphries LA, Tomassian T, Mittelstadt P, Zhang M, Miceli MC. Scaffold protein Dlgh1 coordinates alternative p38 kinase activation, directing T cell receptor signals toward NFAT but not NF-kappaB transcription factors. Nat Immunol. 2007;8(2):154-61.
217. Lasserre R, Charrin S, Cuche C, Danckaert A, Thoulouze MI, de Chaumont F, et al. Ezrin tunes T-cell activation by controlling Dlg1 and microtubule positioning at the immunological synapse. EMBO J. 2010;29(14):2301-14.
218. Berger P, Tersar K, Ballmer-Hofer K, Suter U. The CMT4B disease-causing proteins MTMR2 and MTMR13/SBF2 regulate AKT signalling. J Cell Mol Med. 2011;15(2):307-15.
219. Mizuno K. Signaling mechanisms and functional roles of cofilin phosphorylation and dephosphorylation. Cell Signal. 2013;25(2):457-69.
220. Ramirez-Munoz R, Castro-Sanchez P, Roda-Navarro P. Ultrasensitivity in the Cofilin Signaling Module: A Mechanism for Tuning T Cell Responses. Front Immunol. 2016;7:59.
221. Peng Y, Du K, Ramirez S, Diamond RH, Taub R. Mitogenic up-regulation of the PRL-1 protein-tyrosine phosphatase gene by Egr-1. Egr-1 activation is an early event in liver regeneration. J Biol Chem. 1999;274(8):4513-20.

222. Mou Z, You J, Xiao Q, Wei Y, Yuan J, Liu Y, et al. HuR posttranscriptionally regulates early growth response-1 (Egr-1) expression at the early stage of T cell activation. FEBS Lett. 2012;586(24):4319-25.
223. Onnis A, Finetti F, Baldari CT. Vesicular Trafficking to the Immune Synapse: How to Assemble Receptor-Tailored Pathways from a Basic Building Set. Front Immunol. 2016;7:50.
224. Das V, Nal B, Dujeancourt A, Thoulouze MI, Galli T, Roux P, et al. Activation-induced polarized recycling targets T cell antigen receptors to the immunological synapse; involvement of SNARE complexes. Immunity. 2004;20(5):577-88.
225. Purbhoo MA, Liu H, Oddos S, Owen DM, Neil MA, Pageon SV, et al. Dynamics of subsynaptic vesicles and surface microclusters at the immunological synapse. Sci Signal. 2010;3(121):ra36.
226. Valitutti S, Muller S, Salio M, Lanzavecchia A. Degradation of T cell receptor (TCR)-CD3-zeta complexes after antigenic stimulation. J Exp Med. 1997;185(10):1859-64.
227. Barr VA, Balagopalan L, Barda-Saad M, Polishchuk R, Boukari H, Bunnell SC, et al. T-cell antigen receptor-induced signaling complexes: internalization via a cholesterol-dependent endocytic pathway. Traffic. 2006;7(9):1143-62.
228. Bouchet J, Del Rio-Iniguez I, Lasserre R, Aguera-Gonzalez S, Cuche C, Danckaert A, et al. Rac1-Rab11-FIP3 regulatory hub coordinates vesicle traffic with actin remodeling and T-cell activation. EMBO J. 2016;35(11):1160-74.
229. Zhang W, Sloan-Lancaster J, Kitchen J, Trible RP, Samelson LE. LAT: the ZAP-70 tyrosine kinase substrate that links T cell receptor to cellular activation. Cell. 1998;92(1):83-92.
230. Bai Y, Yu ZH, Liu S, Zhang L, Zhang RY, Zeng LF, et al. Novel Anticancer Agents Based on Targeting the Trimer Interface of the PRL Phosphatase. Cancer Res. 2016;76(16):4805-15.
231. Zeng Q, Dong JM, Guo K, Li J, Tan HX, Koh V, et al. PRL-3 and PRL-1 promote cell migration, invasion, and metastasis. Cancer Res. 2003;63(11):2716-22.
232. Tribioli C, Droetto S, Bione S, Cesareni G, Torrisi MR, Lotti LV, et al. An X chromosome-linked gene encoding a protein with characteristics of a rhoGAP predominantly expressed in hematopoietic cells. Proc Natl Acad Sci U S A. 1996;93(2):695-9.
233. Hai TW, Liu F, Allegretto EA, Karin M, Green MR. A family of immunologically related transcription factors that includes multiple forms of ATF and AP-1. Genes Dev. 1988;2(10):1216-26.
234. Samten B, Townsend JC, Weis SE, Bhoumik A, Klucar P, Shams H, et al. CREB, ATF, and AP-1 transcription factors regulate IFN-gamma secretion by human T cells in response to mycobacterial antigen. J Immunol. 2008;181(3):2056-64.
235. Takenawa T, Miki H. WASP and WAVE family proteins: key molecules for rapid rearrangement of cortical actin filaments and cell movement. J Cell Sci. 2001;114(Pt 10):1801-9.
236. Genot EM, Arrieumerlou C, Ku G, Burgering BM, Weiss A, Kramer IM. The T-cell receptor regulates Akt (protein kinase B) via a pathway involving Rac1 and phosphatidylinositide 3-kinase. Mol Cell Biol. 2000;20(15):5469-78.
237. Quast T, Tappertzhofen B, Schild C, Grell J, Czeloth N, Forster R, et al. Cytohesin-1 controls the activation of RhoA and modulates integrin-dependent adhesion and migration of dendritic cells. Blood. 2009;113(23):5801-10.
238. Kolanus W, Nagel W, Schiller B, Zeitlmann L, Godar S, Stockinger H, et al. Alpha L beta 2 integrin/LFA-1 binding to ICAM-1 induced by cytohesin-1, a cytoplasmic regulatory molecule. Cell. 1996;86(2):233-42.
239. Giagulli C, Scarpini E, Ottoboni L, Narumiya S, Butcher EC, Constantin G, et al. RhoA and zeta PKC control distinct modalities of LFA-1 activation by chemokines: critical role of LFA-1 affinity triggering in lymphocyte in vivo homing. Immunity. 2004;20(1):25-35.

ADDENDA

ADDENDA

1. Curriculum vitae

PERSONAL INFORMATION Patricia Castro Sánchez

patriciacastro@ucm.es / patriciacastro.ctm@gmail.com

Date of birth 23/04/1989 | Nationality Spanish

WORK EXPERIENCE

• Jan-Dec 2016: **PhD contract** associated to the research project 2012-CIG-321858 of the Marie Curie Career Reintegration Grants, titled *Dynamic regulation of cytokine signaling in lymphocytes during inflammation* (PI: Pedro Roda-Navarro) at the Complutense University of Madrid (UCM).

• Jan 2014- Dec 2015: **PhD contract** associated to the research project *Dynamic regulation of the cytokine signaling in lymphocytes during inflammation* (SAF2012-33218), financed by the Spanish Ministry of Economy and Competitiveness (MINECO) (PI: Pedro Roda Navarro) at the Universidad Complutense de Madrid.

EDUCATION

• 2012-2013: **Biochemistry, Molecular Biology and Biomedicine MSc** (90 ECTS) at Universidad Complutense de Madrid. Final overall grade (from 1 to 10): 8,27. Participation in a research project for the realization of the **MSc thesis** *CD3ζ chain expression in T lymphocytes of patients with gastric adenocarcinoma* under the supervision of José Manuel Martín Villa, PhD.

• 2007 – 2012: **Biology Bachelor's Degree (330 ECTS)** by UCM. Major in Biomedicine. Average degree (from 1 to 10): 7,48.

PUBLICATIONS

• Patricia Castro-Sanchez, Rocío Ramírez-Muñoz, Noa Martín-Cófreces, Sara Hernández-Pérez, Raquel Reyes, Carlos Cabañas, Philippe I. Bastiaens, Francisco Sánchez-Madrid, and Pedro Roda-Navarro. Phosphatase of regenerating liver (PRL)-1 regulates T cell activation at the immunological synapse. Manuscript in preparation.

• Castro-Sánchez P, Ramirez-Munoz R, Lamana A, Ortiz A, Gonzalez-Alvaro I, Roda-Navarro P. mRNA profiling identifies low levels of DUSP7 and CDC25B phosphatases in patients with early arthritis. *Clin Exp Immunol*. 2017 Jul;189(1):113-119. doi: 10.1111/cei.12953. Epub 2017 Mar 28.

ADDENDA

• Castro-Sánchez P., Ramirez-Munoz R., and Roda-Navarro P. Gene expression profiles of human phospho-tyrosine phosphatases consequent to Th1 polarisation and effector function. J Immunol Res. 2017; 2017:8701042. doi: 10.1155/2017/8701042. Epub 2017 Mar 14

• Ramirez-Munoz R, Castro-Sánchez P, Roda-Navarro P. Ultrasensitivity in the cofilin phosphorylation monocycle: a mechanism for regulating the activation threshold in lymphocytes?. *Front. Immunol.* 2016 Feb 19;7:59. doi: 10.3389/fimmu.2016.00059. eCollection 2016.

• Castro-Sánchez P, Martín-Villa JM. Gut immune system and oral tolerance. *Br J Nutr*. 109 (2):S3-11. 2013.

BOOK CHAPTERS

• Castro-Sánchez P and Roda-Navarro P. 2017. Physiology and Pathology of Autoimmune Diseases: Role of CD4+ T-cells in Rheumatoid Arthritis. In *Physiology and Pathology of Immunology.* InTech Open Books. Accepted.

CONFERENCE COMMUNICATIONS

International Communications

• Castro-Sánchez P, Ramirez-Munoz R, Roda-Navarro P. Phosphatase of regenerating liver-1 regulates T cell activation at the immunological synapse. EMBO conference Europhosphatase 2017: phosphatases in cell fates and decisions. Paris (France). July 2017

• Castro-Sánchez P, Ramirez-Munoz R, Roda-Navarro P. Phosphatase of regenerating liver-1 regulates T cell activation at the immunological synapse. EMBO conference Lymphocyte antigen receptor signalling (cfs5-16-01). Siena (Italy). September 2016

• Ramirez-Munoz R, Castro-Sánchez P, Krummel MF, Roda-Navarro P. Unraveling the role of SSH-1 in T cell immune responses. EMBO conference Lymphocyte antigen receptor signalling (cfs5-16-01). Siena (Italy). September 2016

• Ramirez-Munoz, R[1].; Castro-Sanchez, P[1]. & Roda-Navarro, P. Intracellular dynamics of phosphatase of regenerating liver 1 in T lymphocytes. 4th European Congress of Immunology. Vienna (Austria). September 2015.
[1]Equal contribution to this work.

• Castro-Sanchez, P. Ramirez-Munoz, R.; & Roda-Navarro, P. Analysis of expression profiles reveals coordinated regulation of phosphotyrosine phosphatases during CD4+ T cell activation and Th1 polarization. EMBO conference Europhosphatase 2015: phosphorilation switches and cellular homeostasis. Turku (Finland). June 2015

• Castro-Sanchez, P[1]. Ramirez-Munoz, R[1].; & Roda-Navarro, P. Phosphatase of regenerating liver 1 (PRL-1) enhances T cell activation at the immunological synapse. EMBO conference Europhosphatase 2015: phosphorilation switches and cellular homeostasis. Turku (Finland). June2015.
[1]Equal contribution to this work.

National Communications

•Ramirez-Munoz[1], R.; Castro-Sanchez, P.[1] & Roda-Navarro, P. mRNA profiling identifies low levels of DUSP7 and CDC25B phosphatases in patients with early arthritis. 40TH Meeting of the Spanish Society of Immunology. 2017 May; Zaragoza, Spain.

•Ramirez-Munoz[1], R.; Castro-Sanchez, P.[1] & Roda-Navarro, P. Phosphatase of regenerating liver 1 (PRL-1) redistributes to the immune synapse and promotes T cell activation. SICAM 5th Meeting, 2014 Dec; Madrid, Spain.
[1]Equal contribution to this work.

•Castro-Sanchez, P.; Ramirez-Munoz, R. & Roda-Navarro, P.
Expression profile of genes encoding protein tyrosine phosphatases in CD4 T cells: from naïve to Th1. SICAM 5th Meeting, 2014 Dec; Madrid, Spain.

•Ramirez-Munoz, R.; Castro-Sanchez, P. & Roda-Navarro, P. Soluble IL-15, but not mature dendritic cells, upregulates NKG2D surface expression in primary human NK cells.
Presented at: SICAM 5th Meeting, 2014 Dec; Madrid, Spain.

PARTICIPATION IN RESEARCH PROJECTS

•Title: Mecanismos reguladores y función de las fosfatasas de especificidad dual en la respuesta inmunológica de los linfocitos T. (Regulatory mechanisms and function of dual-specificity phosphatases in the immune response of T lymphocytes).
Funding: MINECO (Spanish Ministry of Economy, industry and competitiveness)
Duration: 2016-2020
PI: Pedro Roda Navarro

•Title: Descubriendo la rápida dinámica molecular que gobierna las funciones celulares. (Discovering the rapid molecular dynamics that regulates cell function).
Reference: SAF2012-33218-EXP
Funding: MINECO (Spanish Ministry of Economy, industry and competitiveness)
Duration: 2014-2016
PI: Pedro Roda Navarro.

• Title: Dynamic regulation of cytokine signalling in lymphocytes during inflammation.
Reference: FP7-PEOPLE-2012-CIG-321858
Funding: European Comission
Duration: 2013-2016

ADDENDA

PI: Pedro Roda Navarro.

• Title: Regulación dinámica de la señalización por citocinas en linfocitos durante la inflamación. (Dynamic regulation of cytokine signalling in lymphocytes during inflammation)
Reference: SAF2012-33218
Funding: Spanish Ministry of Education
Duration: 2013-2015
PI: Pedro Roda Navarro.

• Title: Estudio de los componentes celulares T (Th1, Th2, Th17 y Treg) y regulación de la expresión de la cadena ζ del complejo CD3 en pacientes con adnocarcinoma gástrico. (Study of T cell subsets (Th1, Th2, Th17 y Treg) and regulation of the expression of the ζ of the CD3 complex in patients with gastric adenocarcinoma)
Reference: FIS PS09/02096
Funding: Carlos III Health Institute
Duration: 2010-2012
PI: José Manuel Martín Villa.

INTERNSHIPS IN RESEARCH INSTITUTES

• Host institution: Beatson Institute for Cancer Research (Glasgow, UK)
Project: Search for PRL-1 interaction partners during T cell activation
Duration: October 2016-January 2017
Supervisor: Shehab Ismail

• Host institution: Centro Nacional de Investigaciones Oncológicas (CNIO) (Madrid, Spain)
Project: Genomic edition of PRL-1 by CRISPR/Cas9
Duration: February-March 2017
Supervisor: Sandra Rodríguez and Raúl Torres

GRANTS

• EMBO short term fellowship (ASTF 344-2016) awarded by EMBO (European Molecular Biology Organization) to do an internship at the Beatson Institute for Cancer Research (Glasgow, UK). September-December 2016

• 2012-2013: **Collaboration scholarship** awarded by the Spanish Ministry of Education, participating in the research project *Study of cellular T populations (Th1, Th2, Th17 and Treg) and regulation of the expression of the ζ chain of the CD3 complex in patients with gastric adenocarcinoma* (FIS PS09/02096) at the Immunology Department of the Faculty of Medicine, UCM (PI: José Manuel Martín Villa).

TEACHING EXPERIENCE

- 2011-2017: Organization and teaching of practicals of the Immunology courses of the Medicine degree at UCM.

- 2013/2014: Honorary collaborator at the Immunology Department of the Faculty of Medicine, UCM.

LANGUAGES

Mother tongue: Spanish
Other languages:

- English: Certificate in Advanced English. University of Cambridge. June 2014.
- Italian: education at the Liceo Scientifico Italiano E. Fermi (1994-2005).

2. Publications relevant to this thesis

Clinical & Experimental Immunology
The Journal of Translational Immunology

Clinical and Experimental Immunology ORIGINAL ARTICLE doi:10.1111/cei.12953

mRNA profilin identifies low levels of phosphatases dual-specific phosphatase-7 (DUSP7) and cell division cycle-25B (CDC25B) in patients with early arthritis

P. Castro-Sánchez,* R. Ramirez-Munoz,* A. Lamana,† A. Ortiz,† I. González-Álvaro† and P. Roda-Navarro

*Department of Microbiology I (Immunology), School of Medicine, Complutense University and '12 de Octubre' Health Research Institute, Madrid, Spain, and †Rheumatology Service, Hospital Universitario de La Princesa, IIS-IP, Madrid, Spain

Accepted for publication 25 February 2017
Correspondence: P. Roda-Navarro, Departamento de Microbiología I (Inmunología). Facultad de Medicina. Universidad Complutense de Madrid. Avda. Complutense s/n 28040. Madrid. Spain.
E-mail: proda@med.ucm.es

Summary

Phosphotyrosine phosphatases (PTPs) control phosphorylation levels and, consequently, regulate the output of intracellular signalling networks in health and disease. Despite the high number of PTPs expressed in CD4 T cells and their involvement in autoimmunity, information about the expression profile of PTPs in these cells has not been obtained in patients diagnosed with autoimmune diseases. Here, we compare the expression profile of PTPs in CD4 T cells of healthy volunteers and patients submitted to an early arthritis clinic, due to suspicion of rheumatoid arthritis, an autoimmune disease mediated by CD4 T cells. We found lower transcript levels of the mitogen-activated protein kinase (MAPK) phosphatase dual-specific phosphatase-7 (DUSP7) and the cell division cycle-25B (CDC25B) in T cells of patients. While the low expression level of DUSP7 was restricted to patients with positive rheumatoid factor and anti-citrullinated protein antibodies, the altered expression of CDC25B correlated with the activity of the disease. Low levels of CDC25B might contribute to the progression of the autoimmune arthritis and/or might be consequence of the inflammatory environment in the active disease. The possible role of DUSP7 and CDC25B as biomarkers of the disease in clinical protocols is discussed.

Keywords: CD4 T cells, CDC25B, DUSP7, early arthritis, PTPs

Introduction

Rheumatoid arthritis (RA) is a systemic autoimmune disease that affects approximately 0·5% of the population worldwide and processes with inflammation of synovial joints and bone destruction [1]. RA is a multi-factorial disease resulting from the combination of environmental and genetic factors. Although the aetiology of this disorder seems to be heterogeneous and to involve several cell subsets of the immune system, currently there is compelling evidence indicating that the pathogenesis involves the specific autoimmune response of T cells [2,3]. Underscoring the role of T helper (Th) cells in RA, several alleles of the human leucocyte antigen D-related (HLA-DR) are associated with the disease [4].

Phospho-tyrosine phosphatases (PTPs) constitute a complex family of more than 100 related enzymes classified into four classes: class I, containing the classical PTPs and the dual-specific phosphatases (DSPs); class II, containing the low molecular weight PTP; class III, containing cell division cycle-25 PTPs (CDC25s); and class IV, containing the eyes absent PTPs [5]. Lymphocytes express 60–70 PTPs expected to be critical to balance phosphorylation levels [6], which are essential for a normal immune response while preventing diseases [7,8]. Some alterations in genes coding for classical PTPs that regulate intracellular signalling in T cells have been involved in autoimmunity, including single nucleotide polymorphisms of PTPN22 and PTPN2, aberrant mRNA processing of protein tyrosine phosphatase, receptor type C (PTPRC) and altered expression levels of PTPN6 and PTPN2 [8–11]. None the less, there is no detailed information concerning the expression profiles of PTPs in immune cells involved in human autoimmune diseases.

Due to the relevant role of CD4 T cell immune responses in RA, we aimed to compare the expression profile of PTPs in total peripheral blood CD4 T cells of healthy individuals and patients submitted to an early arthritis (EA) clinic. In order to avoid the potential effects of specific RA therapy in gene expression, we recruited patients before the

Table 1. Demographic and clinical data of the population included in this study

	Healthy donors (n = 16)	RA (n = 30)	UA (n = 12)	Test result
Female, n (%)	11 (79·2)	22 (73·3)	7 (58·3)	n.s.
Age [years; p50 (IQR)]	47 (40·25–61·00)	57·5 (46·75–66·75)	52·5 (40·5–59·75)	n.s.
Smoking, n (%)				n.s.
Never	7 (43·75)	14 (46·67)	7 (58·33)	
Ever	8 (50·00)	11 (36·67)	5 (41·66)	
Current	1 (6·25)	5 (16·67)	–	
Disease duration [months; p50 (IQR)]	–	5·1 (2·8–10·1)	7·2 (2·1–12·2)	n.s.
RF, n (%)	–	18 (60·00)	4 (33·33)	0·06
ACPA, n (%)	–	16 (53·33)	5 (41·66)	n.s.
ANA, n (%)	–	12 (40·00)	5 (41·66)	n.s.
DAS28 [p50 (IQR)]	–	4·1 (3·1–5·7)	3·5 (2·7–4·8)	n.s.
SDAI [p50 (IQR)]	–	19·1 (11·25–35·33)	13·1 (7·8–25·0)	n.s.
HUPI [p50 (IQR)]	–	7 (4–10·3)	5·25 (3·8–10·4)	n.s.
HAQ [p50 (IQR)]	–	0·875 (0·375–1·438)	0·8125 (0·4063–1·531)	n.s.

The P-value is shown of Fisher's exact or Mann–Whitney test for comparing qualitative or quantitative variables, respectively. Three groups were compared by the Kruskal–Wallis test. IQR = interquartile range; n.s. = non-significant; RF = rheumatoid factor; ACPA = anti-citrullinated peptide antibodies; ANA = anti-nuclear antibodies; DAS28 = 28-joint Disease Activity Score; SDAI = Simplified Disease Activity Index; HUPI = 'Hospital Universitario de La Princesa' Index; HAQ = Health Assessment Questionnaire.

administration of any drug at their initial visit to the hospital. Insights into the potential role of transcript levels of PTPs as biomarkers of the disease were obtained by comparing seropositive and seronegative patients, as well as patients with different disease activity.

Materials and methods

Patients and clinical parameters

We used 42 patients from the Princesa Early Arthritis Register Longitudinal (PEARL) study, a prospective register of patients submitted to an EA clinic. The protocol includes the collection of sociodemographic, clinical, analytical and therapeutic information, as well as biological samples at five structured visits. Rheumatoid factor (RF) was assessed by nephelometry and anti-citrullinated peptide antibodies (ACPA) and anti-nuclear antibodies (ANA) by enzyme-linked immunosorbent assay (ELISA) with QUANTA Lite CCP3 and ANA kits, respectively (Inova Diagnostics, San Diego, CA, USA). CD4 T cells were isolated during the baseline visit, so only one patient had received treatment (methotrexate) before sample collection.

Of these 42 patients, 30 fulfilled the 2010 American College of Rheumatology/European League Against Rheumatism criteria for RA [12] and 12 were classified as undifferentiated arthritis (UA) [13]. Considering the discrepancies found when assessing the activity of the RA, we categorized global disease activity by combining 28-joint Disease Activity Score (DAS28) [14], 'Hospital Universitario de La Princesa' Index (HUPI) [15] and Simplified Disease Activity Index (SDAI) [16] in the following subsets: remission, low, moderate and high disease activity when the three indices were in agreement, and remission/low, low/moderate and moderate/high disease activity when disagreement was observed. Healthy volunteers (n = 16) were also recruited and all information concerning the population included in the study is shown in Table 1.

This study was conducted according to the recommendations of the Declaration of Helsinki and the protocol approved by the Clinical Research Ethics Committee of the 'Hospital Universitario La Princesa' (Madrid, Spain). All patients signed a written consent before being included into the PEARL study.

Isolation of peripheral blood CD4 T cells

Peripheral blood mononuclear cells were obtained by density gradient centrifugation on Lymphoprep™ (Rafer, Spain). CD4 T cells were isolated using the Dynabeads® Untouched™ human CD4 T cells kit (Invitrogen, Carlsbad, CA, USA). Purities above 95% were typically obtained.

Real-time quantitative polymerase chain reaction (RT–qPCR)

RNA was extracted using the Absolutely RNA Microprep Kit (Agilent Technologies, Santa Clara, CA, USA) and 2 μg were reverse-transcribed using the high-capacity cDNA reverse transcription kit (Applied Biosystems, Carlsbad, CA, USA). Using TaqMan low-density arrays (TLDAs, ThermoFisher, Fremont, CA, USA), three healthy donors and three RA patients were compared initially for the expression profiles of genes coding for DSPs and class II, III and IV PTPs, as well as for suppressors of cytokine signalling (SOCS). Age and gender were paired in each comparison performed per TLDA (Fig. 1a). The three patients were diagnosed with seropositive ($ACPA^+/RF^+$) RA and

 © 2017 British Society for Immunology, *Clinical and Experimental Immunology*, **189:** 113–119

(a)

Pair	Age (C vs RA)	Gender	Smoking
C1 vs RA1	50 vs 46	Male	Ever vs Current
C2 vs RA2	40 vs 49	Female	Never
C3 vs RA3	63 vs 77	Female	Ever vs Never

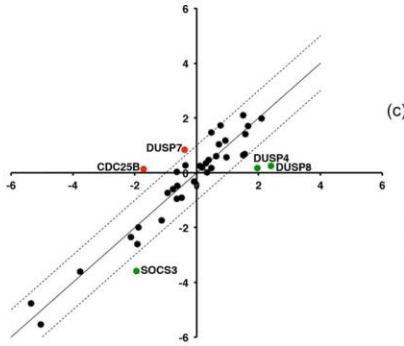

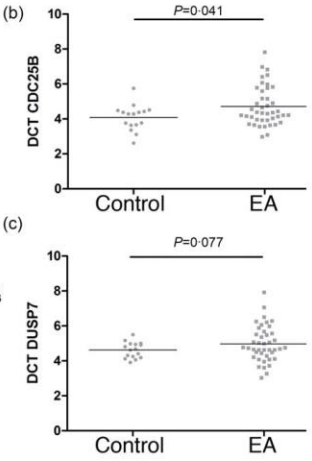

Fig. 1. Analysis of the expression of phospho-tyrosine phosphatases (PTPs) in healthy donors and patients with early arthritis (EA). (a) The table provides information for healthy and diseased donors used in the initial comparisons. Cn and RAn indicate the number of healthy donors and RA patients, respectively. Plot of average dCT values obtained for each gene in the three comparisons of healthy donors (*x*-axis) and rheumatoid arthritis (RA) patients (*y*-axis). Diagonal line labels the position of genes with the same expression. Dashed lines identify genes whose average dCT differs in an absolute value higher than one CT. Genes with lower and higher transcript levels in RA patients are labelled in red and green, respectively. (b,c) Transcript levels of CDC25B (b) and dual-specific phosphatase-7 (DUSP7) (c) in control volunteers and EA patients. Dots in graphs represent the dCT value in each individual analysed. The horizontal line indicates the average value. The probability of the Student's *t*-test is indicated.

had not received any treatment at the time of sample extraction. Genes with CT values > 33 were rejected, and the delta (D)CT was calculated using as reference the average CT of all genes analysed. A difference equal to or higher than 1 CT was indicative of genes with different expression levels.

Data obtained with TLDAs were studied further in higher samples of healthy volunteers and patients submitted to the EA clinic. qPCR reactions were performed with TaqMan Gene Expression Master Mix and the following predesigned qPCR assays (Applied Biosystems): GNB2L1 (Hs00272002_m1), dual-specific phosphatase (DUSP)8 (Hs00792712_g1), DUSP7 (Hs00997002_m1), DUSP4 (Hs01027785_m1) and CDC25B (Hs00244740_m1). GNB2L1 was used as housekeeping gene in these sets of qPCRs.

Statistical analysis

A Student's *t*-test for comparing groups of qPCR data was implemented in GraphPad Prism (GraphPad Software, Inc., San Diego, CA, USA). The Welch correction was applied when variances were different according to a *F*-test. For comparing sociodemographic, clinical and analytical variables, Fisher's exact, Mann–Whitney and Kruskal–Wallis tests were used (Table 1). *P*-values $\leq 0{\cdot}05$ were considered statistically significant.

Results

Expression profile of PTPs in CD4 T cells of healthy donors and RA patients

Despite the similar expression profile of PTPs found in CD4 T cells from RA patients and healthy donors in the initial comparison (see Materials and methods), the expression level of four PTPs was found to be substantially different (Fig. 1a). The transcript levels of the mitogen activated protein kinase (MAPK) phosphatase (MKP) DUSP7 and the cell division cycle-25B (CDC25B) were substantially lower and the MKPs DUSP8 and DUSP4 substantially higher in RA patients. Expression of the suppressor of cytokine signalling-3 (SOCS-3) was higher in RA patients, consistent with a proinflammatory cytokine environment in the pathology. This result is in agreement with the overexpression of SOCS-3 in T cells of RA patients documented previously [17].

The expression level of these genes was analysed further in a higher sample of healthy donors and patients with EA. While transcript levels of DUSP4 and DUSP8 were not different (data not shown), a significantly lower expression of CDC25B was found in CD4 T cells obtained from patients (Fig. 1b). A lower expression of DUSP7 was also observed,

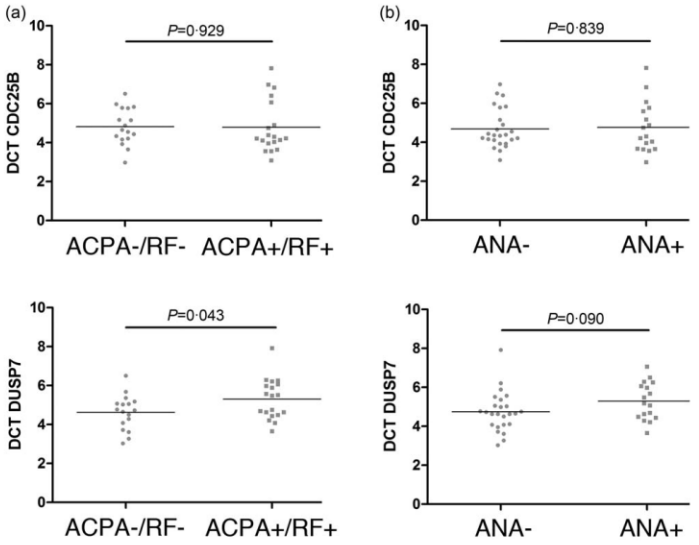

Fig. 2. Low expression of dual-specific phosphatase-7 (DUSP7) in anti-citrullinated peptide antibodies $(ACPA)^+$/rheumatoid factor $(RF)^+$ seropositive patients. (a,b) Graphs represent the dCT value of CDC25B or DUSP7 in EA patients seronegative or seropositive for ACPA and RF or anti-nuclear antibodies (ANA). The horizontal line indicates the average value. The probability of the Student's *t*-test is indicated.

although the difference was not statistically significant (Fig. 1c). Transcript levels of CDC25B and DUSP7 were not different in cells of patients classified as RA and UA (Supporting information, Fig. S1). We found neither correlation between the expression level of CDC25B or DUSP7 and the age of donors nor the genes showing expression levels associated with gender or smoking habit (data not shown).

Lower transcript levels of DUSP7 in seropositive ($ACPA^+/FR^+$) patients

We also studied the relationship of the expression levels of CDC25B or DUSP7 with the serum title of RF, ACPA and ANA. The expression level of DUSP7, but not of CDC25B, was significantly lower in seropositive ($ACPA^+/FR^+$) than in seronegative patients (Fig. 2a). Lower transcript levels of DUSP7 were also found in ANA^+ patients, although differences were not statistically significant (Fig. 2b). In any case, correlation was found with the title of the sera (data not shown). No significant difference in CDC25B was found depending on the ANA status (Fig. 2b).

Low expression levels of CDC25B correlated with the disease activity

We studied the correlation of DUSP7 or CDC25B transcript levels with the global disease activity determined by combining the DAS28, HUPI and SDAI clinical parameters (see Material and methods). The expression of DUSP7 and CDC25B was analysed in the different subsets of disease activity, including remission (R), remission/low (R/L), low (L), low/moderate (L/M), moderate (M), moderate/high (M/H) and high (H). The expression level of CDC25B in patients with active disease was lower than in patients in remission groups or in healthy volunteers ($<dCT>_{active} = 4{\cdot}90 \pm 1{\cdot}17$, $<dCT>_{remission} = 3{\cdot}93 \pm 0{\cdot}25$ and $<dCT>_{controls} = 4{\cdot}08 \pm 0{\cdot}7$) (Fig. 3a,b). None the less, the transcript level of DUSP7 was not different among subsets (Fig. 3c).

Discussion

Despite the multi-factorial nature of the RA aetiology, it is currently proposed that CD4 T cells play a major role in the pathogenesis of this disease. Owing to the critical role of phosphorylation levels in regulating intracellular signalling networks that control normal CD4 T cell immune responses, we aimed to compare the expression profile of genes coding for PTPs in cells of healthy volunteers and patients submitted to an EA clinic before being exposed to specific RA therapy.

In this study we have analysed CD4 T cells, which cooperate for B cell activation. It will be also interesting to study the expression profile of PTPs in other cells involved in the pathology, such as B cells. Besides the secretion of autoantibodies, B cells are thought to participate in RA pathogenesis by presenting antigen to T cells and by secreting cytokines [18]. Thus, the proper function of signalling networks regulating these processes should be investigated. Consistent with B cell relevance in RA pathogenesis, an improvement of the clinical symptoms of the pathology

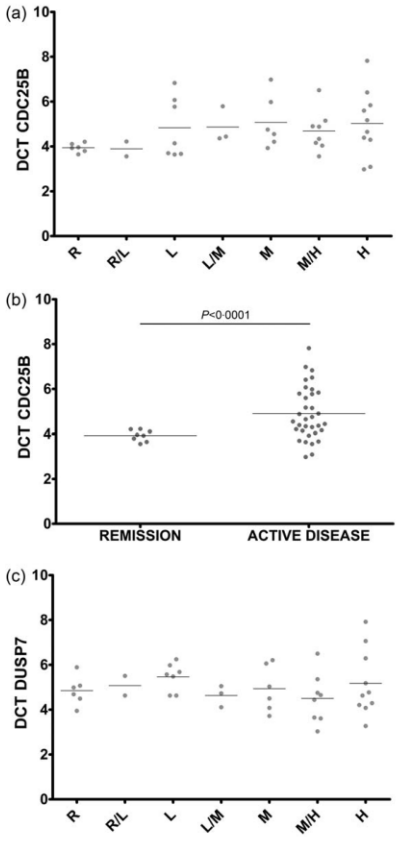

Fig. 3. Low expression of CDC25B in patients with active arthritis. Graphs represent the dCT values of CDC25B (a) and dual-specific phosphatase-7 (DUSP7) (c) in patients in different subsets of disease activity, including: remission (R), remission/low (R/L), low (L), low/moderate (L/M), moderate (M), moderate/high (M/H) and high (H). (b) The graph represents the dCT values of CDC25B in the remission group, resulting from grouping R and R/L subsets, or in the active disease group, resulting from grouping all the remaining subsets. The probability of the Student's *t*-test is indicated.

has been demonstrated by the treatment of patients with rituximab [19], an anti-CD20 antibody, which promotes antibody-dependent cellular cytotoxicity of B cells [20].

The transcript level of DUSP7 was lower in seropositive patients. DUSP7 is a cytoplasmic DSP belonging to the MKPs that regulate the phosphorylation state of the MAPK extracellular-regulated kinase (ERK) [21]. The function of this DSP in T cells is currently not known, and the lower transcript level of DUSP7 in $ACPA^+/RF^+$ patients might indicate a regulatory role in processes deregulated in the seropositive pathology. Association of lymphoid-specific phosphatase (LYP) polymorphism C1858T (R620W) with seropositive RA patients has also been shown [22]. Interestingly, LYP regulates TCR signalling and whether it is also the case for DUSP7 should be investigated. The possible role of DUSP7 as a biomarker of seropositive RA should be assessed further in a larger cohort of patients.

Lower levels of CDC25B were observed in those patients with marked active disease. CDC25B is a known regulator of G2/M transition during the cell cycle [23]. None the less, the function of this molecule in CD4 T cells has not been evaluated. CDC25B is phosphorylated and activated at the centrosome by Aurora A kinase [24], which has been proposed to be required for the dynamics of microtubules supporting intracellular signalling subjacent to the activation of T cells [25]. Thus, it is tempting to speculate that lower levels of CDC25B might promote a higher disease activity by altering T cell sensitivity or activation. The regulatory role of CDC25B during T cell activation should be investigated. The cross-sectional design of our study does not allow determining whether the low level of CDC25B is the origin or the consequence of the inflammatory process. Supporting the latter, we have found that pharmacological activation of PKC and cytosolic Ca^{2+} elevation in CD4 T cells of healthy individuals resulted in down-modulation of CDC25B transcript levels [26]. Whether the treatment of active RA with typical immunosuppressants may restore the expression level of this enzyme should be tested further in a longitudinal follow-up study.

RA pathology has been associated with an anticipated ageing of the immune system. This pathological ageing seems to be due to premature dysfunction of the thymus in RA patients. Early thymus dysfunction promotes an increase in self-replication of T cells promoting an accelerated senescence characterized by short telomeres, cell cycle arrest and secretion of proinflammatory cytokines [27]. This enhanced replicative stress, directed to compensate for the loss of new thymic emigrants to the periphery, renders cells with a low capacity to proliferate. Consistently, the number of T cells in cell cycle in RA patients has been proposed to be lower than in healthy individuals [28]. Interestingly, low levels of CDC25B, which promote cell division, might participate or be a consequence of this process.

Changes in transcript levels might be due to different frequencies of CD4 T cell subtypes in patients. Thus, a deeper analysis of transcript levels in CD4 T cell subpopulations will be needed to understand more clearly the changes found in this work. Importantly, no difference has been found previously in the percentage of peripheral blood naive and memory T cells in RA patients [29]. Although other authors found a reduction in the central memory compartment in RA, the cohort used contained

therapy-submitted patients of long-duration disease [30]. Thus, it is not comparable with the cohort used in this work. In addition, an expansion of effector-memory T cells ($CD4^+CD28^-$) has been broadly found, in particular in patients with severe extra-articular RA [31]. These cells are characterized by a senescent phenotype associated with the expression of NK cell stimulatory molecules, such as NKG2D [32]. We did not find a substantial expansion of $CD4^+CD28^-$ $NKG2D^+$ cells in our cohort, although a slightly higher percentage of this T cell subpopulation was observed in some patients (data not shown). Our finding is consistent with an early stage of the pathology with no signs of severe extra-articular RA.

The most remarkable information in this study was that low transcript levels of CDC25B were associated with subsets of patients with higher disease activity. Whether low expression levels may contribute to the origin or the progression of autoimmune arthritis should be investigated. Lower transcript levels may be the consequence of higher cell activation in a more inflammatory environment in patients with active disease or of recent episodes of enhanced self-replicative stress. Our data suggest that measuring the expression levels of CDC25B might assist in the evaluation of the activity or prognosis of the disease. None the less, a longitudinal study in a larger cohort of patients will be needed in order to assess how patients evolve during the disease or respond to different therapies. This will provide information about the relation between gene expression and the pathogenesis of the RA. We are currently working in this direction.

Acknowledgements

This work was supported by funds of the Spanish Ministry of Economy and Competitiveness (MINECO) (SAF2012-33218 and SAF2016-75656-P) and the European Union (FP7-PEOPLE-2012-CIG) to P. R.-N. These projects support P. C.-S. and R. R.-M. The PEARL study is supported by PI14/00442 to IG-A and the work of A. L. was supported by PIE13/00041, both grants from the MINECO ('Instituto de Salud Carlos III'), co-funded by 'Fondo Europeo de Desarrollo Regional' (FEDER). A. L. was co-funded by SER (Sociedad Española de Reumatología) to A. O.

Disclosure

The authors declare that there is no financial or commercial conflict of interest regarding the publication of this paper.

References

1 Scott DL, Wolfe F, Huizinga TWJ. Rheumatoid arthritis. Lancet 2010; **376**:1094–108.
2 Conigliaro P, Chimenti MS, Triggianese P *et al.* Autoantibodies in inflammatory arthritis. Autoimmun Rev 2016; **15**:673–83.
3 Bossini-Castillo L, de Kovel C, Kallberg H *et al.* A genome-wide association study of rheumatoid arthritis without antibodies against citrullinated peptides. Ann Rheum Dis 2015; **74**:e15.
4 Bax M, van Heemst J, Huizinga TWJ, Toes REM. Genetics of rheumatoid arthritis: what have we learned?. Immunogenetics 2011; **63**:459–66.
5 Alonso A, Sasin J, Bottini N *et al.* Protein tyrosine phosphatases in the human genome. Cell 2004; **117**:699–711.
6 Arimura Y, Yagi J. Comprehensive expression profiles of genes for protein tyrosine phosphatases in immune cells. Sci Signal 2010; **3**:rs1.
7 Mustelin T, Vang T, Bottini N. Protein tyrosine phosphatases and the immune response. Nat Rev Immunol 2005; 5:43–57.
8 Rhee I, Veillette A. Protein tyrosine phosphatases in lymphocyte activation and autoimmunity. Nat Immunol 2012; **13**:439–47.
9 The Wellcome Trust Case Control Consortium. Genome-wide association study of 14,000 cases of seven common diseases and 3,000 shared controls. Nature 2007; **447**:661–78.
10 Doody KM, Bussieres-Marmen S, Li A, Paquet M, Henderson JE, Tremblay ML. T cell protein tyrosine phosphatase deficiency results in spontaneous synovitis and subchondral bone resorption in mice. Arthritis Rheum 2012; **64**:752–61.
11 Vang T, Miletic AV, Arimura Y, Tautz L, Rickert RC, Mustelin T. Protein tyrosine phosphatases in autoimmunity. Annu Rev Immunol 2008; **26**:29–55.
12 Aletaha D, Neogi T, Silman AJ *et al.* 2010 Rheumatoid arthritis classification criteria: an American College of Rheumatology/European League Against Rheumatism collaborative initiative. Arthritis Rheum 2010; **62**:2569–81.
13 Verpoort KN, van Dongen H, Allaart CF, Toes REM, Breedveld FC, Huizinga TWJ. Undifferentiated arthritis - disease course assessed in several inception cohorts. Clin Exp Rheumatol 2004; **22**:S12–S7.
14 Prevoo ML, van 't Hof MA, Kuper HH, van Leeuwen MA, van de Putte LB, van Riel PL. Modified disease activity scores that include twenty-eight-joint counts. Development and validation in a prospective longitudinal study of patients with rheumatoid arthritis. Arthritis Rheum 1995; **38**:44–8.
15 Gonzalez-Alvaro I, Castrejon I, Ortiz AM, Toledano E *et al.* Cut-offs and response criteria for the Hospital Universitario La Princesa Index (HUPI) and their comparison to widely-used indices of disease activity in rheumatoid arthritis. PLOS ONE 2016; **11**:e0161727.
16 Aletaha D, Smolen J. The simplified disease activity index (SDAI) and the clinical disease activity index (CDAI): a review of their usefulness and validity in rheumatoid arthritis. Clin Exp Rheumatol 2005; **23**:S100–8.
17 Isomaki P, Alanara T, Isohanni P *et al.* The expression of SOCS is altered in rheumatoid arthritis. Rheumatology 2007; **46**:1538–46.
18 Bugatti S, Vitolo B, Caporali R, Montecucco C, Manzo A. B cells in rheumatoid arthritis: from pathogenic players to disease biomarkers. BioMed Res Int 2014; **2014**:681678.
19 Edwards JC, Szczepanski L, Szechinski J *et al.* Efficacy of B-cell-targeted therapy with rituximab in patients with rheumatoid arthritis. N Engl J Med 2004; **350**:2572–81.
20 Edwards JCW, Cambridge G. Sustained improvement in rheumatoid arthritis following a protocol designed to deplete B lymphocytes. Rheumatology 2001; **40**:205–11.

21 Caunt CJ, Keyse SM. Dual-specificity MAP kinase phosphatases (MKPs): Shaping the outcome of MAP kinase signalling. FEBS J 2013; **280**:489–504.
22 Taylor LH, Twigg S, Worthington J *et al.* Metaanalysis of the association of smoking and PTPN22 R620W genotype on autoantibody status and radiological erosions in rheumatoid arthritis. J Rheumatol 2013; **40**:1048–53.
23 Sur S, Agrawal DK. Phosphatases and kinases regulating CDC25 activity in the cell cycle: clinical implications of CDC25 overexpression and potential treatment strategies. Mol Cell Biochem 2016; **416**:33–46.
24 Dutertre S, Cazales M, Quaranta M *et al.* Phosphorylation of CDC25B by Aurora-A at the centrosome contributes to the G2-M transition. J Cell Sci 2004; **117**:2523–31.
25 Blas-Rus N, Bustos-Moran E, de Castro IP *et al.* Aurora A drives early signalling and vesicle dynamics during T-cell activation. Nat Commun 2016; **7**:11389.
26 Castro-Sánchez P, Ramirez-Munoz R, Roda-Navarro P. Gene expression profiles of human phospho-tyrosine phosphatases consequent to Th1 polarisation and effector function. J Immunol Res 2017; 8701042, 12pp.
27 Weyand CM, Fulbright JW, Goronzy JJ. Immunosenescence, autoimmunity, and rheumatoid arthritis. Exp Gerontol 2003; **38**:833–41.
28 Goronzy JJ, Weyand CM. Thymic function and peripheral T-cell homeostasis in rheumatoid arthritis. Trends Immunol 2001; **22**:251.
29 Dejaco C, Duftner C, Klauser A, Schirmer M. Altered T-cell subtypes in spondyloarthritis, rheumatoid arthritis and polymyalgia rheumatica. Rheumatol Int 2010; **30**: 297–303.
30 Matsuki F, Saegusa J, Miyamoto Y, Misaki K, Kumagai S, Morinobu A. CD45RA-Foxp3(high) activated/effector regulatory T cells in the CCR7 $^{+}$ CD45RA-CD27 $^{+}$ CD28^{+}central memory subset are decreased in peripheral blood from patients with rheumatoid arthritis. Biochem Biophys Res Commun 2013; **438**: 778–83.
31 Martens PB, Goronzy JJ, Schaid D, Weyand CM. Expansion of unusual CD4^{+} T cells in severe rheumatoid arthritis. Arthritis Rheum 1997; **40**:1106–14.
32 Groh V, Bruhl A, El-Gabalawy H, Nelson JL, Spies T. Stimulation of T cell autoreactivity by anomalous expression of NKG2D and its MIC ligands in rheumatoid arthritis. Proc Natl Acad Sci USA 2003; **100**:9452–7.

Supporting information

Additional Supporting information may be found in the online version of this article at the publisher's web-site:

Fig. S1. Expression of CDC25B and dual-specific phosphatase-7 (DUSP7) in patients classified as rheumatoid arthritis (RA) or undifferentiated arthritis (UA). Graphs represent the dCT value in patients. The horizontal line indicates the average value. The probability of the Student's *t*-test is indicated.

Hindawi
Journal of Immunology Research
Volume 2017, Article ID 8701042, 12 pages
http://dx.doi.org/10.1155/2017/8701042

Research Article

Gene Expression Profiles of Human Phosphotyrosine Phosphatases Consequent to Th1 Polarisation and Effector Function

Patricia Castro-Sánchez, Rocio Ramirez-Munoz, and Pedro Roda-Navarro

Department of Microbiology I (Immunology), School of Medicine, Complutense University and "12 de Octubre" Health Research Institute, Madrid, Spain

Correspondence should be addressed to Pedro Roda-Navarro; proda@med.ucm.es

Received 4 December 2016; Accepted 14 February 2017; Published 14 March 2017

Academic Editor: Andréia M. Cardoso

Phosphotyrosine phosphatases (PTPs) constitute a complex family of enzymes that control the balance of intracellular phosphorylation levels to allow cell responses while avoiding the development of diseases. Despite the relevance of CD4 T cell polarisation and effector function in human autoimmune diseases, the expression profile of PTPs during T helper polarisation and restimulation at inflammatory sites has not been assessed. Here, a systematic analysis of the expression profile of PTPs has been carried out during Th1-polarising conditions and upon PKC activation and intracellular raise of Ca^{2+} in effector cells. Changes in gene expression levels suggest a previously nonnoted regulatory role of several PTPs in Th1 polarisation and effector function. A substantial change in the spatial compartmentalisation of ERK during T cell responses is proposed based on changes in the dose of cytoplasmic and nuclear MAPK phosphatases. Our study also suggests a regulatory role of autoimmune-related PTPs in controlling T helper polarisation in humans. We expect that those PTPs that regulate T helper polarisation will constitute potential targets for intervening CD4 T cell immune responses in order to generate new therapies for the treatment of autoimmune diseases.

1. Introduction

CD4 T cells are important components of adaptive immune responses. During antigen stimulation, T cells polarise towards a type of effector cell specialised in controlling different sorts of infections by secreting different cytokines: Effector T helper 1 (Th1) secretes IFNγ and is specialised against intracellular pathogens, Th2 secretes IL-4 and is specialised against helminths, and Th17 secretes IL-17 and is specialised against extracellular bacterial and fungi. Despite having a crucial role in the immunity against pathogens, helper T cells are also involved in immune system-related diseases, including allergies and autoimmune pathologies. It is well established that Th2 responses mediate allergy and, currently, major efforts are directed to understand the pathological balance of Th1, Th2, and Th17 polarisation in autoimmune diseases [1–4].

In humans, protein tyrosine phosphatases (PTPs) constitute a family of more than 100 enzymes that regulate the phosphorylation state of molecular components of signalling networks. The folding of the PTP domain classifies PTPs in four classes: class I, containing the classical nonreceptor and receptor PTPs (NRPTPs and RPTPs, respectively) and the dual specific phosphatases (DSPs) [5]; class II, containing the low molecular weight PTP (LM-PTP); class III, containing cell division cycle-25 PTPs (CDC25s); and class IV, containing the eyes absent PTPs (EYAs) [6]. Catalytic activity of classes I to III is based on a Cysteine residue, while in the case of class IV it is based on an Aspartic acid residue [5, 6]. Despite their important role in balancing phosphorylation levels, it is becoming clear that they also regulate intracellular signalling by mechanisms not dependent on the phosphatase activity, including the competition for the binding of inhibitors, like in the case of phosphatase of regenerating liver-1 (PRL-1) [7], the control of the spatial regulation of nonphosphorylated substrates, like in the case of MAPK phosphatases (MKPs) [8], and the control of the catalytic activity of other PTPs, like in the case of noncatalytic myotubularins (MTMs) [9]. These mechanisms underscore the relevance of the dose and the spatial

regulation of PTPs in the signalling networks that control cell responses.

Lymphocytes express around 60 to 70 genes coding for PTPs [10–12] and the significance of the above-mentioned regulatory mechanisms for the immune responses by human CD4 T cells has been barely established. Studying these mechanisms is needed in order to understand how CD4 T cells achieve normal immune responses while preventing diseases. In this regard, the critical role of some classical PTPs in lymphocyte activation and the association of genetic variants to autoimmune disease have been described [13, 14]. Nonetheless the dose and the regulatory role of the majority of DSPs and class II to IV PTPs (for simplicity called in this study nonclassical PTPs or NCs) in T helper polarisation and effector function have not been studied. Here, we characterise the expression profile of the genes coding for these groups of PTPs in human naïve CD4 T cells, during the polarisation to Th1 effector cells and in response to PKC stimulation and cytosolic raise of Ca^{2+}. Our data suggest that changes in the dose of MAPK phosphatases (MKPs) might dramatically affect the regulation of the MAPK module during T cell polarisation and stimulation at the inflammatory sites. Gene expression changes found in our study suggest the existence of previously nonnoted regulators of Th1 polarisation and effector functions and, consequently, potential targets for the manipulation of CD4 T cell immune responses in future research directed to obtain therapies for the treatment of autoimmune diseases.

2. Materials and Methods

2.1. Cell Isolation, Culture, and Stimulation. Blood cells of healthy adult donors (<65 year old) where obtained from buffy coats processed at the transfusion centre of the "Comunidad de Madrid," Spain. Peripheral blood mononuclear cells (PBMCs) were obtained by Lymphoprep™ (Rafer, Spain) density gradient centrifugation. Naïve CD4 T cells were isolated from PBMCs using the Naïve $CD4^+$ T cell Isolation Kit II (Miltenyi Biotec, Germany). Purities over 95% were typically obtained as assessed by flow cytometry. For Th1 polarising conditions, the obtained naïve CD4 T cells were cultured for 12 days in RPMI 1640 (Lonza Group, Switzerland) supplemented with 10% FCS (Gibco, USA), Penicillin-Streptomycin 100 U/mL and 100 μg/mL, respectively, and 2 mM L-Glutamine (all from Lonza Group, Switzerland) in the presence of Dynabeads Human T-Activator CD3/CD28 (Invitrogen, USA) and 10 ng/ml of IL-12 (Peprotech, USA). Th1 cells were then restimulated for 4 hours with 10 ng/mL Phorbol 12-myristate 13-acetate (PMA) plus 1 μM Ionomycin (Th1-PI) (both from Sigma Aldrich, USA).

2.2. Flow Cytometry. Th1 polarisation was assessed by analysing the production of IFNγ in response to stimulation with PMA and Ionomycin. Th1 cells were stimulated as explained in Section 2.1 in the presence of 5 μg/mL Brefeldin A (Sigma Aldrich, USA). Cells were then washed, fixed with 4% paraformaldehyde (Sigma Aldrich, USA) permeabilized with 0,1% saponin (Sigma Aldrich, USA), and stained with anti-IFNγ antibody (BD pharmingen, USA). Flow cytometry data were collected using a FacsCalibur flow cytometer (BD Biosciences, USA).

2.3. Real-Time Quantitative Polymerase Chain Reaction (qPCR). RNA was extracted from naïve, Th1, and Th1-PI cells using the Absolutely RNA Microprep Kit (Agilent Technologies, USA) and the RNA integrity was assessed using the Agilent 2100 Bioanalyzer (Agilent Technologies, USA). 2 μg of RNA was used to synthesize cDNA with the High Capacity cDNA Reverse Transcription Kit (Applied Biosystems, USA). Expression profiles were obtained by qPCR implemented with TaqMan Low Density Arrays (TLDA, ThermoFisher, USA) in a 7900HT Fast Real-Time PCR System (Applied Biosystems, USA). Genes with CT values under 33 were considered to be nonexpressed. Delta (D)CT was calculated by using as housekeeping gene the average of CT values obtained for the genes 18S and GNB2L1. RQ was calculated using the $2^{-\Delta\Delta CT}$ method [48].

2.4. Data and Statistical Analysis. An agglomerative hierarchical tree was implemented in MATLAB (The Mathworks, Inc, USA) by using Euclidean metrics and the ward method. Statistical analysis was implemented in GraphPad Prism version 5.04 (GraphPad Software, USA). Changes in mRNA levels between different conditions (Naïve, Th1, and Th1-PI) obtained for each donor were analysed with a paired t-test. A consistent change in the expression level was considered when it was obtained a difference in expression equal or higher than 1,5 CTs in the majority of donors analysed and a p value under 0.1 in the t-test. In each data and statistical analysis, only those donors were used in which all the conditions that wanted to be compared were obtained ($n = 3$ donors in analysis of Table 2 and Figures 2 and 3, $n = 2$ in analysis of Figure 4(a) and $n = 4$ donors in the analysis of Figure 4(b)).

3. Results and Discussion

3.1. Th1 Polarisation of Human Naïve CD4 T Cells. Human naïve CD4 T cells were isolated and polarised to Th1 conditions as detailed in materials and methods. The polarisation was confirmed by the production of IFNγ. The majority of cells in the population produced IFNγ in response to phorbol esters and Ionomycin (PI) treatment (Figure 1(a)). The induction of the Th1 master regulator transcription factor Tbet was also corroborated (Figure 1(b)). PKC activation and cytosolic raise of Ca^{2+}, induced by PI treatment, mimic antigen stimulation via the T cell receptor (TCR) during T cell effector functions at inflammatory sites. By using this in vitro model, we studied the amount of mRNA, which indicates the dose of each PTP in naïve and Th1 effector cells.

3.2. Expression Profile of PTPs Associated with Human CD4 T Cells. We included in this study all NCs given the unknown function of the majority of them in T cells and some classical RPTPs and NRPTPs, due to their regulatory role in the signalling downstream the TCR and cytokine receptors and in the dynamics of the cellular machinery or due to their

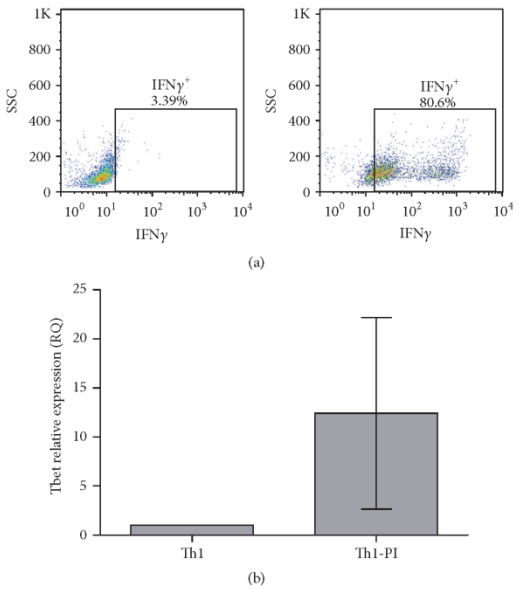

FIGURE 1: Assessment of Th1 polarisation. (a) Flow cytometry dot plots represent the IFNγ production against the size scatter of Th1-polarised cells without (Th1) or with PI treatment (Th1-PI). The percentage of IFNγ producing cells is indicated. A representative experiment is shown. (b) Determination of the RQ of the transcription factor Tbet in naïve and Th1 cells. The average and the standard deviations of 3 donors are shown.

association with autoimmune diseases [13–25, 27, 28, 30–35, 37–39, 49–52] (Table 1). An agglomerative hierarchical tree and statistical analysis were used to characterise the obtained expression profiles (see materials and methods). Consistent with the high number of PTP-coding genes that are expressed in the lymphoid compartment in mice [11], the mRNA of all 14 classical PTPs and 55 out of 65 NCs was detectable in the analysed human naïve and Th1 cells. This fact underscored the relevant role of the family of PTPs in Th1 polarisation and function. Agglomerative hierarchical tree revealed clusters of PTPs, which share not only the expression level and profile during Th1 polarisation but also, in some cases, related functions (Figure 2). The change in the expression profile during Th1 polarisation might be indicative of previously nonnoted regulators of T cell activation/polarisation.

3.2.1. Expression of Classical PTPs. The majority of classical PTPs analysed (10 out of 14) were found inside the group of high expression, including *PTPRC* (CD45), *PTPN1* (PTP1B), *PTPN7* (HePTP), *PTPN6* (SHP1), *PTPRJ* (CD148 or DEP-1), *PTPN4* (MEG1), *PTPN12* (PTP-PEST), *PTPN2* (TC-PTP), *PTPN22* (LYP), and *PTPRA* (PTP-alpha) (Figure 2). Consistent with the established knowledge, PTPRC, an important regulator of Lck activation [14, 16, 17], showed the highest expression levels of all PTPs studied. PTPs found inside the group of middle and low expression included *PTPRK* (PTP-Kappa), *PTPN13* (FAP-1 or PTP-BAS), *PTPN18* (BDP1 or PTP-HSCF), and *PTPN9* (MEG-2) (Figure 2).

PTPRJ, PTPN6, and *PTPN7*, which are known to regulate intracellular phosphotyrosine levels during T cell activation [18, 19, 28, 30, 31], were upregulated with Th1 polarisation (Table 2). Consistent with our data, upregulation of *PTPRJ* in response to TCR stimulation has been previously described [18]. Interestingly, mouse Shp1 limits IL-4 signals and then controls abnormal skewing to Th2 polarisation [49]. Therefore, our data indicate that SHP1 might also have a role in balancing Th1/Th2 polarisation in human CD4 T cells.

Our analysis uncovered a relation between the upregulated expression and the function of some PTPs. For example, *PTPN9*, which regulates the fusion of secretory vesicles with the plasma membrane [32, 33], shared cluster with the myotubularin *MTMR2* (Figure 2), a known regulator of endosomal dynamics (see below). The higher gene expression found in Th1 cells (Figure 2 and Table 2) suggests an important role of these PTPs in endosomal dynamics during the immune responses of Th1 cells. Another example was found inside the group of low expressed PTPs: *PTPN18* and *PTPN13* were found upregulated in the same cluster (Figure 2). Both PTPs have been suggested to regulate *(PTPN18)* or associate with *(PTPN13)* the actin cytoskeleton [50, 51]. Interestingly, they also shared cluster with the DSP

Table 1: Class-I classical RPTP and NRPTP included in this study.

Phosphatase	Substrate	Regulation of T cell activation	Involved in autoimmunity	References
PTPRA (RPTPα)	SFK	Regulation of TCR signalling:	Not reported	[15]
PTPRC (CD45)	SFK and JAK family kinases	Regulation of TCR and cytokine signalling	MS, AH	[13, 16, 17]
PTPRJ (CD148)	SFK	Regulation of TCR signalling	Not reported	[18, 19]
PTPRK (RPTPκ)	STAT3	Regulation of CD4 T cell development	Not reported	[20, 21]
PTPN1 (PTP1B)	STAT6	Not reported	Not reported	[22]
PTPN2 (TC-PTP)	SFK, JAK1, JAK3	Regulation of TCR and cytokine signalling	T1D, CD, S	[23–26]
PTPN4 (PTP-MEG1)	CD247	Regulation of TCR signalling	Not reported	[27]
PTPN6 (SHP1)	SFK, ITAMs, ZAP70, SLP-76	Regulation of TCR signalling	PS	[28, 29]
PTPN7 (HePTP)	ERK1/2, p38	Regulation of TCR signalling	Not reported	[30, 31]
PTPN9 (PTP-MEG2)	NSF	Regulation of cytokine secretion	Not reported	[32, 33]
PTPN12 (PTP-PEST)	Pyk2	Positive regulator of secondary T cell responses	Not reported	[34]
PTPN13 (PTP-BAS)	STAT4, STAT6	Regulation of cytokine signalling	Not reported	[35]
PTPN18 (PTP20)	HER2	Not reported	Not reported	[36]
PTPN22 (LYP)	ZAP70, LCK, FYN	Regulation of TCR signalling	T1D, RA, SLE	[37–39]

SFK: Src family kinases, MS: multiple sclerosis, AH: autoimmune hepatitis, T1D: type 1 diabetes, CD: Crohn's disease, S: synovitis, PS: psoriasis, RA: rheumatoid arthritis, and SLE: systemic lupus erythematosus.

Table 2: PTP regulated during Th1 polarization. PTPs whose expression levels were regulated during Th1 polarization are shown. Changes in expression were determined as explained in materials and methods. Asterisks represent the result of the paired t-test of DCt values obtained from the comparison of naïve and Th1 cells in 3 donors. $p < 0.1$ (*), $p < 0.05$ (**), or $p < 0.01$ (***). Absolute values in column 4 indicate the average change in the DCT, generated by subtracting the DCT value obtained for each condition (DCT_Th1 minus DCT_Naïve) in the 3 individual donors analysed, and obtaining the average. DUSP13 and DUSP21 were considered as repressed genes since their expressions were only detectable in naïve but not in Th1 cells. MTMR11 and CDC25C were considered as induced genes since their expression was detectable in Th1 but not in naïve cells.

Group	Phosphatase	Regulation during Th1 polarization	|Average change in DCT|/p value	Substrate	Regulation of T cell activation or polarisation/Involvement in autoimmunity
Classical	*PTPRJ* (CD148)	Upregulation	2.02/**	SFK	Regulation of TCR signalling/Not reported [18, 19]
	PTPN6 (SHP1)	Upregulation	2.08/**	SFK, ITAMs, ZAP70, SLP-76, Vav1	Regulation of TCR signalling/PS [28, 29]
	PTPN7 (HePTP)	Upregulation	1.54/**	ERK1/2, p38	Regulation of TCR signalling/Not reported [30, 31]
	PTPN9 (PTP-MEG2)	Upregulation	2.45/**	NSF	Regulation of cytokine secretion/Not reported [32, 33]
	PTPN12 (PTP-BL)	Upregulation	2.40/**	STAT4, STAT6	Regulation of cytokine signalling/Not reported [35]
	PTPN18 (PTP20)	Upregulation	1.9/*	HER2	Not reported/Not reported
MKPs and Atypical DSPs	DUSP1	Downregulation	3.07/***	p38, JNK, ERK	T cell activation/Not reported [40]
	DUSP7	Upregulation	2.10/*	ERK	Not reported/Not reported
	DUSP8	Downregulation	4.55/**	JNK, p38	Not reported/Not reported
	DUSP13	Repression		JNK, p38	Not reported/Not reported
	DUSP16	Downregulation	1.20/*	JNK, p38	Th1/Th2 balance/Not reported [41, 42]
	STYXL1	Upregulation	1.19/*	Catalytically inactive	Not reported/Not reported
	DUSP21	Repression		Unknown	Not reported/Not reported
	DUSP22	Upregulation	2.10/**	JNK, ERK2, Lck	Regulation of TCR signaling/EAE, SLE [43–45]
	DUSP23	Upregulation	1.57/***	p38, JNK	Not reported/SLE [46]
Myotubularins	MTMR1	Upregulation	1.43/***	PI(3)P, PI(3,5)P2	Not reported/Not reported
	MTMR2	Upregulation	2.61/**	PI(3)P, PI(3,5)P2	Not reported/Not reported
	MTMR11	Induction		Catalytically inactive	Not reported/Not reported
SSHs, CDC14s and PTEN DSPs	SSH2	Downregulation	1.68/**	Cofilin	Not reported/Not reported
	SSH3	Upregulation	2.63/***	Cofilin	Not reported/Not reported
	TPTE2	Downregulation	1.96/*	PIP	Not reported/Not reported
	CDKN3	Upregulation	5.81/**	CDK2	Inhibition of cell cycle/Not reported [47]
Class III Cys-based PTPs	CDC25A	Upregulation	6.80/**	CDKs	Promotion of cell cycle/Not reported [42]
	CDC25B	Upregulation	2.45/**	CDKs	Not reported/Not reported
	CDC25C	Induction		CDKs	Not reported/Not reported

PS: psoriasis. EAE: experimental autoimmune encephalomyelitis. SLE: systemic lupus erythematosus.

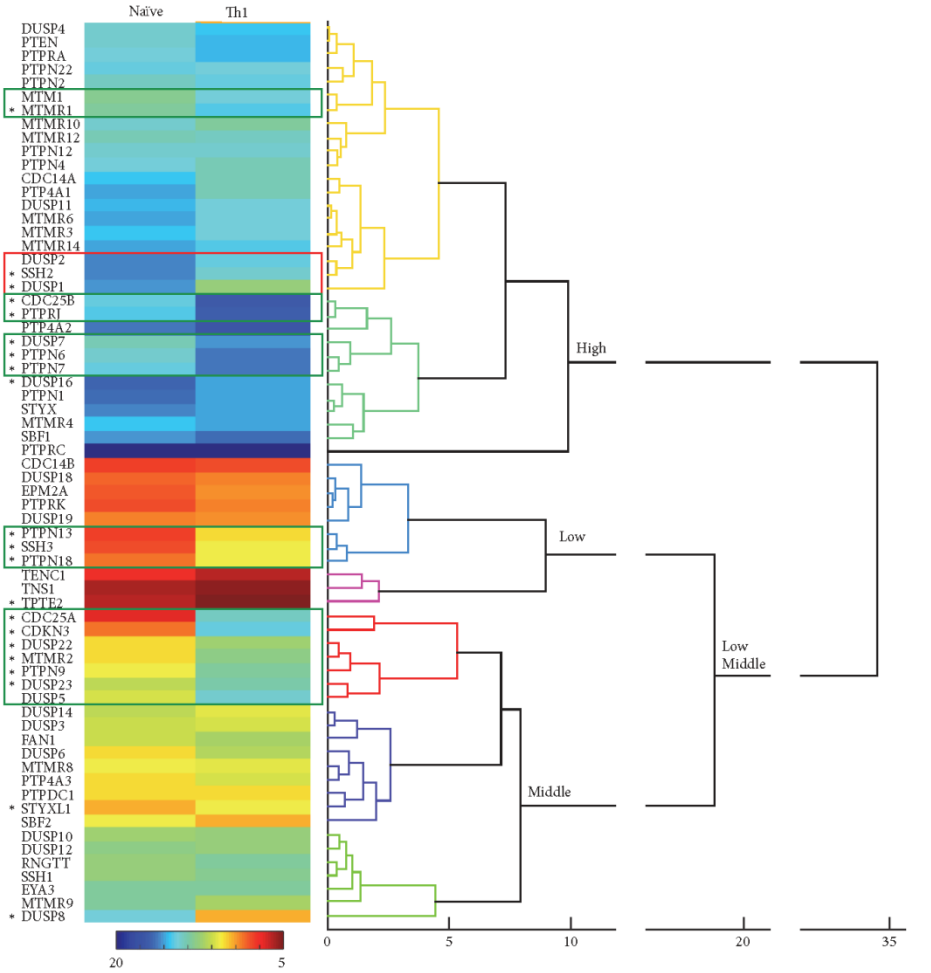

Figure 2: Agglomerative hierarchical tree of the gene expression patterns in naïve and Th1 cells. Numbers below the tree indicate the distance among gene patterns. Hitmap represents the average DCT obtained for each gene in both conditions and 3 donors. The calibration bar is shown between 5 and 20 DCTs. Green and red squares point to clusters of upregulated and downregulated genes, respectively. Asterisks indicate those genes whose expression levels were considered to significantly change, as detailed in Table 2, and explained in materials and methods. Clusters are indicated of high, middle, and low expression.

Slingshot-3 (SSH3), another regulator of the actin cytoskeleton. Thus, the function of *PTPN18* and *PTPN13* in the actin dynamics subjacent T cell activation should be investigated. Consistent with our data, these PTPs have also been found to be expressed in T cells of mice [11]. Interestingly, a regulatory role of *PTPN13* in Th1 and Th2 polarisation has also been proposed [35].

The genes *PTPN1*, *PTPN2*, *PTPN4*, *PTPN12*, *PTPN22*, *PTPRA*, and *PTPRK* were not regulated with Th1-polarising conditions, although the function of some of them in TCR or cytokine signalling has been described (Table 1).

3.2.2. Expression of NCs. We did not detect mRNA of the atypical MKPs *DUSP13*, *DUSP15*, *DUSP26*, and *DUSP27*,

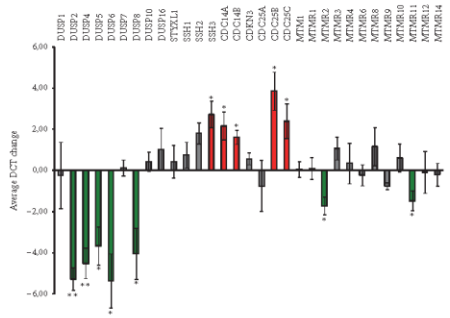

FIGURE 3: Expression change of NCs phosphatases induced by the PI treatment. The graph represents the average of the change in DCT between Th1 and Th1-PI cells. Genes upregulated and downregulated are labelled in green and red, respectively. Assessment of regulated genes is explained in materials and methods. $^{**}p < 0.01$ and $^{*}p < 0.05$ correspond to the probability of paired t-test used in comparison of the DCT values obtained in Th1 and Th1-PI cells from 3 donors.

the classical MKP *DUSP9*, the tensin homolog *TPTE*, the eyes absent *EYA1*, *EYA2,* and *EYA4,* and the myotubularin *MTMR7*. The reported expression of the *Eya1*, *Eya2,* and *Eya3* mouse orthologs [11] suggests a different requirement of this group of PTPs in mice and humans. The same might apply for the myotubularin *MTMR7*, which seems to have a regulatory role in Th polarisation in mice [53]. The expression of tensin homologs was very low and only *PTEN* was highly expressed particularly in Th1 cells (Figure 2). Although very lowly expressed, *TPTE2* was consistently downmodulated with Th1-polarising conditions (Figure 2 and Table 2). Nonexpressed MKPs in our study matched previous data in mice [11].

22 NCs were found in the group of highly expressed PTPs (Figure 2). Substantial changes in expression levels associated with Th1 polarisation were found in genes coding for regulators of the phosphorylation state of phosphoinositides (MTMs), the MAPK signalling module (MKPs), the actin cytoskeleton (Slingshots or SSHs), and the cell cycle (CDC25s and CDKN3) (Table 2). Interestingly, the role of some of these enzymes, including MTMR1, MTMR2, DUSP7, DUSP8, DUSP23, STYXL1, and CDC25B, has not been studied in T cells. To investigate the expression profile of these different groups of PTPs during the effector functions of Th1 cells at inflammatory sites, we analysed the change in expression levels induced by the PI treatment (Figure 3).

MTMs dephosphorylate the position 3 of phosphatidylinositol phosphate (PIP) molecules PI(3)P and PI(3,5)P_2, making them important regulators of the endosomal compartment, the cytoskeleton, and ion channels [9]. Eight out of 12 MTMs were found in the group of highly expressed PTPs (Figure 2), which suggests that they finely tune PIP levels for a proper function of these components of the cellular machinery in T cells. For example, MTMR14 controls the activity of the Ryanodine Receptor (RyR), which is essential for the homeostasis of Ca^{2+} [9]. RyR is needed for Ca^{2+} signalling and proper IL-2 production and proliferation of activated T cells [54]. MTMR14 shared cluster with MTMR6 (Figure 2), which has been described to control naïve CD4 T cell activation by inhibiting the KCa3. $1K^{+}$ channel, which is essential for Ca^{2+} influx [55]. Consistently, a slightly higher mRNA level was found in naïve T cells than in Th1 cells. Other MTM of this cluster was MTMR3, which, along with MTMR6, has been described to regulate autophagy [9], an essential process for the metabolic changes required during T cell activation [56]. Among the highly expressed MTMs, only MTMR1 was found significantly upregulated (Table 2) and shared cluster with MTM1 (Figure 2), which was also weakly upregulated. MTM1 interacts with desmin [57] and might have an important role in cytoskeleton dynamics in T cells.

We also found phosphatase death (PD) MTMs expressed in CD4 T cells, including the highly expressed SBF1 (MTMR5), MTMR10, and MTMR12, the middle expressed MTMR9, and the inducible with Th1 polarisation MTMR11 (Figure 2 and Table 2). PD MTMs have been found to physically interact and increase the catalytic activity of MTMs [9]. For example, MTMR9 regulates the activity of MTMR6 [9] and MTMR8, a previously described regulator of the PI3K/AKT pathway in zebrafish [58]. MTMR9 might constitute an important regulator of CD4 T cell polarisation as has been proposed in mice [53]. The PI treatment upregulated MTMR11 levels in Th1 cells (Figure 3), suggesting a previously unknown regulatory role in effector functions at inflammatory sites. The MTMs regulated by MTMR11 have not been described.

Inside the group of middle expressed PTPs, MTMR2 was found upregulated by Th1-polarising conditions and PI treatment (Table 2 and Figure 3). These data suggest a previously unknown role of this MTM in T cells during Th1 immune responses. MTMR2 catalytic activity is increased by the PD MTMs SBF1, MTMR12, and SBF2 (MTMR13). Although none of these MTMs were found upregulated upon polarisation, the expression level of SBF1 and MTMR12 seems to be enough to allow this regulatory mechanism to take place in naïve and Th1 cells. MTMR2 dephosphorylates PI(3,5)P, which regulates membrane homeostasis and endosomal transport and has been described to interact with Disc large-1 (Dlg-1), which is involved in polarised membrane trafficking [59]. Recently, it has been proposed that ezrin controls tubulin cytoskeleton dynamics, immunological synapse organization, and NFAT activation by interacting with Dlg-1 [60]. Thus, it is tempting to speculate that MTMR2 has a regulatory role in the dynamics of the endosomal compartment during the activation of Th1 cells at inflammatory sites.

The cytoskeleton regulators SSH2 and SSH3 were found downregulated and upregulated, respectively, by Th1-polarising conditions (Table 2). These data underscore the relevance of SSH3 for the cytoskeleton rearrangements during Th1 polarisation or effector function. Despite both proteins being downmodulated by PI treatment (Figure 3), SSH1 expression was not regulated under any treatment. Interestingly, the role of SSHs, including the middle

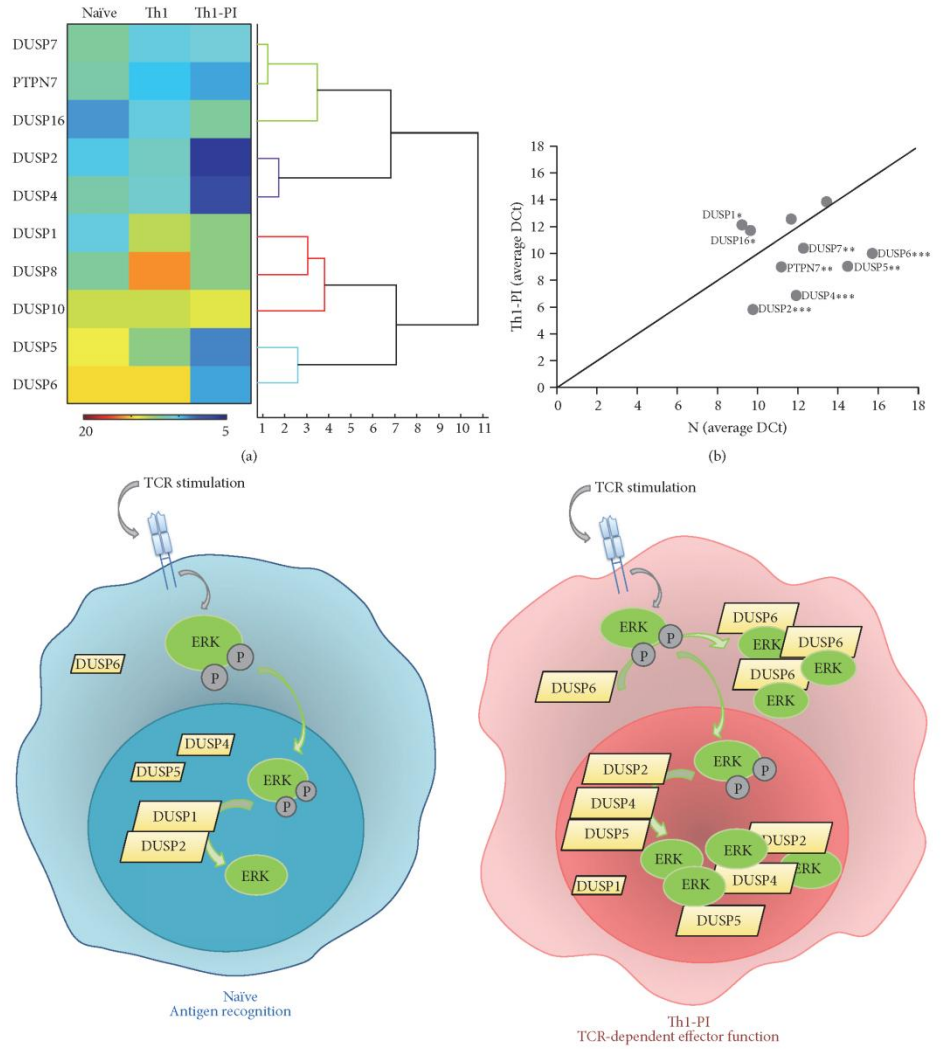

FIGURE 4: Expression of regulators of the MAPK signalling module in naïve and Th1 cells. (a) Agglomerative hierarchical tree of the expression profile of MAPKs phosphatases in naïve, Th1, and Th1-PI samples. Numbers under the tree indicate the distance among the expression profile. Hitmap represents the average DCT obtained for each gene in all samples and 2 donors. Calibration bar is shown between 5 and 20 DCTs. (b) The average DCT obtained for classical MPKs and PTPN7 in naïve (N) and PI treated Th1 cells (Th1-PI) is plotted. The diagonal line labels the position of genes with equal expression levels in both samples. Labelled genes are those with different expression level assessed as explained in material and methods. $^{***}p < 0.001$, $^{**}p < 0.01$, and $^{*}p < 0.05$ correspond to the probability of paired t-test used in comparisons of the DCT values obtained for each gene in naïve and Th1-PI samples from 4 donors. (c) Schematic of proposed spatial regulation of ERK during CD4 T cell immune responses. Dominance of partners of the dephosphorylated ERK in cytoplasm or nucleus might mediate the accumulation of this MAPK and, consequently, promote ERK functions nonmediated by the kinase activity in restimulated Th1 cells.

expressed SSH1, in the intracellular signalling operating during antigen-induced T cell stimulation is not completely understood [61].

Among the 9 out of 10 classical MKPs [8] whose expression was detected, DUSP1, DUSP2, DUSP4, DUSP7, and DUSP16 were found in the group of highly expressed PTPs (Figure 2). Nuclear DUSP1 has been found to be required for proper T cell activation [40] and nuclear/cytoplasmic DUSP16 has been proposed to be downregulated and upregulated during Th1 and Th2 polarisation, respectively, being, in mice, a regulator of the Th1/Th2 balance [41]. Consistently, the expression levels of DUSP16 were found downmodulated during Th1-polarising conditions (Table 2), suggesting a role in balancing human T helper differentiation or in initial T cell immune responses by naïve cells. The cytoplasmic ERK-specific MKP DUSP7 was upregulated with Th1-polarising conditions and shared cluster with the SHP1 and the ERK regulator He-PTP (Table 2 and Figure 2). Interestingly, its function and regulatory mechanism in T cells are not known, and our data might indicate a role of DUSP7 in Th1 polarisation or effector function. The nuclear ERK-specific MKPs DUSP2 and DUSP4 have been described to interact with phosphorylated and dephosphorylated ERK and were upregulated by the PI treatment (Figure 3). Thus, they might be involved in both ERK inactivation and/or accumulation of the dephosphorylated form in the nucleus (see below). DUSP5, DUSP6, DUSP8, and DUSP10 were found inside the group of middle expressed PTPs. Nuclear DUSP5 has been proposed to modulate T cell development and activation [62] and Cytosolic DUSP6 has been proposed to decrease T cell sensitivity by dephosphorylating ERK and, consequently, inhibiting the Lck-ERK positive feedback loop established upon strong T cell stimulation [63]. Interestingly, DUSP5 shared cluster with genes upregulated with polarisation (Figure 2) and both MKPs were upregulated by the PI treatment (Figure 3). The function of the p38- and JNK-specific DUSP8 and DUSP10 in T cell immune responses is not known. DUSP8 was found substantially more abundant in naïve than in Th1 cells (Figure 2) and was upregulated with PI treatment (Figure 3). DUSP10 was not regulated by Th1-polarising conditions or PI treatment.

The group of MKPs are characterised by sharing MAPK substrates. For example, ERK is dephosphorylated by 13 different MKPs. Interestingly, it has been proposed that the spatial distribution of dephosphorylated MAPKs is regulated by the binding of MKPs, such as the nucleocytoplasmic location of ERK by nuclear DUSP5 and cytoplasmic DUSP6, and the accumulation of ERK in the nucleus by DUSP2, DUSP4, and DUSP5 [64–66]. Thus, the coordinated expression levels of MKPs are expected to be essential for the proper function of the MAPK signalling module. Dephosphorylated MAPKs can have functions nondependent on the kinase activity, for example, as transcription factors [8], and they bind with high affinity and increase the activity of MKPs [67]. Thus, more than simply having a role in down-modulating the response of the module, MKPs regulate the subcellular localisation and crosstalk of MAPKs [8, 65]. In this regard, changes in the dose, as may be achieved by regulating their expression levels, may enable MKPs to compete with other molecules for the binding of MAPKs.

Consistent with this complex scenario, Th1 polarisation and PI treatment of Th1 cells induced dramatic changes in the expression profile of ERK-directed MKPs and, consequently, remarkable differences were found between naïve and Th1 restimulated cells (Th1-PI) (Figures 4(a) and 4(b)). While the relative expression of nuclear DUSP1 and DUSP2 was dominant in naïve cells, in Th1 restimulated cells there was a clear dominance of partners of dephosphorylated ERK, including DUSP2, DUSP4, and DUSP5 in the nucleus, and DUSP6 in the cytoplasm. These data suggest that interactions between MKPs and dephosphorylated ERK might accumulate ERK in the cytoplasm and/or the nucleus of restimulated Th1 cells, while in naïve cells nuclear translocation and transient phosphorylation of ERK should dominate the response (Figure 4(c)). DUSP7 was also more abundant in restimulated Th1 cells (Figure 4(b)). Whether it can also bind dephosphorylated ERK should be investigated. Thus, functions nonrelated to its kinase activity of dephosphorylated ERK in the cytoplasm and the nucleus of effector T cells at inflammatory sites and the regulatory role of MKPs in the spatial distribution of dephosphorylated ERK should be investigated. Dynamic compartmentalisation of MAPK signalling module by MKPs warrants future research.

Some atypical MKPs were found regulated by Th1-polarising conditions (Table 2). The JNK- and ERK-specific DUSP22 and DUSP23 were found upregulated in our analysis, suggesting an important role in controlling intracellular signalling during Th1 polarisation or effector function. DUSP22 has been proposed to regulate TCR signalling [43] while the function of DUSP23 in T cell activation is not known. The JNK- and p38-specific DUSP13 and DUSP21 (whose substrates are unknown) were repressed with polarisation. The function of these proteins in T cell biology is also unknown.

Among cell cycle regulators, CDC14A and CDC25B were found in the group of highly expressed PTPs. Interestingly, CDC25B, a negative regulator of the cell cycle was upregulated by Th1-polarising conditions (Table 2). CDC25A and CDKN3 constitute a cluster of strongly upregulated cell cycle regulators (Figure 2) and CDC25C was induced with Th1-polarising conditions (Table 2). These data suggest a relevant function of these enzymes for Th1 polarisation, proliferation, or effector function. Consistently, inhibition of T cell proliferation by PD-1 is mediated by suppression of CDC25A [42]. Whether there is a role of these cell cycle regulators during antigen-mediated T cell stimulation, as has been recently described for the CDC25B-specific kinase Aurora A [68], should be investigated.

4. Conclusions: Perspective on Autoimmune Diseases

The systematic analysis performed in this study reveals several genes coding for PTPs that are regulated during Th1 polarisation and restimulation of effector cells. Interestingly, the mRNA level of the majority of the regulated genes coding for NCs was increased during Th1 polarisation, which

suggests a regulatory role of these PTPs in Th1 polarisation or effector function. By contrast downmodulated genes during polarising conditions might be involved in initial immune responses by naïve T cells. In general, changes in expression levels found during polarisation might indicate a role in achieving a healthy balance of T helper polarisation. Our data also suggest an important compartmentalisation of dephosphorylated ERK functions during the T cell responses at inflammatory sites. Finally, the obtained results also suggest the existence of PTPs that might regulate components of the cellular machinery (including the endosomal compartment, the cytoskeleton, and the activity of ion channels) during T cell immune responses. The regulatory role of these PTPs should be investigated.

Regarding autoimmunity, the expression of *PTPN6* has been found reduced in psoriatic T cells [29] and in blood cells of psoriatic arthritis [69]. Our data suggest that balanced nonpathological T helper polarisation requires a highly upregulated expression of SHP1 during the generation of IFNγ producing cells. By contrast, although the polymorphism rs1893217(C) in the *PTPN2* gene has been associated with a decrease in the expression levels that promotes autoimmunity [23, 70] and to a reduced response to IL-2 [26], the regulation of the expression levels of this gene does not seem to be necessary during the generation of IFNγ producing cells. Single nucleotide polymorphisms (SNPs) in nonregulated PTPs *PTPN22* and *PTPRC* have been associated with human autoimmune diseases, including multiple sclerosis and autoimmune hepatitis in the case of *PTPRC* and type I diabetes, rheumatoid arthritis, and systemic lupus erythematosus in the case of *PTPN22* [13, 23, 37, 52].

In the mouse model the atypical DUSP22 has been proposed to inhibit TCR signalling and to control the development of experimental autoimmune encephalomyelitis [44]. Interestingly, low expression of DUSP22 in human T cells has been proposed to be a potential biomarker for systemic lupus erythematosus nephritis [45]. Thus, it seems that this protein is relevant in controlling T cell responses in order to prevent autoimmune diseases. Interestingly, overexpression of DUSP23 in CD4 T cells of patients with systemic lupus erythematosus has been described [46]. The upregulation of DUSP22 and DUSP23 found in our work by Th1-polarising conditions suggests a regulatory role of these enzymes during T helper polarisation and, consequently, their contribution to the control or development of pathological polarisation should be investigated. In general, our data encourage comparing the expression profile of PTPs in T cells of patients diagnosed with autoimmune diseases and healthy individuals. Some of the genes regulated during Th1 polarisation as assessed herein might also constitute biomarkers or might be involved in the pathogenesis or severity of autoimmune diseases.

Conflicts of Interest

The authors declare that there are no conflicts of interest regarding the publication of this paper.

Acknowledgments

This work was supported by funds of the Spanish Ministry of Economy and Competitiveness (SAF2012-33218) and the European Union (FP7-PEOPLE-2012-CIG) to Pedro Roda-Navarro. These projects supported Patricia Castro-Sánchez. Rocio Ramirez-Munoz was supported by a fellowship for educating researchers (FPI Fellowship) assigned to the SAF2012-33218 Project.

References

[1] C. Fournier, "Where do T cells stand in rheumatoid arthritis?" *Joint Bone Spine*, vol. 72, no. 6, pp. 527–532, 2005.

[2] R. Baccala, D. H. Kono, and A. N. Theofilopoulos, "Interferons as pathogenic effectors in autoimmunity," *Immunological Reviews*, vol. 204, pp. 9–26, 2005.

[3] K. Miyake, M. Akahoshi, and H. Nakashima, "Th subset balance in lupus nephritis," *Journal of Biomedicine and Biotechnology*, vol. 2011, Article ID 980286, 7 pages, 2011.

[4] M. Diani, G. Altomare, and E. Reali, "T helper cell subsets in clinical manifestations of psoriasis," *Journal of Immunology Research*, vol. 2016, Article ID 7692024, 7 pages, 2016.

[5] N. K. Tonks, "Protein tyrosine phosphatases: from genes, to function, to disease," *Nature Reviews Molecular Cell Biology*, vol. 7, no. 11, pp. 833–846, 2006.

[6] A. Alonso, J. Sasin, N. Bottini et al., "Protein tyrosine phosphatases in the human genome," *Cell*, vol. 117, no. 6, pp. 699–711, 2004.

[7] Y. Bai, Y. Luo, S. Liu et al., "PRL-1 protein promotes ERK1/2 and RhoA protein activation through a non-canonical interaction with the Src homology 3 domain of p115 Rho GTpase-activating protein," *The Journal of Biological Chemistry*, vol. 286, no. 49, pp. 42316–42324, 2011.

[8] C. J. Caunt and S. M. Keyse, "Dual-specificity MAP kinase phosphatases (MKPs): shaping the outcome of MAP kinase signalling," *FEBS Journal*, vol. 280, no. 2, pp. 489–504, 2013.

[9] K. Hnia, I. Vaccari, A. Bolino, and J. Laporte, "Myotubularin phosphoinositide phosphatases: cellular functions and disease pathophysiology," *Trends in Molecular Medicine*, vol. 18, no. 6, pp. 317–327, 2012.

[10] T. Mustelin, T. Vang, and N. Bottini, "Protein tyrosine phosphatases and the immune response," *Nature Reviews Immunology*, vol. 5, no. 1, pp. 43–57, 2005.

[11] Y. Arimura and J. Yagi, "Comprehensive expression profiles of genes for protein tyrosine phosphatases in immune cells," *Science Signaling*, vol. 3, no. 137, p. rs1, 2010.

[12] A. Hijikata, H. Kitamura, Y. Kimura et al., "Construction of an open-access database that integrates cross-reference information from the transcriptome and proteome of immune cells," *Bioinformatics*, vol. 23, no. 21, pp. 2934–2941, 2007.

[13] T. Vang, A. V. Miletic, Y. Arimura, L. Tautz, R. C. Rickert, and T. Mustelin, "Protein tyrosine phosphatases in autoimmunity," *Annual Review of Immunology*, vol. 26, pp. 29–55, 2008.

[14] I. Rhee and A. Veillette, "Protein tyrosine phosphatases in lymphocyte activation and autoimmunity," *Nature Immunology*, vol. 13, no. 5, pp. 439–447, 2012.

[15] L. Maksumova, Y. Wang, N. K. Y. Wong, H. T. Le, C. J. Pallen, and P. Johnson, "Differential function of PTPα and PTPα Y789F in T cells and regulation of PTPα phosphorylation at Tyr-789 by

CD45," *The Journal of Biological Chemistry*, vol. 282, no. 29, pp. 20925–20932, 2007.

[16] T. Mustelin, K. M. Coggeshall, and A. Altman, "Rapid activation of the T-cell tyrosine protein kinase pp56lck by the CD45 phosphotyrosine phosphatase," *Proceedings of the National Academy of Sciences of the United States of America*, vol. 86, no. 16, pp. 6302–6306, 1989.

[17] J. Irie-Sasaki, T. Sasaki, W. Matsumoto et al., "CD45 is a JAK phosphatase and negatively regulates cytokine receptor signalling," *Nature*, vol. 409, no. 6818, pp. 349–354, 2001.

[18] J. Lin and A. Weiss, "The tyrosine phosphatase CD148 is excluded from the immunologic synapse and down-regulates prolonged T cell signaling," *Journal of Cell Biology*, vol. 162, no. 4, pp. 673–682, 2003.

[19] J. E. Baker, R. Majeti, S. G. Tangye, and A. Weiss, "Protein tyrosine phosphatase CD148-mediated inhibition of T-cell receptor signal transduction is associated with reduced LAT and phospholipase Cγ1 phosphorylation," *Molecular and Cellular Biology*, vol. 21, no. 7, pp. 2393–2403, 2001.

[20] N. Erdenebayar, Y. Maekawa, J. Nishida, A. Kitamura, and K. Yasutomo, "Protein-tyrosine phosphatase-kappa regulates CD4+ T cell development through ERK1/2-mediated signaling," *Biochemical and Biophysical Research Communications*, vol. 390, no. 3, pp. 489–493, 2009.

[21] R. Iwata, N. Sasaki, and T. Agui, "Contiguous gene deletion of Ptprk and Themis causes T-helper immunodeficiency (thid) in the LEC rat," *Biomedical Research*, vol. 31, no. 1, pp. 83–87, 2010.

[22] X. Lu, R. Malumbres, B. Shields et al., "PTP1B is a negative regulator of interleukin 4-induced STAT6 signaling," *Blood*, vol. 112, no. 10, pp. 4098–4108, 2008.

[23] K. M. Doody, S. Bussières-Marmen, A. Li, M. Paquet, J. E. Henderson, and M. L. Tremblay, "T cell protein tyrosine phosphatase deficiency results in spontaneous synovitis and subchondral bone resorption in mice," *Arthritis and Rheumatism*, vol. 64, no. 3, pp. 752–761, 2012.

[24] F. Wiede, B. J. Shields, S. H. Chew et al., "T cell protein tyrosine phosphatase attenuates T cell signaling to maintain tolerance in mice," *Journal of Clinical Investigation*, vol. 121, no. 12, pp. 4758–4774, 2011.

[25] P. D. Simoncic, A. Lee-Loy, D. L. Barber, M. L. Tremblay, and C. J. McGlade, "The T cell protein tyrosine phosphatase is a negative regulator of Janus family kinases 1 and 3," *Current Biology*, vol. 12, no. 6, pp. 446–453, 2002.

[26] S. A. Long, K. Cerosaletti, J. Y. Wan et al., "An autoimmune-associated variant in PTPN2 reveals an impairment of IL-2R signaling in CD4+ T cells," *Genes and Immunity*, vol. 12, no. 2, pp. 116–125, 2011.

[27] J. A. Young, A. M. Becker, J. J. Medeiros et al., "The protein tyrosine phosphatase PTPN4/PTP-MEG1, an enzyme capable of dephosphorylating the TCR ITAMs and regulating NF-κB, is dispensable for T cell development and/or T cell effector functions," *Molecular Immunology*, vol. 45, no. 14, pp. 3756–3766, 2008.

[28] J. Brockdorff, S. Williams, C. Couture, and T. Mustelin, "Dephosphorylation of ZAP-70 and inhibition of T cell activation by activated SHP1," *European Journal of Immunology*, vol. 29, no. 8, pp. 2539–2550, 1999.

[29] K. W. Eriksen, A. Woetmann, L. Skov et al., "Deficient SOCS3 and SHP-1 expression in psoriatic T cells," *Journal of Investigative Dermatology*, vol. 130, no. 6, pp. 1590–1597, 2010.

[30] K. Nika, C. Charvet, S. Williams et al., "Lipid raft targeting of hematopoietic protein tyrosine phosphatase by protein kinase Cθ-mediated phosphorylation," *Molecular and Cellular Biology*, vol. 26, no. 5, pp. 1806–1816, 2006.

[31] M. Saxena, S. Williams, J. Brockdorff, J. Gilman, and T. Mustelin, "Inhibition of T cell signaling by mitogen-activated protein kinase-targeted hematopoietic tyrosine phosphatase (HePTP)," *Journal of Biological Chemistry*, vol. 274, no. 17, pp. 11693–11700, 1999.

[32] H. Huynh, N. Bottini, S. Williams et al., "Control of vesicle fusion by a tyrosine phosphatase," *Nature Cell Biology*, vol. 6, no. 9, pp. 831–839, 2004.

[33] Y. Wang, E. Vachon, J. Zhang et al., "Tyrosine phosphatase MEG2 modulates murine development and platelet and lymphocyte activation through secretory vesicle function," *Journal of Experimental Medicine*, vol. 202, no. 11, pp. 1587–1597, 2005.

[34] D. Davidson, X. Shi, M.-C. Zhong, I. Rhee, and A. Veillette, "The phosphatase PTP-PEST promotes secondary t cell responses by dephosphorylating the protein tyrosine kinase Pyk2," *Immunity*, vol. 33, no. 2, pp. 167–180, 2010.

[35] M. Nakahira, T. Tanaka, B. E. Robson, J. P. Mizgerd, and M. J. Grusby, "Regulation of signal transducer and activator of transcription signaling by the tyrosine phosphatase PTP-BL," *Immunity*, vol. 26, no. 2, pp. 163–176, 2007.

[36] H.-M. Wang, Y.-F. Xu, S.-L. Ning et al., "The catalytic region and PEST domain of PTPN18 distinctly regulate the HER2 phosphorylation and ubiquitination barcodes," *Cell research*, vol. 24, no. 9, pp. 1067–1090, 2014.

[37] S. M. Stanford, T. M. Mustelin, and N. Bottini, "Lymphoid tyrosine phosphatase and autoimmunity: human genetics rediscovers tyrosine phosphatases," *Seminars in Immunopathology*, vol. 32, no. 2, pp. 127–136, 2010.

[38] J. S. Wu, A. Katrekar, L. A. Honigberg et al., "Identification of substrates of human protein-tyrosine phosphatase PTPN22," *The Journal of Biological Chemistry*, vol. 281, no. 16, pp. 11002–11010, 2006.

[39] S. M. Stanford and N. Bottini, "PTPN22: the archetypal non-HLA autoimmunity gene," *Nature Reviews Rheumatology*, vol. 10, no. 10, pp. 602–611, 2014.

[40] Y. Zhang, J. M. Reynolds, S. H. Chang et al., "MKP-1 is necessary for T cell activation and function," *Journal of Biological Chemistry*, vol. 284, no. 45, pp. 30815–30824, 2009.

[41] T. Musikacharoen, K. Bandow, K. Kakimoto et al., "Functional involvement of Dual Specificity Phosphatase 16 (DUSP16), a c-Jun N-terminal kinase-specific phosphatase, in the regulation of T helper cell differentiation," *Journal of Biological Chemistry*, vol. 286, no. 28, pp. 24896–24905, 2011.

[42] N. Patsoukis, D. Sari, and V. A. Boussiotis, "PD-1 inhibits T cell proliferation by upregulating p27 and p15 and suppressing Cdc25A," *Cell Cycle*, vol. 11, no. 23, pp. 4305–4309, 2012.

[43] A. Alonso, J. J. Merlo, S. Na et al., "Inhibition of T cell antigen receptor signaling by VHR-related MKPX (VHX), a new dual specificity phosphatase related to VH1 related (VHR)," *Journal of Biological Chemistry*, vol. 277, no. 7, pp. 5524–5528, 2002.

[44] J.-P. Li, C.-Y. Yang, H.-C. Chuang et al., "The phosphatase JKAP/DUSP22 inhibits T-cell receptor signalling and autoimmunity by inactivating Lck," *Nature Communications*, vol. 5, article 3618, 2014.

[45] H. C. Chuang, Y. M. Chen, W. T. Hung et al., "Downregulation of the phosphatase JKAP/DUSP22 in T cells as a potential new biomarker of systemic lupus erythematosus nephritis," *Oncotarget*, vol. 7, no. 36, pp. 57593–57605, 2016.

ADDENDA

[46] E. Balada, L. Felip, J. Ordi-Ros, and M. Vilardell-Tarres, "DUSP23 is over-expressed and linked to the expression of DNMTs in $CD4^+$ T cells from systemic lupus erythematosus patients," *Clinical & Experimental Immunology*, vol. 187, no. 2, pp. 242–250, 2017.

[47] C.-F. Chen, X. Feng, H.-Y. Liao et al., "Regulation of T cell proliferation by JMJD6 and PDGF-BB during chronic hepatitis B infection," *Scientific Reports*, vol. 4, article 6359, 2014.

[48] K. J. Livak and T. D. Schmittgen, "Analysis of relative gene expression data using real-time quantitative PCR and the 2-ΔΔCT method," *Methods*, vol. 25, no. 4, pp. 402–408, 2001.

[49] D. J. Johnson, L. I. Pao, S. Dhanji, K. Murakami, P. S. Ohashi, and B. G. Neel, "Shp1 regulates T cell homeostasis by limiting IL-4 signals," *Journal of Experimental Medicine*, vol. 210, no. 7, pp. 1419–1431, 2013.

[50] M. Shiota, T. Tanihiro, Y. Nakagawa et al., "Protein tyrosine phosphatase PTP20 induces actin cytoskeleton reorganization by dephosphorylating p190 RhoGAP in rat ovarian granulosa cells stimulated with follicle-stimulating hormone," *Molecular Endocrinology*, vol. 17, no. 4, pp. 534–549, 2003.

[51] M. Van Ham, L. Kemperman, M. Wijers, J. Fransen, and W. Hendriks, "Subcellular localization and differentiation-induced redistribution of the protein tyrosine phosphatase PTP-BL in neuroblastoma cells," *Cellular and Molecular Neurobiology*, vol. 25, no. 8, pp. 1225–1244, 2005.

[52] Wellcome Trust Case Control Consortium, "Genome-wide association study of 14,000 cases of seven common diseases and 3,000 shared controls," *Nature*, vol. 447, no. 7145, pp. 661–678, 2007.

[53] L. Guo, C. Martens, D. Bruno et al., "Lipid phosphatases identified by screening a mouse phosphatase shRNA library regulate T-cell differentiation and Protein kinase B AKT signaling," *Proceedings of the National Academy of Sciences of the United States of America*, vol. 110, no. 20, pp. E1849–E1856, 2013.

[54] S. Dadsetan, L. Zakharova, T. F. Molinski, and A. F. Fomina, "Store-operated Ca^{2+} influx causes Ca^{2+} release from the intracellular Ca^{2+} channels that is required for T cell activation," *Journal of Biological Chemistry*, vol. 283, no. 18, pp. 12512–12519, 2008.

[55] S. Srivastava, K. Ko, P. Choudhury et al., "Phosphatidylinositol-3 phosphatase myotubularin-related protein 6 negatively regulates CD4 T cells," *Molecular and Cellular Biology*, vol. 26, no. 15, pp. 5595–5602, 2006.

[56] A. W. Bronietzki, M. Schuster, and I. Schmitz, "Autophagy in T-cell development, activation and differentiation," *Immunology and Cell Biology*, vol. 93, no. 1, pp. 25–34, 2015.

[57] K. Hnia, H. Tronchère, K. K. Tomczak et al., "Myotubularin controls desmin intermediate filament architecture and mitochondrial dynamics in human and mouse skeletal muscle," *The Journal of Clinical Investigation*, vol. 121, no. 1, pp. 70–85, 2011.

[58] J. Mei, Z. Li, and J.-F. Gui, "Cooperation of Mtmr8 with PI3K regulates actin filament modeling and muscle development in zebrafish," *PLoS ONE*, vol. 4, no. 3, 2009.

[59] A. Bolino, A. Bolis, S. C. Previtali et al., "Disruption of *Mtmr2* produces CMT4B1-like neuropathy with myelin outfolding and impaired spermatogenesis," *Journal of Cell Biology*, vol. 167, no. 4, pp. 711–721, 2004.

[60] R. Lasserre, S. Charrin, C. Cuche et al., "Ezrin tunes T-cell activation by controlling Dlgl and microtubule positioning at the immunological synapse," *The EMBO Journal*, vol. 29, no. 14, pp. 2301–2314, 2010.

[61] R. Ramirez-Munoz, P. Castro-Sánchez, and P. Roda-Navarro, "Ultrasensitivity in the cofilin signaling module: a mechanism for tuning T cell responses," *Frontiers in Immunology*, vol. 7, article 59, 2016.

[62] S.-J. Moon, M.-A. Lim, J.-S. Park et al., "Dual-specificity phosphatase 5 attenuates autoimmune arthritis in mice via reciprocal regulation of the Th17/Treg cell balance and inhibition of osteoclastogenesis," *Arthritis & Rheumatology*, vol. 66, no. 11, pp. 3083–3095, 2014.

[63] O. Acuto, V. D. Bartolo, and F. Michel, "Tailoring T-cell receptor signals by proximal negative feedback mechanisms," *Nature Reviews Immunology*, vol. 8, no. 9, pp. 699–712, 2008.

[64] J. Rodriguez and P. Crespo, "Working without kinase activity: phosphotransfer-independent functions of extracellular signal-regulated kinases," *Science Signaling*, vol. 4, no. 196, article re3, 2011.

[65] C. J. Caunt, S. P. Armstrong, C. A. Rivers, M. R. Norman, and C. A. McArdle, "Spatiotemporal regulation of ERK2 by dual specificity phosphatases," *Journal of Biological Chemistry*, vol. 283, no. 39, pp. 26612–26623, 2008.

[66] M. Mandl, D. N. Slack, and S. M. Keyse, "Specific inactivation and nuclear anchoring of extracellular signal-regulated kinase 2 by the inducible dual-specificity protein phosphatase DUSP5," *Molecular and Cellular Biology*, vol. 25, no. 5, pp. 1830–1845, 2005.

[67] B. Zhou and Z.-Y. Zhang, "Mechanism of mitogen-activated protein kinase phosphatase-3 activation by ERK2," *Journal of Biological Chemistry*, vol. 274, no. 50, pp. 35526–35534, 1999.

[68] N. Blas-Rus, E. Bustos-Morán, I. P. de Castro et al., "Aurora A drives early signalling and vesicle dynamics during T-cell activation," *Nature Communications*, vol. 7, Article ID 11389, 2016.

[69] F. M. Batliwalla, W. Li, C. T. Ritchlin et al., "Microarray analyses of peripheral blood cells identifies unique gene expression signature in psoriatic arthritis," *Molecular Medicine*, vol. 11, no. 1-12, pp. 21–29, 2005.

[70] F. Wiede, F. Sacirbegovic, Y. A. Leong, D. Yu, and T. Tiganis, "PTPN2-deficiency exacerbates T follicular helper cell and B cell responses and promotes the development of autoimmunity," *Journal of Autoimmunity*, vol. 76, pp. 85–100, 2017.